NEURAL BASIS OF LOCOMOTION IN *DROSOPHILA* MELANOGASTER LARVAE

by

MATTHEW CLARK

A DISSERTATION

Presented to the Department of Biology
and the Graduate School of the University of Oregon
in partial fulfillment of the requirements
for the degree of
Doctor of Philosophy

December 2017

DISSERTATION APPROVAL PAGE

Student: Matthew Clark

Title: Neural Basis Of Locomotion In *Drosophila Melanogaster* Larvae

This dissertation has been accepted and approved in partial fulfillment of the requirements for the Doctor of Philosophy degree in the Department of Biology by:

Tory Herman	Chairperson
Chris Doe	Advisor
Shawn Lockery	Core Member
Janis Weeks	Core Member
Matt Smear	Institutional Representative

and

Sara D. Hodges	Interim Vice Provost and Dean of the Graduate School

Original approval signatures are on file with the University of Oregon Graduate School.

Degree awarded December 2017.

DISSERTATION ABSTRACT

Matthew Clark

Doctor of Philosophy

Department of Biology

December 2017

Title: Neural Basis Of Locomotion In *Drosophila Melanogaster* Larvae

Drosophila larval crawling is an attractive system to study patterned motor output at the level of animal behavior. Larval crawling consists of waves of muscle contractions generating forward or reverse locomotion. In addition, larvae undergo additional behaviors including head casts, turning, and feeding. It is likely that some neurons are used in all these behaviors (e.g. motor neurons), but the identity (or even existence) of neurons dedicated to specific aspects of behavior is unclear. To identify neurons that regulate specific aspects of larval locomotion, we performed a genetic screen to identify neurons that, when activated, could elicit distinct motor programs. We defined 10 phenotypic categories that could uniquely be evoked upon stimulation, and provide further in depth analysis of two of these categories to understand the origins of the evoked behaviors.

We first identified the evolutionarily conserved Even-skipped^{+} interneuron phenotype (Eve/Evx). Activation or ablation of Eve^{+} interneurons disrupted bilaterally symmetric muscle contraction amplitude, without affecting left-right synchronous timing. TEM reconstruction places the Eve^{+} interneurons at the heart of a sensorimotor circuit capable of detecting and modifying body wall muscle contraction

We then went on to identify a unique pair of descending neurons dubbed the

'Mooncrawler' descending neurons (McDNs) to be sufficient to generate reverse locomotion. We show that the McDNs are present at larval hatching, function during larval life, and are remodeled during metamorphosis while maintaining basic morphological features and neural functions necessary to generate backwards locomotion. Finally, using serial section Transmission Electron Microscopy (ssTEM) to map neural connections to upstream and downstream elements provides a mechanistic view of how sensory information is received by the McDNs and transmitted to the VNC motor system to perform backwards locomotion. Finally, we show that these McDNs are the same as those identified in recent work in *Drosophila* adults (Bidaye et al. 2014) to be sufficient to generate reverse locomotion.

This dissertation includes previously published and unpublished co-authored material

CURRICULUM VITAE

NAME OF AUTHOR: Matthew Clark

GRADUATE AND UNDERGRADUATE SCHOOLS ATTENDED:

University of Oregon, Eugene
University of Arizona, Tucson
Pima Community College, Tucson

DEGREES AWARDED:

Doctor of Philosophy, Biology, 2017, University of Oregon
Bachelor of Science, Biochemistry & Molecular Biophysics and Molecular & Cellular Biology, 2009, University of Arizona
Associate of Science, 2004, Pima Community College

AREAS OF SPECIAL INTEREST:

Developmental Neuroscience
Systems Neuroscience

PROFESSIONAL EXPERIENCE:

Graduate Research Assistant, Richard Baines lab, January-March 2013

Postbaccalaureate Research Education Program (PREP) Research Assistant, Bing Ye lab, 2010-2011

Research Technician, Luceome Laboratory Technician 2009-2010

GRANTS, AWARDS, AND HONORS:

American Physiological Society William Porter Graduate Fellowship, University of Oregon, 2015

NIH Genetics Training Grant, University of Oregon, 2013

NIH Development Training Grant, University of Oregon, 2012

University of Oregon Graduate School Promising Scholar, University of Oregon, 2011

PUBLICATIONS:

Hirono, K., Kohwi, M., Clark, M. Q., Heckscher, E. S., & Doe, C. Q. (2017). The Hunchback temporal transcription factor establishes, but is not required to maintain, early-born neuronal identity. *Neural development*, *12*(1), 1.

Clark, M. Q., McCumsey, S. J., Lopez-Darwin, S., Heckscher, E. S., & Doe, C. Q. (2016). Functional genetic screen to identify Interneurons governing Behaviorally distinct aspects of Drosophila larval motor programs. *G3: Genes, Genomes, Genetics*, *6*(7), 2023-2031.

Heckscher, Ellie S., Aref Arzan Zarin, Serge Faumont, Matthew Q. Clark, Laurina Manning, Akira Fushiki, Casey M. Schneider-Mizell et al. "Even-skipped+ interneurons are core components of a sensorimotor circuit that maintains left-right symmetric muscle contraction amplitude." *Neuron* 88, no. 2 (2015): 314-329.

ACKNOWLEDGMENTS

This work would not exist without the guidance and support I have received from mentors throughout my career. Drs. Michael Wells and Roger Meisfeld have been scientific mentors, and advocates in early days giving my first chance at research. Reena Zutshi helped me to clarify my thinking and develop my use of the scientific method.

My thesis advisor, Dr. Chris Doe, guided me through several years of tremendous personal and professional growth. I admire him immensely and am grateful to have had the chance to work in his laboratory. Several of my colleagues have been instrumental to my progress on this work. Ellie Heckscher set my sights on a fascinating line of inquiry and trained me in techniques that have been critical to the experiments presented here. Keiko Hirono taught me molecular genetics. Laurina Manning helped me to be a microscopist and gather beautiful images. Sereno Lopez and Stephanie McCumsey also provided pivotal support throughout my time in graduate school. Syed Mubarak for partnership in countless outreach events helping to spread the gospel of the Fruit Fly. I would also like to thank the members of my thesis committee: Tory Herman, Matt Smear, Shawn Lockery and Janis Weeks for many constructive discussions of my research and for supporting my scientific career.

I am also grateful to my mom, Debra Clark, for encouraging me and supporting my work as a scientist. 10 years ago the goal of getting a PhD seemed impossible, but through it all my lovely wife Hannah has been by my side.

For Frank

TABLE OF CONTENTS

LIST OF FIGURES

CHAPTER I

NEURAL CONTROL OF LOCOMOTION IN *DROSOPHILA* MELANOGASTER LARVAE

INTRODUCTION

Our central nervous system (CNS) is composed of billions of neurons with orders of magnitude more synaptic connections that form the basis of neural circuitry. The instructions for making and maintaining proper functional circuits are encoded within the genome. However, general principles for understanding the genetic basis of neural circuit formation remain elusive. Due to the precise nature of development, subtle disruptions in the biochemical signals used to form circuits can produce serious deleterious effects (Wu et al. 2011). Gaining an understanding of the molecular and genetic basis of circuit formation can help us to understand how improper establishment and maintenance of circuits arise. Understanding the genetic logic guiding circuit formation holds the promise of one day being able to develop therapeutic interventions for conditions such as autism, epilepsy and schizophrenia (Gage and Temple 2013).

The ability to compare conserved principles of neural circuit development and function of in vertebrates and invertebrates is relatively new, but as circuits and their genetic origins are understood we can begin to understand how genes influence circuit form and function. Bilaterally symmetric organisms such as *Drosophila* and mice share a common body plan where they do share some principles of brain organization. Both have ascending, descending and local interneuronal input which all interact with each other at various scales. Sensory feedback from the periphery gives feedback to the motor system

to instruct axial propagation speed and duration. In mice descending input into local systems originates in the cortical and basal ganglia regions of the brain (Grillner *et al.* 2005), whereas in *Drosophila* they originate from the supraesophageal and subesophageal ganglia (Ito *et al.* 2014). Circuit–level comparisons between larval *Drosophila* and embryonic mice may be confounding due to the different modes of locomotion (walking vs. crawling), however common genetic fingerprints of neuronal populations do exist (Eve/EVX, Engrailed, Dbx etc.) and may inform analysis of general principles of circuit function and shed insight into mechanism of the evolution of neural circuits (Thor and Thomas 2002; Denes *et al.* 2007). Owing to the genetic accessibility of major groups of progenitor domain neurons, certain functions can be attributed to mammalian spinal locomotor circuits. For example, functional properties of the V0 and V2 subtypes include left/right alternation of gait, V1 (engrailed+ interneurons) help dictate the speed of axial propagation, while V3 interneurons ensure a stable pattern is propagated along the spinal column. While these genetically accessible populations are still broad their heterogeneity is just beginning to be understood (Stepien *et al.* 2010).

More than 30 years of studies into *Drosophila* neurogenesis have revealed fundamental insights into our understanding of axon guidance mechanisms, neural differentiation, and early cell fate decisions (Siller and Doe 2009; Kohwi and Doe 2013; Zarin et al. 2014). What is less understood is how a group of neurons from disparate locations, lineages and developmental periods of neurogenesis can join together to form a functional circuit. A recently published collection of neural fragment enhancer Gal4 driver lines allows unprecedented access to interneurons within the CNS of *Drosophila* larvae (Manning et al. 2012; Li et al. 2014). Using neurogenetic techniques developed in

Drosophila it is now possible to study the neural substrates of behavior at single cell resolution and to determine their functional properties. New and exciting mapping tools allow researchers to chart neural connectivity and to investigate their developmental origins. Combining these tools we can now begin to assess the genetic framework that guides neural circuit development.

In order to understand how diverse groups of neurons can form functional circuitry, many labs have begun to address these challenges using larval locomotion as a model for analysis. By studying how neural networks that govern *Drosophila* larval locomotion are specified and assembled, we can gain a greater understanding of the genetic principles of neural circuit development. However, before we can analyze how circuits form, we must first identify neurons that form the circuits. Indeed, challenges faced by 21st century neuroscientists, as articulated by the BRAIN initiative, include discovering diversity, making maps at various scales, observing the brain in action and demonstrating causality (Bargmann and Newsome 2014).

Patterned motor behaviors such as breathing and locomotion require the coordination of neural circuits which is accomplished by central pattern generators (CPGs) (Marder and Bucher 2001). CPGs are complex microcircuits comprised of excitatory and inhibitory interneurons that synapse upon motor neurons. Motor neurons can simply reflect the net output of a CPG, or may influence its ouput. For example, leech peristaltic movements rely on excitatory motor neurons that receive input from interneuronal CPGs, however there is not input back to the CPG from the excitatory motor neurons. In contrast, inhibitory motor neurons synapse onto CPG neurons and can affect their activity (Mullins *et al.* 2011). In the crustacean stomatogastric system, motor

neurons innervate stomach muscles and also synapse with each other to form a CPG that governs mastication (Marder and Bucher 2007). The net activity of CPGs can be observed at the level of rhythmic activity in muscles or motor neurons. Understanding basic motor patterns is necessary to further understand how these patterns are generated within the central nervous system. A core component of CPGs is their ability to function independent of modulation via sensory systems.

Much of our understanding of the origins of motor pattern generation is from the study of 'simple' invertebrates such as locust, crabs, crayfish, lobsters and shrimp (Nusbaum and Beenhakker 2002). Indeed, our first understanding of CPGs came from the study of locusts (Wilson 1961; Wilson and Wyman 1965). Wilson and colleagues first used the term 'central *nervous* pattern generator' to describe a 'fugue' pattern of signals emanating from the flight system of a wing-deaffererted and decapitated locust(Wilson and Wyman 1965). Owing to their small size, complex neural circuits in *Drosophila* have traditionally proven difficult to study. However, a recent confluence of a number of integrative tools has ushered in a golden age of neural circuit analysis in *Drosophila.* Researchers can leverage the tools of connectomics, optogenetics, sophisticated dual binary transcriptional systems, high-throughput computational methods to quantify behavior, and computational methods for modeling behavior (Lai and Lee 2006; Risse, Thomas, Otto, Löpmeier, *et al.* 2013; Lemon *et al.* 2015; Schneider-Mizell *et al.* 2015; Pehlevan *et al.* 2016). *Drosophila* larvae are also advantageous to study because of their stereotyped behaviors, anatomical simplicity, genetic accessibility, and transparent cuticle, which allows for live imaging of neuronal activity. This model system holds the promise of linking developmental history to circuit formation and function.

CIRCUIT CRACKING TOOLS

The generation of the Janelia Rubin Gal4 and Vienna Tiles Gal4 libraries (Pfeiffer *et al.* 2008; Kvon *et al.* 2014), has allowed researchers increasingly refined precision to access various cell types within the nervous system and to elucidate their function. Due to the nature of the library, defined cis-regulatory module (CRM) DNA fragments can be used to generate various constructs such as a LexA driver instead of GAL4, and to reintegrate these elements in a site-specific manner back into the genome. This modularity allows for intersectional strategies to subdivide a pattern, monitor different cell populations at the same time, or optogenetically activate one group while monitoring the response of others (Kohsaka, Takasu, Morimoto, and Nose 2014; Dolan *et al.* 2017; Turner-Evans *et al.* 2017).

Coupled to the advent of refined cellular targeting technologies, we now have an array of constructs that can be expressed in a cell-type-specific manner. These UAS, LexAop, and QUAS constructs allow us to anatomically mark, monitor and perturb neurons (Nicolai *et al.* 2010; Akerboom *et al.* 2012; Klapoetke *et al.* 2014; Nern *et al.* 2015). Refinements in the translational efficiency of transgenes has allowed for stable expression at robust levels using translational enhancer elements such as p10, syn21, WPRE (Pfeiffer *et al.* 2008, 2010, 2012). MultiColor FlpOut (MCFO) is one such technique to benefit from these enhancements as well as others including attaching myristoylated moieties for improved trafficking to the cell membrane. MCFO allows for detailed morphological studies of individual neurons that may be part of a broader population. This method stochastically expresses various cell membrane tagged markers within a population so that neurons can be visualized in different colors. With detailed

morphology captured via confocal microscopy, we can then find a morphological match for those neurons in the CATMAID ssTEM data set based on their unique morphology and cell body position (see below).

Within the field, a widely adopted neural effector known as CsChrimson came from an algal transcriptomics screen for new channelrhodopsins (Klapoetke *et al.* 2014). It is a red-shifted cation channel that can depolarize the membrane of neurons and trigger behaviors within an intact moving animal. It is beneficial for behavior studies since red light is deeper penetrating and has less behavioral artifacts compared to the previous blue-shifted channelrhodopsins. For loss-of-function experiments a blue-light activated Guillardia theta anion channelrhodopsin (GtACR) has been proven to be a hardy substitute for the poorly performing Halorhodopsin anion pump (NpHR) (Mohammad *et al.* 2017). While these tools show the most promise, there are many on the market and an investigator must be careful when considering their assay and tools to choose (Pauls et al. 2015). With current optogenetic tools it is now possible to go "all-optical" in interrogating neural circuits. For example, a researcher may want to trigger a pulse of activity in a putative upstream neuron and monitor the downstream neurons for effect. To achieve this it is possible to express an effector in one expression system (Gal4/LexA), and monitor in the other (UAS/LexAop).

To begin to understand the functions of neurons relevant to behavior, researchers now have the ability to optogenetically silence or activate various populations (or individual) neurons and assay the behavioral perturbations. A major advantage to using *Drosophila* larvae for behavior assays is the ability to observe many animals in one experiment, to perturb neural activity from a distance and track the response in each

individual animal. Using off-the-shelf components one can build a rig and use freely available software to track behavior (Pulver *et al.* 2011; Risse *et al.* 2014; Aleman-Meza *et al.* 2015; Titlow *et al.* 2015; Brooks *et al.* 2016; Maia Chagas *et al.* 2017). Gain-of-function optogenetic assays revealed unique and distinct evocable 'behaviotypes' or phenotypic categories from which larval behaviors could be linked to neuronal expression patterns (Vogelstein *et al.* 2014; Clark *et al.* 2016). In this manner we can begin to connect neural expression patterns to their functional role in larval crawling. For instance, a group demonstrated that interneurons that are of the downstream of mechanonociception sensory neurons were the same A08n neurons identified in a behaviotype screen (Hu *et al.* 2017), providing a path to explore nervous system function. With the ability to perturb and monitor unique, identifiable and reproducible neuronal subtypes comes the ability to functionally map circuits. Via a broad international collaborative effort initiated by Albert Cardona and colleagues, we are gaining progress at mapping the entire connectome of the roughly 10,000 neurons in the first instar larva at synaptic resolution. Through a semi-automated method of tracing synaptic connections, the mushroom body, antennal lobe, and visual system have been mapped, with descending neurons, gustatory, and motor neurons and sensory neurons of the VNC partially done or are nearing completion. These maps allow researchers to generate hypotheses related to circuit form and function and then in conjunction with the circuit cracking tools outlined above, functionally test their ideas.

Natural crawling behaviors

Drosophila larvae spend their lives continually foraging for food as they have a limited time to obtain a nutrient-dependent critical weight that must be met in order to

undergo metamorphosis (Mirth *et al.* 2005). Throughout developmental instars larvae display similar behavioral traits until a hormonal pulse of ecdysone triggers the wandering stage where they leave their substrate to find a suitable surface to begin metamorphosis (Almeida-Carvalho et al. 2017). Recent studies have demonstrated that basic neuronal architecture and connectivity remain consistent during this growth phase, though what differs is the degree of connectivity (Zwart *et al.* 2013; Gerhard *et al.* 2017). Natural crawling behaviors include turns, head sweeps, pauses, hunching, bending, burrowing, rolling and forward and backwards locomotion (Green et al. 1983). Larval forward and reverse locomotion is generated by abdominal somatic body wall muscle contractions moving from posterior to anterior (forward locomotion) or anterior to posterior (reverse locomotion) (Heckscher *et al.* 2012). Consecutive bouts of forward or backward waves are called runs. Asymmetric contractions of thoracic body wall musculature generate turns (Lahiri et al. 2011). A bout of left-right swings of the thoracic head region is known as head casting.

All of these complex movements are enabled by a larval body plan that is regionally specified by Hox genes. Hox genes give segmental identity and regional specification to the central brain, subesophageal zone (SEZ) and the ventral nerve cord (VNC) which includes the thorax, abdomen and terminal ganglion (Dixit et al. 2008). It is hypothesized that Hox gene networks may govern the regional specification of peristaltic locomotion circuits through modifying CPG organization. There is evidence that supports this idea. For example, neural control of turning movements is located within the thoracic segments of the VNC (Berni 2015) while the CPGs that drive larval locomotion reside in the thoracic and abdominal segments of the VNC (Berni *et al.* 2012; Pulver *et al.* 2015a).

However, little is known about the interneurons specifically used in aspects of locomotion, such as forward or reverse movements, head sweeps, and pauses. Making progress identifying specialized neurons may help shed light on this question of regional specialization.

A defined 'simple' system

Fast neurotransmission that governs *Drosophila* larval locomotion is achieved primarily by patterns of connections and the activity of glutamatergic and GABAergic inhibitory interneurons as well as excitatory cholinergic interneurons within the VNC (Rohrbough and Broadie 2002). These networks influence the firing patterns of motor neurons that drive muscle contractions. While the highly stereotyped anatomy of the neuromuscular system is well known, the nature of the upstream interneuronal network remains to be investigated. The topological arrangement of the neuromuscular system is well characterized, with dendritic domains of the motor neurons forming a myotopic map with respect to dorsoventral organization of the functional muscle groups (Landgraf, Sanchez-Soriano, *et al.* 2003; Tripodi *et al.* 2008; Mauss *et al.* 2009).

Drosophila larvae have two main types of motor neurons that provide excitatory drive for muscle contraction, type Ib and Is where b and s denote features of synaptic bouton size big and small, respective (Landgraf and Thor 2006; Peron et al. 2009). Type Is are broadly innervating to synergistic muscle groups, whereas 1b typically innervates individual muscles. Based on their innervation patterns, morphology and physiological properties, it is thought that Ib with its low threshold of activation, and Is with its high threshold, are similar to motor neurons of other animals such as crayfish and humans where low and high activation threshold motor neurons facilitate powerful or precise

movements (Mendell 2005; Atwood 2008). In these systems individual motor neurons are organized into common pools that are recruited to fire in concert to perform locomotory drive. Though motor patterns can be generated independent of sensory input (Fox et al. 2006), the activity of these motor pools is altered in the presence or absence of sensory stimuli (Hughes and Thomas 2007). Several studies have looked at the intrinsic physiological properties of individual motor neurons and found diversity in firing properties (Choi *et al.* 2004; Srinivasan *et al.* 2012; Wolfram *et al.* 2012). In a study by Schaefer and colleagues, whole-cell patch-clamp dual recordings were performed on type Is and Ib motor neurons and they observed that 1b motor neurons are more easily recruited than Is motor neurons (Schaefer *et al.* 2010). Their work also suggests that certain motor groups share common drive potential. This evidence is in agreement with muscle contraction patterns (Heckscher *et al.* 2012) and recent live imaging of bouton activity at the neuromuscular junction (Newman et al. 2017). Live imaging of Ib and Is boutons showed that muscle contraction is most closely associated with type Ib activity. Interestingly, when type Is activity was silenced, it did not change activity of type Ib boutons, and muscle contractions appeared normal. However, intersegmental muscle contraction failed, suggesting that type Is contribute to the propagation of muscle contraction waves. Furthermore, it appears that motor neurons convey electrical information via gap junction synapses to the CPGs (Matsunaga *et al.* 2017).

There are 42 sensory neurons that bilaterally tile each hemi-segment of the body wall in a modality specific array (Merritt and Whitington 1995; Singhania and Grueber 2014). Four classes of sensory neurons that tile the body wall with their “naked dendrites’, send projections into the brain and their axons innervate a very specific region

of the neuropil. These dendritic arborization (DA) neurons, class I-IV, vary in the degree of branching with I being the simplest and IV the most complex. They span the ability to sense all modalities including heat, touch, light, stretch, and vibrations. Each modality innervates a discrete region of the neuropil forming a somatotopic map (Landgraf, Sánchez-Soriano, *et al.* 2003; Zlatic *et al.* 2009). Interestingly, each somatosensory modality is further subdivided according to a fine-scale somatotopy within the neuropil (Kaneko and Ye 2015). This allows the dorso-ventral axis (and it's accompanying region specific sensory information) to coherently be represented in the neuropil.

Within the ventral nerve cord (VNC) there are there are ~270 bilateral pairs of interneurons (INs), each displaying a unique morphological features with varying local, ascending and descending neurite projections. Until recently, very little was known about the discrete structure and function of these interneurons. Early attempts to catalogue interneuronal diversity used DiI labeling to trace the morphologies of individual neurons and lineages of origin, however it was difficult glean a deeper understanding due to the randomness of the labeling technique (Schmid *et al.* 1999a; Rickert *et al.* 2011). Certain features could be discerned for example the fasciculation of projections of neurons from common neuroblasts clones. It was also apparent that there were unique features such as ascending, descending and local interneurons. An array of 30 neuroblasts per hemisegment progressively generates diversity in the VNC according to a stereotyped set of temporal instructions (Kohwi and Doe 2013). These neuroblasts are the same that are used later in the larva to make adult walking and flying circuits (Harris *et al.* 2015; Lacin *et al.* 2016). When an interneuron can be properly assigned to a lineage, and is annotated in the EM, a standard nomenclature has been adopted based on larval neuroblast lineage

of origin. There are 30 NBs so for example if neurons are from abdominal lineage 27 they are named A27a, b, c etc.. Orphan neurons that haven't been ascribed to a particular lineage contain numbers above 30 (for example A31k)(Ohyama *et al.* 2015b; Schneider-Mizell *et al.* 2016).

A recently published integrative tool allows for the characterization of interneuronal diversity according to developmentally expressed molecular markers and cell body position (Heckscher *et al.* 2014). Known as the eNeuro atlas this tool assigns a unique number to a cell body position (for example a Rubin Gal4 expression pattern) and allows us to look at other overlapping expression patterns of other Gal4s or known transcription factors. This tool has been successfully used to predict overlapping expression patterns of Gal4 drivers that was then used to generate split Gal4s for use in an intersectional manner.

To begin to explore relevant interneurons mediating behavior we take two general approaches: 1) screen for functionally relevant interneurons and map the connective and 2) map neurons anatomically and test for function. Pre-Rubin Gal4 behavior screens (Suster et al. 2003; Iyengar et al. 2011) yielded some interesting observations yet, the pattern we often to broad, without any means to considerably (and reproducibly) narrow target population. The recent larval behavior screens using the Rubin lines has allowed researcher the ability to pinpoint unique groups (or individual) neurons important for a given behavior (Ohyama *et al.* 2013a; Vogelstein *et al.* 2014; Clark *et al.* 2016; Yoshikawa *et al.* 2016).

Chapters II and III of this dissertation were published in with the follwoing co-authors: McCumsey, S. J., Lopez-Darwin, S., Heckscher, E. S., & Doe, C. Q. and

Heckscher, E.S., Zarin, A.A., Faumont, S., Clark, M.Q., Manning, L., Fushiki, A., Schneider-Mizell, C.M., Fetter, R.D., Truman, J.W., Zwart, M.F., Landgraf, M., Cardona, A., Lockery, S.R., Doe, C.Q. (respective). Chapters I and IV contain unpublished materials.

CHAPTER II
FUNCTIONAL GENETIC SCREEN TO IDENTIFY INTERNEURONS GOVERNING BEHAVIORALLY DISTINCT ASPECTS OF *DROSOPHILA* LARVAL MOTOR PROGRAMS

Reproduced with permission from Clark, M. Q., McCumsey, S. J., Lopez-Darwin, S., Heckscher, E. S., & Doe, C. Q. (2016). Functional genetic screen to identify Interneurons governing Behaviorally distinct aspects of *Drosophila* larval motor programs. *G3: Genes, Genomes, Genetics*, *6*(7), 2023-2031. **Author contributions**

Abstract

Drosophila larval crawling is an attractive system to study patterned motor output at the level of animal behavior. Larval crawling consists of waves of muscle contractions generating forward or reverse locomotion. In addition, larvae undergo additional behaviors including head casts, turning, and feeding. It is likely that some neurons are used in all these behaviors (e.g. motor neurons), but the identity (or even existence) of neurons dedicated to specific aspects of behavior is unclear. To identify neurons that regulate specific aspects of larval locomotion, we performed a genetic screen to identify neurons that, when activated, could elicit distinct motor programs. We used 165 Janelia *CRM-Gal4* lines – chosen for sparse neuronal expression – to express the warmth-inducible neuronal activator TrpA1 and screened for locomotor defects. The primary screen measured forward locomotion velocity, and we identified 63 lines that had locomotion velocities significantly slower than controls following TrpA1 activation (28^{o}C). A secondary screen was performed on these lines, revealing multiple discrete behavioral phenotypes including slow forward locomotion, excessive reverse locomotion, excessive turning, excessive feeding, immobile, rigid paralysis, and delayed paralysis. While many of the Gal4 lines had motor, sensory, or muscle expression that may account for some or all of the phenotype, some

lines showed specific expression in a sparse pattern of interneurons. Our results show that distinct motor programs utilize distinct subsets of interneurons, and provide an entry point for characterizing interneurons governing different elements of the larval motor program.

Introduction

Understanding the neurobiological basis of behavior and brain disorders is a grand challenge of the 21st century as outlined by the BRAIN Initiative (Jorgenson *et al.* 2015). The study of invertebrates has yielded numerous insights into the neural basis of behavior (Marder 2007). Invertebrates offer an elegant platform to investigate behavioral patterns due to the stereotypy of behaviors as well as the ability to reproducibly identify individual neurons that generate behaviors. Examples include detailed studies of escape behaviors driven by command neurons of crayfish (Edwards *et al.* 1999), central pattern generating circuits of crustaceans (Hooper and DiCaprio 2004), reciprocal inhibition motifs in the visual system of the horseshoe crabs (HARTLINE and RATLIFF 1957, 1958), and learning and memory habituation in the sea hare (Kandel 2001). While these principles were discovered in invertebrates, they are broadly applicable to aspects of neural circuit function in vertebrates.

An integral component of all of motor systems are central pattern generators (CPGs), which underlie the generation of rhythmic motor patterns (Marder and Calabrese 1996; Marder and Bucher 2001). CPGs are diverse and modular and can be recruited to function depending on context and exposure to aminergic neuromodulators such as serotonin (Harris-Warrick 2011). Neural circuits that comprise CPGs can function autonomous of sensory or descending inputs (Pulver *et al.* 2015b). The study of insects has led to advances in understanding unique aspects of motor programs including patterned motor output, sensory or descending inputs and the local control of musculature (Burrows 1996; Büschges *et al.* 2011).

Although it is possible to study neural circuits in *Drosophila melanogaster* (Wilson *et al.* 2004; Stockinger *et al.* 2005; Yu *et al.* 2010a; Ruta *et al.* 2010), historically it has been challenging due to the small size and inaccessibility of their neurons. However, the recent advent of advanced techniques to target, label and monitor physiological input and output has made *Drosophila* an excellent model to investigate the neurobiological basis of behaviors and the development of neural circuits (Pfeiffer *et al.* 2008, 2010; Pulver *et al.* 2009; Chen *et al.* 2013; Klapoetke *et al.* 2014; Heckscher *et al.* 2015; Nern *et al.* 2015). Furthermore, serial section Transmission Electron Microscopy (ssTEM) maps of neural connectivity (Saalfeld *et al.* 2009; Cardona *et al.* 2010; Cardona 2013; Takemura *et al.* 2013; Ohyama *et al.* 2015a; Schneider-Mizell *et al.* 2015; Berck *et al.* 2016a) and advanced computational 'ethomic' approaches to establish behavioral categories (Branson *et al.* 2009; Kabra *et al.* 2013; Vogelstein *et al.* 2014) will greatly aid future investigations.

With approximately 10,000-15,000 neurons (Scott *et al.* 2001), *Drosophila* larvae offer a relatively simple preparation for investigating neural circuit formation at single cell resolution. Considerable progress has been made in understanding larval and embryonic neurogenesis with markers of neuroblasts and progeny well characterized (Doe 1992; Schmid *et al.* 1999b; Birkholz *et al.* 2015; Harris *et al.* 2015). Recent anatomical studies show that many, if not all, interneurons of the ventral nerve cord (VNC) have a unique morphology (Rickert *et al.* 2011), and possibly unique molecular profile (Heckscher *et al.* 2014). Importantly, there are over 7,000 Gal4 lines generated by the Rubin lab (Jenett *et al.* 2012); we previously screened these lines for late embryonic expression, and identified several hundred expressed in sparse numbers of neurons within the VNC (Manning *et al.* 2012). These tools allow us and other researchers genetic access to the majority of interneurons within the VNC,

and allow us to characterize their role in late embryonic or newly hatched larval behaviors by expression of ion channels to silence neuronal activity (KiR; (Baines *et al.* 2001)) or induce neuronal activity (TrpA1; (Pulver *et al.* 2009)). By screening these Gal4 patterns for unique behavioral phenotypes it becomes possible to connect neuronal anatomy to neuronal function and development. Recent work in adults has used this approach to connect adult behaviors to their neurogenic origins in the late larva (Harris *et al.* 2015).

Drosophila larval locomotion is an excellent model to study patterned rhythmicity. Stereotypic movements include turns, head sweeps, pauses, and forward and backwards locomotion (Figure 1A) (Green *et al.* 1983). Larval forward and reverse locomotion is generated by abdominal somatic body wall muscle contractions moving from posterior to anterior (forward locomotion) or anterior to posterior (reverse locomotion) (Heckscher *et al.* 2012). Consecutive bouts of forwards or backwards waves are called runs (Figure 1B). Asymmetric contractions of thoracic body wall musculature generate turns (Lahiri *et al.* 2011). Neural control of turning movements is located within the thoracic segments of the VNC (Berni 2015) while the CPGs that drive larval locomotion have also been shown to be located in the thoracic and abdominal segments of the VNC (Berni *et al.* 2012; Pulver *et al.* 2015a). However, the specific neurons that comprise the CPG are currently unknown (Gjorgjieva *et al.* 2013). Similarly, little is known about the neurons specifically used in other aspects of locomotion, such as forward or reverse movements, head sweeps, and pauses.

Here we screen a collection of several hundred Gal4 lines that are sparsely expressed in the CNS to identify neurons that, when activated, can induce specific alterations in the larval locomotor program. The results presented here will provide the basis for future functional studies of motor control and neural circuit formation in the *Drosophila* larva.

Materials and Methods

Imaging Gal4 expression patterns in whole first instar larvae

For every Gal4 line we imaged whole newly-hatched "L0" first instar larvae, defined as between 0-4 hours of hatching, for native GFP fluorescence and nuclear red stinger fluorescence. We used a newly developed protocol to fix and stain intact larvae to confirm the expression pattern. Briefly, intact L0-L3 larvae were prepared for staining by incubation in 100% bleach for 10 min at room temperature (rt), digested with chymotrypsin/collagenase for 1 h at 37C, fixed in 9% formaldehyde for 30 min at rt, incubated in 1:1 methanol:heptane for 1 min at rt, and post-fixed in methanol for 1-3 days at -20C (L. Manning and CQD, in preparation). Subsequently, standard methods were used for staining with chick anti-GFP (1:2000; Aves) [43].

Bright-field whole larva behavioral recordings

All behavior was done using "L0" first instar larvae. Behavior arenas were made of 6% agar in grape juice, 2 mm thick and in 5.5 cm in diameter. Temperature was measured using an Omega HH508 thermometer with type K hypodermic thermocouple directly measuring agar surface temperature. Temperature was controlled using a custom-built thermoelectric controller and peltier device. The arenas were placed under a Leica S8APO dissecting microscope and red light (700 nm, Metaphase Technologies) illuminated a single larva. The microscope was equipped with a Scion1394 monochrome CCD Camera, using Scion VisiCapture software. Images were acquired via ImageJ at either 4 Hz for low magnification videos or 7.5 Hz for high magnification.

TrpA1 screen

Adult UAS-TrpA1 virgin females were crossed to males of select Janelia *CRM-Gal4* lines which were kept in standard collection bottles (Genesee Scientific) and allowed to lay eggs on apple caps with yeast paste. For low magnification screening, a single larva was staged on a behavior arena and given a 5-10 minute period of acclimation. For recordings, larvae were permitted to crawl freely, and the stage was manually re-centered when the larva left the field of view. Individual larvae were recorded at permissive (23ºC) and restrictive (28ºC) for 800 frames at 4 Hz.

Quantification of crawl parameters

We conducted two locomotion assays, low magnification for screening and high magnification in order to discern the etiology of crawl defects. For our initial low magnification screening, we calculated the speed of larval locomotion with automated analysis using custom Matlab scripts. Scripts were written in MATLAB and are available upon request. Object recognition. For low magnification tracking an individual larva was detected in each frame using the following steps. The image was mildly blurred using a Gaussian blurring function to reduce background artifacts and make the appearance of the larva more uniform. The built-in MATLAB thresholding function utilizing Otsu's method was used to segment the image. The image was then made binary and objects were morphologically closed. In each frame a single object was selected as the larva based on empirically determined and manually entered size. Built-in MATLAB functions were used to determine the larval object's area and centroid position in each frame. The script returned no data if more than one object was found or no object was found.

Crawling Speed. An approximate instantaneous speed was calculated by taking the distance traveled by the larval object between two consecutive frames and dividing by the time elapsed. All instantaneous speeds were then averaged to get an average crawling speed. If there was more than one behavioral recording for a given larva, data from up to three recordings were included. Standard deviation was then calculated. To exclude time points in which the larva appeared to travel large distances due to manual repositioning of larva during behavioral recording, if the distance traveled by the larval object between successive frames was farther than half the length of the larva (see below) then the frames were excluded from speed calculations.

Larval length. The mean area of the larva was averaged to get "LarvalLen"; then larval length was calculated as = sqrt(LarvalLen/3.14).

Normalized data. Normalized values (n) refer to values for a given larva at restrictive (r) temperature less the values for that larva at permissive (p) temperature, divided by values at permissive temperature ($n = (r-p)/p$).

Test statistics. Built-in MATLAB function was used to run a 1-tailed, t-test assuming equal means but unequal variance ('ttest2' function).

Representation of slow hits. To represent lines that exhibited crawling defects at restrictive temperature, we chose two criteria to define slow crawls. First were those that were slow at restrictive compared to controls (students t-test) and second those that did not increase their speed by the same rate when shifted from permissive to restrictive when compared to control (students t-test). Then average speed at restrictive was then divided by permissive.

High mag quantification. We manually calculated head sweeps, and forward and reverse wave propagation.

Fly Stocks

The following stocks obtained from the Bloomington *Drosophila* Stock Center (NIH P40OD018537) were used in this study: *10xUAS-IVS-myr::GFP* (BL #32198)*, UAS-RedStinger* (BL# 8546), *UAS-TrpA1* (BL #26263), D42-Gal4 (BL #8816), *OK6-Gal4* (Aberle, 2002), *Mef2-Gal4* (BL #27390), *repo-Gal4* (BL #7415), *elav-Gal4* (BL #8760), EL-Gal4 (Fujioka et al., 2003), *RN2-Gal4* (BL #7470), *CQ-Gal4* (BL #7466), *OK371-Gal4* (BL #26160), *GAD1-Gal4* (BL # 51630), *ple-Gal4* (BL# 8848), *trh-Gal4* (BL# 38389), *painless-gal4* (BL# 27894), *iav-Gal4* BL# (52273), *nan-Gal4* (BL #24903), *en-Gal4* (BL #1973), and *pBDP-Gal4.1Uw* in attP2 (gift from B.D. Pfeiffer). Flies were raised on conventional cornmeal agar medium at 25 °C.

Results

TrpA1 activation of sparse neuronal subsets results in slower, but not faster, larval locomotion

To identify neurons that can generate specific aspects of locomotor behaviors (pause, turn, forward, reverse, etc.), we screened Janelia *CRM-Gal4* lines containing sparse expression patterns at either embryonic stage 16 or in newly hatched "L0" first instar larvae (0-4h after hatching) (Figure 1C). We began with 7000 *CRM-Gal4* patterns; 4500 were screened at embryonic stage 16 with *UAS-nls::GFP* marking the cell nucleus, and 2500 were screened at first instar with *UAS-myr::GFP, UAS-RedStinger* labeling the cell membrane and cell nucleus.

From the initial 4500 we selected 75 patterns that had sparse expression patterns and entered them into the eNeuro atlas (Heckscher *et al.* 2014), which allows us to determine if they are motor neurons, interneurons, or glia. In addition to these 75 lines, we identified an additional 65 lines that had sparse embryonic VNC expression. A final 30 lines with sparse larval (L0) VNC expression were selected from the 2500 first instar expression patterns. We assayed newly hatched L0 larva behavior because it was closest in time to the stage where our Gal4 expression patterns were documented, making it less likely for the pattern to have changed; most embryonic Gal4 patterns are completely different by third larval instar (Manning *et al.* 2012; Jenett *et al.* 2012).

To assess the function of the neurons labeled by each of these Gal4 lines, we screened nearly 200 strains using the warmth-gated neural activator TrpA1 (Pulver *et al.* 2009). In our assay regime we monitored crawl speeds of individual newly hatched larvae at permissive temperature (23ºC) and then at restrictive temperature (28ºC). As with previous behavior experiments using JRC *CRM-Gal4* constructs (Vogelstein *et al.* 2014) we used larvae containing the 'empty' vector pBDP-Gal4U crossed to UAS-TrpA1 flies as our control; this transgene does not express TrpA1 in the VNC, and larva have normal locomotor velocities (Figure 1D, top). This is an appropriate control as the experimental Gal4 lines from the Rubin collection have a similar genetic background. We noted that control larvae increased their speed from 65.0 µm/sec at permissive temperature (+/- 47.0 SD, n=10) to 98.7 µm/sec at restrictive temperature (+/- 66.3 SD, n=10), or an increase of roughly 1.5 fold (Figure 1D, top).

Approximately 40 percent of lines we screened exhibited elements of crawl defects. We defined a genotype as slow by the following criteria: at restrictive temperature they were slower compared to controls (student t-test $p<0.05$) and normalized permissive to restrictive

change was statistically different (one-tailed student t-test $p<0.05$). Of those lines that were slow, approximately half had uniquely evocable behaviors that we describe below. We expected to elicit 'fast' crawl phenotypes, however, we only detected normal or slow phenotypes.

TrpA1 activation of sparse neuronal subsets generates multiple, distinct locomotor phenotypes

Control larvae on naturalistic terrain exhibit pauses, head casts, turns and forward and backward locomotion (Figure 1A,B) (Green *et al.* 1983; Riedl and Louis 2012), but in our assay they showed a strong bias towards forward locomotion, perhaps due to the temperature shift from 23°C to 28°C (Barbagallo and Garrity 2015) (Figure 2A,A'). Each of the *CRM-Gal4 UAS-TrpA1* lines we characterize below has a defect in the frequency or velocity of forward locomotion (Figure 1D, above), and in this section we describe each of the multiple, distinct locomotor phenotypes observed. We present the phenotype of one representative line in Figure 2, larval expression patterns for representative lines in each category are shown in Figure 3, and the cell type expression patterns for all lines in each category are shown in Figure 4.

Reverse

We found one line in this category: R53F07 (Figure 2B,B'). Whereas control larvae normally display a range of movements (Figure 1A,B), larvae in this category are strongly biased towards reverse locomotion. Forward propagating waves were generated occasionally, but they often failed to reach the anterior thoracic head region, instead switching prematurely to reverse waves.

Anatomical characterization shows both interneurons and motor neurons (Figure 3E, 4), but many other lines contained motor neurons without showing the reverse locomotion phenotype. We also did not observe expression in any sensory neurons such as the Bolwig organ or Class IV MD neurons, which have been shown to play a role in light mediated aversive response (Xiang *et al.* 2010). This suggests that the phenotype is due to activation of one or more interneurons in the pattern.

Immobile

We found 12 lines in this category, including R17C07 and 95A04 that showed expression only in interneurons (Figure 2E,E', 3G). Behavioral hallmarks of this category were loss of mobility with infrequent peristaltic waves. At times, some body wall segments appeared to lack tone and showing a smooth, elongated body shape (Figure 2E'). Larvae could move when prodded, however, distinguishing this category from the next two "paralysis" categories.

Anatomical characterization showed sparse interneuron expression as well as a few lines with additional sensory neuron, motor neuron, or muscle expression (Figure 3G, 4).

Rigid paralysis

We found 4 lines in this category, including R23A02 (Figure 2D,D'). Hallmarks of this category include immobility, tonic contraction of all body segments and shortening of larval body length. There was also a nearly complete lack of forward and reverse peristaltic waves. Larvae did not move when prodded.

Anatomical characterization shows lines that contained all body-wall muscles, all motor neurons or large subsets of interneurons (Figure 3A, 4). This last group includes lines that were

picked for our behavioral assay due to sparse numbers of interneurons in the late embryo, but ultimately showed greatly increased numbers of interneurons in newly hatched larvae.

Delayed paralysis

We found one line in this category: R55B12 (Figure 2E,E'). Larvae appeared identical to controls upon shifting to 28^{o}C, but over time exhibited full tonic contraction paralysis (Figure 2C'). Larvae are sometimes observed recovering from this paralysis but continue to cycle through paralysis periodically. Paralyzed larvae did not move when prodded.

Anatomical characterization showed expression of R55B12 restricted to neuropil "astrocyte" glia. A similar phenotype of "delayed paralysis" was obtained by crossing the glial-specific Repo-Gal4 line to UAS-TrpA1 and shifting to 28^{o}C (data not shown), confirming that the phenotype is due to glial activation.

Head cast

We found one line in this category: R15D07 (Figure 2F,F'). Larvae had a "zigzag" pattern of locomotion (Figure 2F) due to persistent head casting (Figure 2F'). Whereas control larvae normally exhibit head casts as part of their exploratory program (Gomez-Marin *et al.* 2011), larvae in this category exhibited continuous head casts during crawls. High magnification time-lapse analysis reveals that posterior to anterior body wall muscle waves characteristic of forward locomotion still occurred in larvae of this category, but the larva often initiated a head cast prior to completion of the wave of muscle contraction (data not shown).

Anatomical characterization showed expression in interneurons in the brain and VNC, plus dorsally projecting motor neurons (Figure 3D, 4). Because other lines contained dorsally

projecting motor neurons without showing the head cast phenotype, we suggest the phenotype is due to activation of brain or VNC interneurons.

Feeding

We found three lines in this category; line 76F05 is shown in Figure 2G. Hallmarks of this category were a bias towards feeding behavior, including pharyngeal pumping, rhythmic ingestion that can be observed as air bubbles entering the midgut through the esophagus (white triangles, Figure 2G'), and frequent mouth hook movements and head tilting (Melcher and Pankratz 2005; Hückesfeld *et al.* 2015). Larvae of one genotype (R21C06) do not move when at restrictive temperature and exhibited elements of the rigid paralysis phenotype while another (R59D01) exhibited a free range a movement while attempting to feed. The genotype expressing only interneurons (76F05) did not move, but showed normal range of motion of the head.

Anatomical characterization showed that all lines had a sparse pattern of interneurons in the brain and VNC (Figure 3H, 4); R21C06 showed additional expression in motor neurons, which is likely to be the cause of the additional rigid paralysis phenotype.

Dorsal contraction

We found 10 lines in this category; the R70H08 and R89F12 lines expressing only in sparse interneuronal patterns are shown in Figure 2H. This phenotype is characterized by the most anterior and posterior segments of the larva lifted vertically off the substrate when viewed laterally (Figure 2H'). The phenotype varies in severity with some larvae permanently stuck with their thoracic head region and tail lifted up. At times some continue crawling but

periodically become stuck in this position. This phenotype may arise from premotor interneurons stimulating dorsal projecting motor neurons, and we have confirmed that TrpA1-induced activation of just two dorsal projecting motor neurons, aCC and RP2, is sufficient to generate a "dorsal contraction" phenotype (RN2-Gal4 UAS-TrpA1; data not shown).

Anatomical characterization showed many lines that had dorsally-projecting motor neuron expression. Interestingly, there were lines that expressed in interneurons only and exhibited a similar phenotype (Figure 3C, 4). These interneurons are strong candidates for excitatory interneurons that directly or indirectly specifically stimulate dorsal-projecting motor neurons. We also found a line (R65D02) with muscle expression in dorsal acute and dorsal oblique muscle groups that gave a similar phenotype (data not shown).

Ventral contraction

We found 8 lines in this category; the R92C05 and R79E03 lines expressing only in sparse interneuronal patterns are shown in Figure 2I. Similar to the dorsal contraction phenotype, yet opposite in conformation, the ventral contraction phenotype was first discovered when we activated Gal4 patterns that expressed in ventrally projecting motor neurons (Nkx6, Hb9 and lim3B Gal4 lines; data not shown). When viewed laterally, the head and tail regions are ventrally contracted towards each other (Figure 2I'). Similar to the dorsal contraction postural phenotypes, we saw a spectrum of severity, with some continually stuck with tonically contracted ventral muscles, while others would go through bouts of ventral contraction, then can made attempts to crawl.

Anatomical characterization showed lines that had ventrally-projecting motor neuron expression. Interestingly, there were lines that expressed in interneurons only and exhibited a

similar phenotype (Figure 3F, 4). These interneurons are strong candidates for excitatory interneurons that directly or indirectly specifically stimulate ventral-projecting motor neurons. We also found two lines (R40D04, R33E02) with muscle expression in ventral acute, ventral oblique and ventral longitudinal muscle groups that gave similar phenotypes (data not shown).

Discussion

We identified a number of distinct behavior phenotypes elicited by activation of sparse subsets of neurons in the larval brain and VNC (Figure 5), but this is by no means an exhaustive exploration of TrpA1-induced larval phenotypes. As noted previously, roughly half of the statistically slow genotypes did not show any of the 'overt' phenotypic categories described in this paper. To fully characterize the remaining lines by phenotype would require advanced annotation of crawl dynamics and quantification of additional parameters. For example, upon high magnification observation of the slow hits, many simply appeared slow. Careful analysis by measuring wave duration and frequency may reveal additional phenotypes. Indeed, using refined analysis we investigated a slow line (R11F02) and discovered it was due to a defect in maintaining left-right symmetric muscle contraction amplitude during forward locomotion (Heckscher *et al.* 2015).

Recently developed larval tracking methods for multiplexed computational analysis would greatly assist the further definition of TrpA1-induced larval phenotypes. Examples of novel tracking methods include FIM, MaggotTracker, Multiple Worm Tracker and idTracker (Risse, Thomas, Otto, Lopmeier, *et al.* 2013; Vogelstein *et al.* 2014; Pérez-Escudero *et al.* 2014; Aleman-Meza *et al.* 2015). For example, MaggotTracker can characterize aberrations in run distance, duration, strides and many other abnormalities in crawl patterns not readily

identifiable by human eyes. A study from Vogelstein et al., used the optogenetic effector Channelrhodopsin and Multiple Worm Tracker to screen third instar *Drosophila* larval Gal4 patterns which yielded both fast and slow hits (Vogelstein *et al.* 2014). Using unsupervised machine learning they were further able to identify and cluster unique behavioral phenotypes or 'behaviotypes'. Post-hoc human analysis of these categories yielded four general categories consisting of still or back-up, turners, escape, turn-avoid and as many as 29 refined sub-type categories. Our study complements this investigation by describing additional categories, while also noting similar behaviotypes such as head cast or turn and immobile or still.

Many of the phenotypes we illustrated contained anatomical expression patterns with only interneurons, suggesting that those behavioral phenotypes were generated in the CNS. However, there were a large majority of lines that also expressed in tissues such as muscles, motor neurons, sensory neurons or glia. Many of these "off target" neurons can be discounted; for example, it is highly unlikely that motor neuron activation induces the head cast, reverse, or feeding phenotypes because our extensive tests of Gal4 lines driving TrpA1 in subsets of motor neurons never produced such phenotypes. Of course, motor neuron expression can lead to complex phenotypes, such as a combination of feeding + paralysis phenotypes (R21C06) or reverse + dorsal contraction phenotype (R53F07).

Some phenotypic categories contained single Gal4 lines, whereas some categories had multiple Gal4 lines that generated a particular behavior. The latter could be due to multiple lines expressed in a common neuron or pool of neurons -- or due to several different neurons being able to produce the same phenotype (e.g. premotor and motor neurons). Further characterization of the expression patterns of lines with similar phenotypes will be necessary to resolve this question.

In the future it will be important to define the neurons within each Gal4 line expression pattern that generates a specific motor pattern. *Drosophila* genetic techniques have made it possible to restrict expression of Gal4 patterns to successfully identify individual neurons that generate a behavior. For example, stochastic flipping (Flood *et al.* 2013; Tastekin *et al.* 2015), the FLP/FRT system (von Philipsborn *et al.* 2011; Sivanantharajah and Zhang 2015), and the split-Gal4 system (Luan, Lemon, *et al.* 2006; Aso *et al.* 2014; Bidaye *et al.* 2014) all allow subdivision of a Gal4 pattern. An intersectional technique has used the FLP/FRT system to successfully dissect the functional elements of the *fru* circuit (Yu *et al.* 2010b; von Philipsborn *et al.* 2011), and we recently used the split Gal4 system to identify a subset of functionally relevant interneurons governing muscle contraction amplitude during forward locomotion (Heckscher *et al.* 2015). Application of these methods should allow identification of the neuron(s) responsible for each of the eight locomotor phenotypes described in this paper.

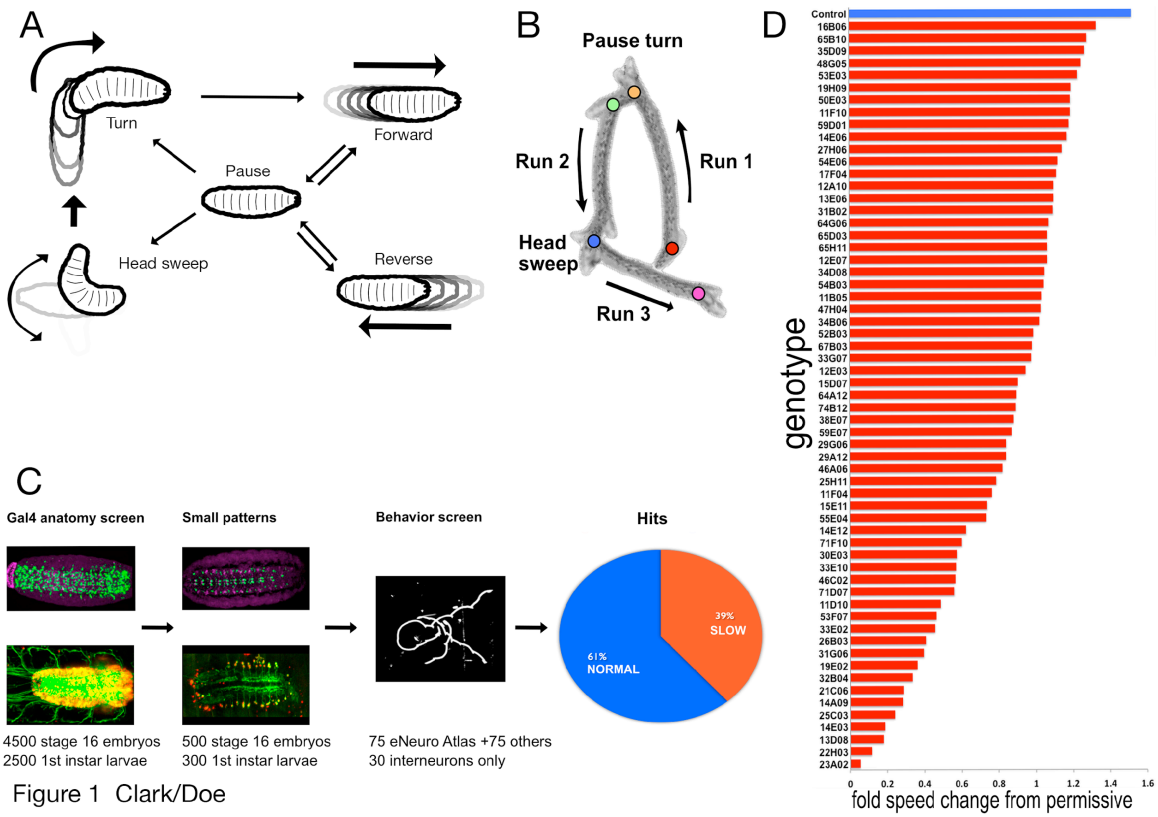

Figure 1. TrpA1 functional screen results and low magnification traces of crawl patterns.

(A) Ethogram of common behaviors during crawling (modified from reference 52).

(B) A time-lapse projection of a typical larval crawl pattern consisting of runs, pause turns and head sweeps.

(C) Initial screening of over 7000 Gal4 patterns yielded at least 700 Gal4 patterns with <15 neurons per hemisegment. 75 of these late stage embryonic Gal4 patterns were entered into eNeuro atlas and screened at first larval instar with ectopically expressed warm-gated cation channel UAS-TrpA1. An additional 100 *CRM-Gal4* expression patterns were screened with TrpA1 resulting in nearly 40% of those exhibiting crawl defects as shown in histogram of speed tracking.

(D) Tracking speed changes from permissive (23ºC) to restrictive (28ºC) yielded genotype-specific fold changes statistically slower when compared to controls (top blue). p-values for all represented in red was <0.05 (student's t-test).

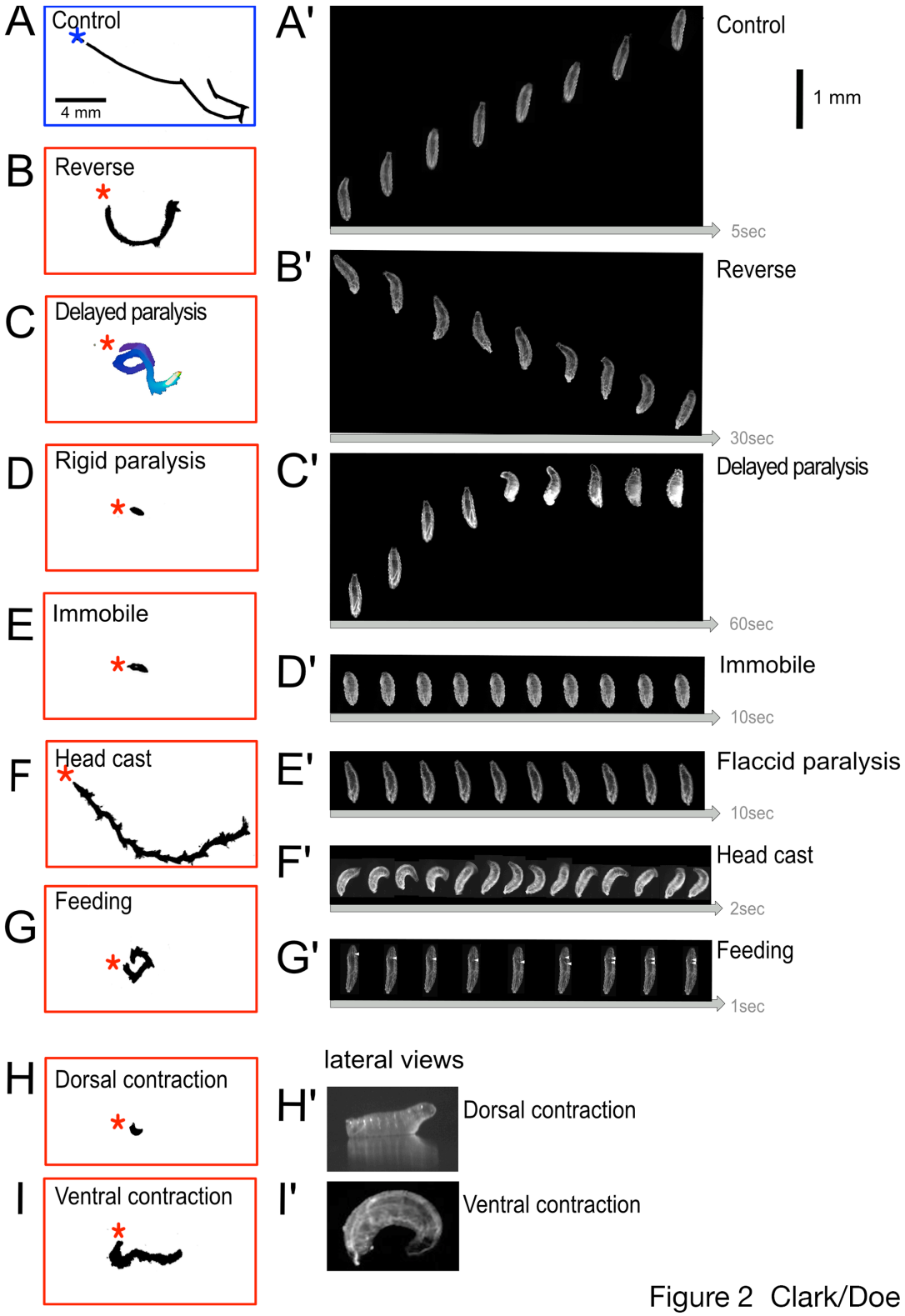

Figure 2 Clark/Doe

(see next page for legend)

Figure 2. Low and High Magnification Analysis of TrpA1-Induced Crawling Phenotypes. Representational traces of crawl trajectories for control (empty transgene cassette) and TrpA1-induced phenotypes of newly hatched larvae observed at low magnification (left) and high magnification still frames (right). Asterisk denotes beginning of crawl. Still frames from videos of larvae at restrictive temperature were taken at 7.5fps. Phenotype categories are indicated; distance scale bar applies to all right column panels, but each set of movie stills has a unique timeline (arrow at bottom of panel).

(A-A') Control. Larva demonstrates a typical crawl with runs and pause turns (left), while larva shown (right) travels ~4 μM in 5 seconds.

(B-B') Reverse. Larva successfully generates complete waves from anterior to posterior only. Translational movements occur strictly in the reverse direction.

(C-C') Delayed paralysis. Characterized by a free range of movements at restrictive, yet progressively slows until all segments are tonically contracted at 60 seconds.

(D-D') Rigid paralysis. All segments are fully contracted with no translational movement.

(E-E') Immobile. All segments are fully relaxed with no translational movement**.**

(F-F') Head cast. Crawl trajectory illustrates the 'back-and-forth' nature of movement. Peristalsis functions similar to controls, however before a peristaltic wave fully traverses from posterior to anterior, the larva has already begun a head sweep.

(G-G') Feeding. Characteristics of ingestion including pharyngeal pumping, mouth hook movement and head tilting. White arrow indicates rhythmic bubble ingestion (larva viewed ventrally).

(H-H') Dorsal contraction. Head and tail off the substrate illustrated in lateral view.

(I-I') Ventral contraction. Ventral contraction displays little movement and most extreme pictured is stuck ventrally curved.

Genotypes: (A) UAS-TrpA1/+; pBDP-Gal4U/+. (B) UAS-TrpA1/+; R53F07-Gal4. (C) UAS-TrpA1/+; R55B12-Gal4/+. (D) UAS-TrpA1/+; R23A02-Gal4. (E) UAS-TrpA1/+; R31G06-Gal4/+. (F) UAS-TrpA1/+; R15D07-Gal4/+. (G) UAS-TrpA1/+; R76F05-Gal4/+. (H) UAS-TrpA1/+; R26B03-Gal4/+. (I) UAS-TrpA1/+; R79E03-Gal4/+.

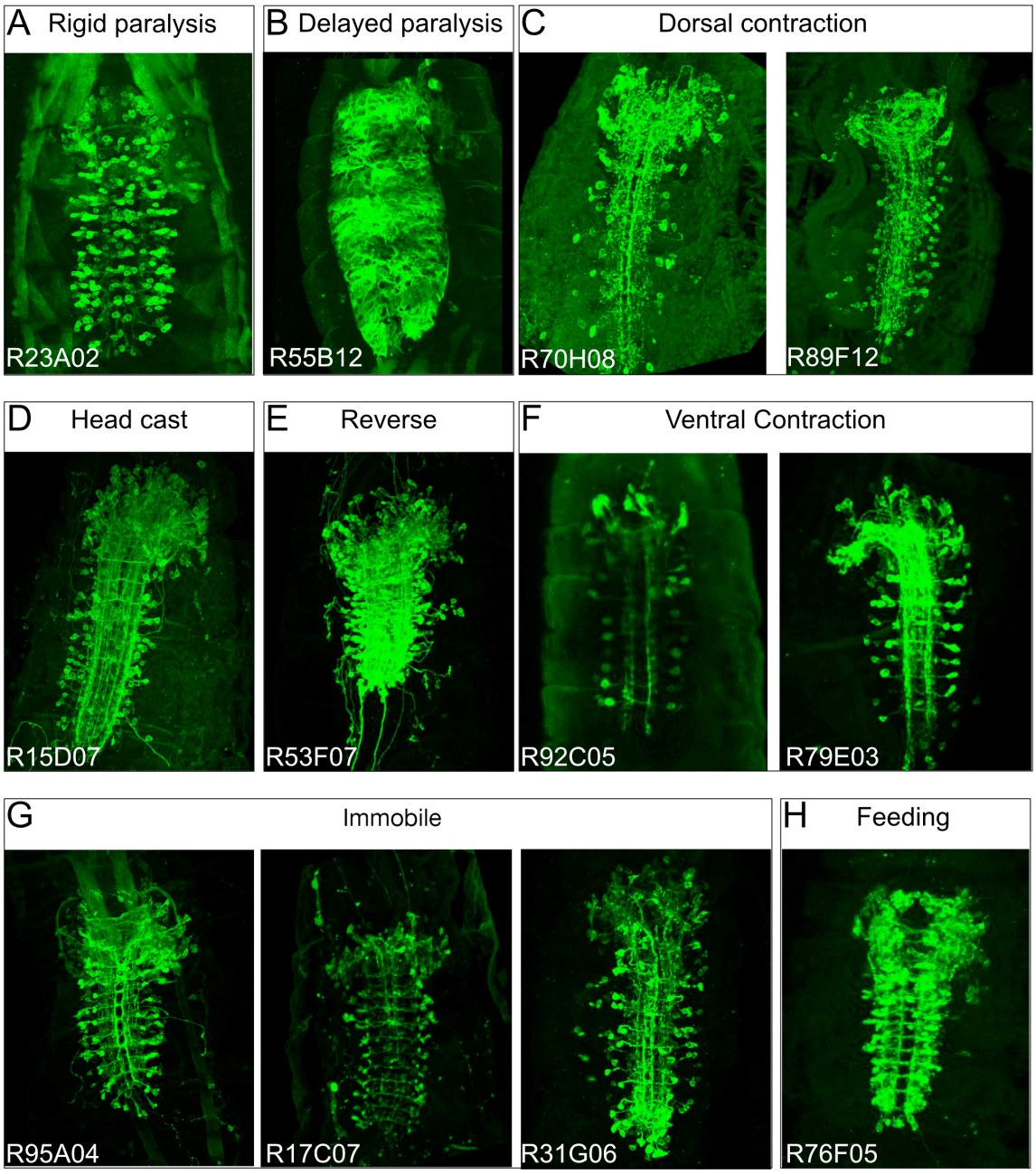

Figure 3 Clark/Doe

(see next page for legend)

Figure 3. Expression patterns for each phenotype group.
Ventral view of Z-stack projections for Gal4 patterns expressing membrane marker UAS-myr::GFP, except delayed paralysis, which is also expressing UAS-RedStinger to show cell nucleus. Anterior is up.
(A) Rigid paralysis. All lines expressed in interneurons and other tissues, with many expressing in all muscles.
(B) Delayed paralysis. Shown is one slice of z-stack to illustrate the reticulated nature of astrocyte glia in the VNC. Cell nuclei in red.
(C) Dorsal contraction. Lines shown are interneuron-specific.
(D) Head cast. This line expresses in interneurons and sporadically in dorsally projecting motor neurons
(E) Reverse. This line expresses in interneurons and in dorsally projecting motor neurons.
(F) Ventral contraction. Lines shown are interneuron-specific.
(G) Immobile. Lines shown are interneuron-specific, with the expression of 31G06 expressed in VO muscles.
(H) Feeding. One line is interneuron-specific; others express in interneurons as well as motor and sensory neurons.

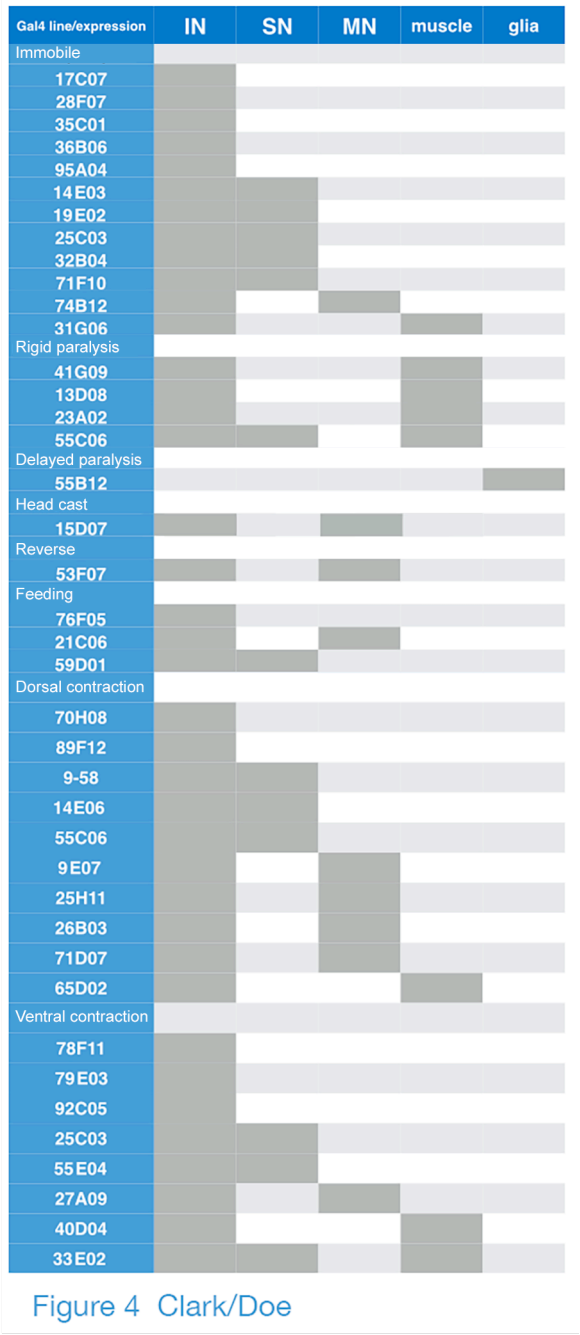

Figure 4. Gal4 line expression patterns in newly hatched larvae.
Left column indicates the Janelia Gal4 line name (nomenclature: Rxxxxx) and relevant phenotypic categories. Dark grey boxes to the right indicate cell type expression patterns of each Gal4 line: interneurons (IN), sensory neurons (SN), motor neurons (MN), muscle, and glia.

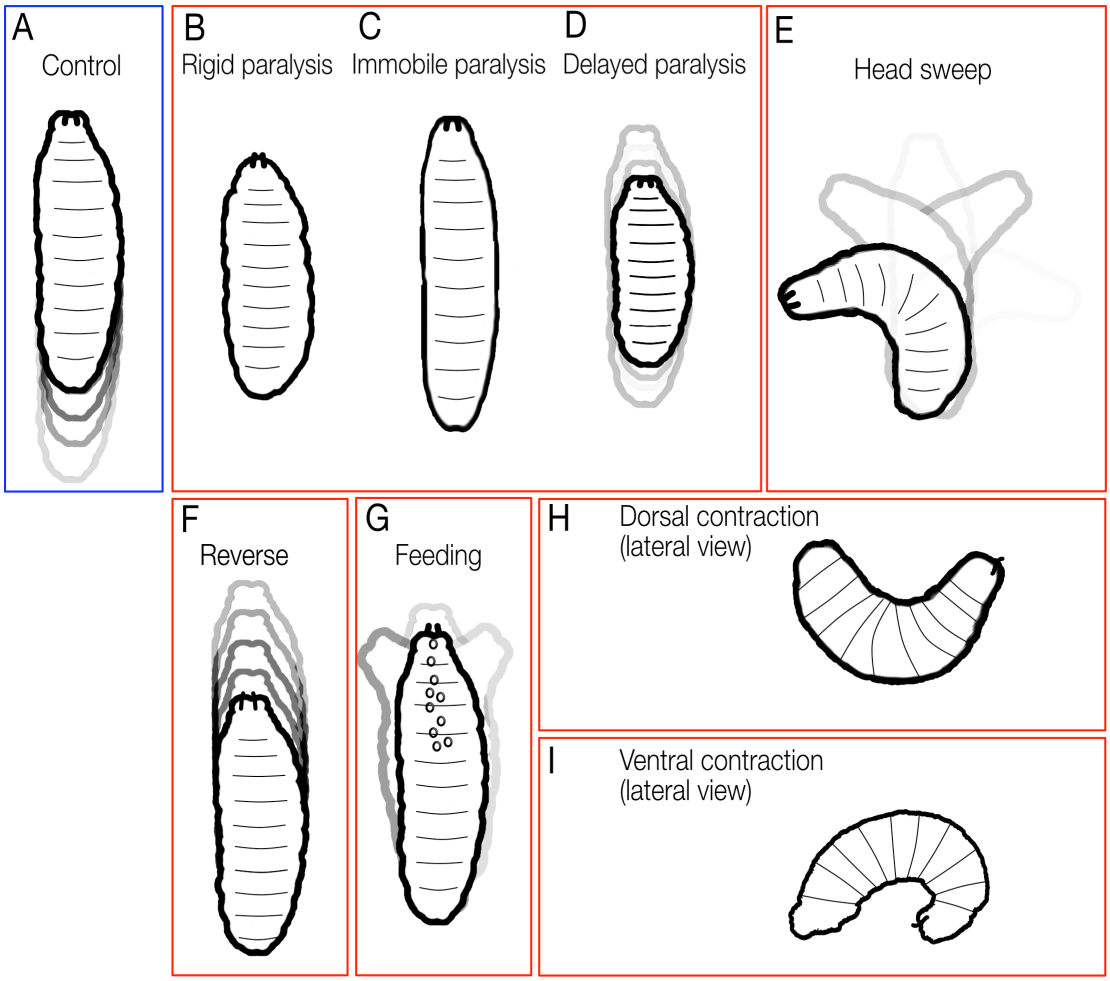

Figure 5 Clark/Doe

Figure 5. Summary of phenotypic groups.
(A) Control larvae have free range of motion, crawling for bouts of forward or reverse (left, blue box).
TrpA1-induced phenotypes bound in red (from left to right):
(B) Rigid paralysis: complete loss of mobility with all segments of the larval body wall muscles fully contracted.
(C) Immobile: complete loss of mobility with body wall segments often lacking tone, appearing smoothened and the larvae becoming languid and lengthened.
(D) Delayed paralysis: gradual slowing of crawl speed over time until finally becoming immobile with tonic contraction of body wall muscles.
(E) **Head cast:** head sweeps back and forth; can occur with thoracic/abdominal paralysis or with normal thoracic/abdominal peristaltic movements.
(F) Reverse: only backward peristaltic movements.
(G) Feeding: constant digging around with mouth hooks and attempts to ingest substrate. Frequent rhythmic ingestion of gaseous bubbles can be observed.

(H) Dorsal contraction: head and tail is raised off substrate.
(I) Ventral contraction: head and tail are curled ventrally toward each other.

BRIDGE TO CHAPTER III

In the previous chapter, we performed a screen. In the next chapter, we examined a pattern from the screen that yielded and interesting phenotype the ELs. The guiding hypotheses for my collaboration with Ellie Heckscher centered on understanding the genetic principles guiding neural circuit formation. Previously, Chris Doe and Ellie hypothesized that neural circuits are specified by 1) shared transcription factors expressed during neurogenesis that help build circuitry 2) the birth-order of neurons is important for wiring properties and 3) neuroblast lineage of origin confers a unique identity important for circuit formation.

At the onset of our collaboration I began screening for behaviorally relevant interneurons that we posited had at least one of these features. Previous graduate student Kat Reinhardt, who subsequently left to pursue other ventures, had piloted aspects of this project using the loss of function tool UAS-KIR2.1. We modified larval speed tracking software Ellie had developed for Kat, and I developed a behavior rig and assay to perform a loss-of-function screen using the neuronal inactivator UAS-Shi(ts1). Though I was able to find statistically significant slow lines, I felt the assay was not robust in yielding tractable findings. Accordingly, I began to assay using the neuronal activator UAS-dTrpA1 as highlighted in my G3 screen paper.

Using the defined GAL4 promoter HB9-GAL4 and Rubin GAL4 candidate lines predicted to target HB9+ INs (Heckscher et al. 2014) we sought to screen for recurring or common phenotypes. The large pattern of HB9-GAL4 made the problem difficult and activation of predicted HB9+ INs did not readily yield emerging themes. Following the transcription factor hypothesis (hypothesis number 1 above), I decided to

test the reagent EL-GAL4 with my assay. EL-GAL4 expresses in 8-10 even-skipped+ interneurons per hemisegment. Much is known about their development. For example, they are all born from the same neuroblast 3-3. However, nothing was known about their function. I was able to show with my gain of function tool altered crawl dynamics for the ELs. I wanted to show that these neurons were both necessary and sufficient for larval locomotion yet various loss-of-function tools proved unsuccessful. Testing through various loss-of-function tools (shibire, KiR, tnt, NpHR), I was finally able to ablate them by ectopically activating the cell apoptosis pathway by overexpressing UAS-reaper in combination with UAS-hid. Both gain-of-function and loss-of-function data comprised the majority of figures 1 and 2 of this publication.

Based on earlier work from the laboratory of Richard Baines (Pym et al., 2006) I hypothesized that loss of eve in the ELs would cause altered electrical properties, which we could observe as altered crawl dynamics. Indeed, further work from Ellie has shown this to be true. Additional collaborative work we had planned, and she has completed includes the activation of the ELs during a free crawl while observing the activity via GCaMP. Using this assay, she has shown these neurons balance muscle symmetries by responding to sensory cues.

CHAPTER III

EVOLUTIONARILY-CONSERVED EVEN-SKIPPED^{+} INTERNEURONS ARE A CORE COMPONENT OF A SENSORIMOTOR CIRCUIT THAT MAINTAINS LEFT-RIGHT BALANCED MOTOR OUTPUT

Reproduced with permission from Heckscher, E.S., Zarin, A.A., Faumont, S., Clark, M.Q., Manning, L., Fushiki, A., Schneider-Mizell, C.M., Fetter, R.D., Truman, J.W., Zwart, M.F., Landgraf, M., Cardona, A., Lockery, S.R., Doe, C.Q. (2015). Even-Skipped(+) Interneurons Are Core Components of a Sensorimotor Circuit that Maintains Left-Right Symmetric Muscle Contraction Amplitude. Neuron **88(2)**: 314--329. Author contributions: MQC devised behavioral assay and demonstrated altered crawling phenotypes in gain-of-function and loss-of-function backgrounds, contributed to the planning and development of the project and helped revise the manuscript. ESH co-wrote the manuscript, did behavioral and calcium imaging experiments as well as analysis. SF and SRL contributed to the Ca^{2+} imaging experiments. AAZ did Chrimson experiments. LM characterized *EL-gal4* expression. HL and JT generated third instar single neuron MCFO data and named the A08 neurons. TEM reconstruction was done by AAZ, AF, CQD, CSM, MZ, ML and AC. CQD guided the project and co-wrote the manuscript.

Summary

Bilaterally symmetric motor patterns—those in which left-right pairs of muscles contract synchronously and with equal amplitude (e.g., breathing, smiling, whisking, locomotion)—are widespread throughout the animal kingdom. Yet surprisingly little is know about the underlying neural circuits. We performed a thermogenetic screen to identify neurons required for bilaterally symmetric locomotion in *Drosophila* larvae, and identified the evolutionarily-conserved Even-skipped^{+} interneurons (Eve/Evx). Activation or ablation of Eve^{+} interneurons disrupted bilaterally symmetric muscle contraction amplitude, without affecting left-right synchronous timing. GCaMP6 calcium

imaging in isolated brains and freely-moving larvae shows Eve^+ interneurons can be left-right asymmetrically activated, which correlates with motor output and behavior. TEM reconstruction places the Eve^+ interneurons at the heart of a sensorimotor circuit capable of detecting and modifying body wall muscle contraction. Our results establish a new system for investigating neural mechanisms underlying bilaterally symmetric locomotion at molecular, developmental, circuit, and behavioral levels.

Introduction

Bilaterally symmetric motor patterns—those in which muscle contractions on the left and right sides of the body occur synchronously and with equal amplitude—are widespread throughout the animal kingdom. They regulate respiration, speech, smiling, whisking, flight, and various locomotor gaits. Surgical manipulations in both vertebrates and invertebrates have shown that contralaterally-projecting, commissural interneurons are required for bilaterally symmetric motor output, demonstrating that this is not merely a default state (Dubayle and Viala, 1996; Jahan-Parwar and Fredman, 1980; Lanuza et al., 2004; Murchison et al., 1993; von der Porten et al., 1982). In the mouse, genetic deletion of $Dbx1^+$ interneurons resulted in left-right asynchronous motor output during respiration and perinatal lethality (Bouvier et al., 2010). Genetic deletion of $Dbx1^+$ affects a subpopulation of ventral, $Evx1^+$ interneurons; more specific loss of just the dorsal, $Dbx1^+$ interneurons, which did not affect the ventral, $Evx1^+$ interneurons had no effect on breathing. Taken together these data implicate $Evx1^+$ interneurons in regulating respiratory motor rhythms (Bouvier et al., 2010). However, this interpretation is clouded by the observation that mice lacking Evx1 appear to breathe normally (Moran-Rivard et al., 2001). These findings demonstrate how little we understand about the molecules and

neural circuitry underlying bilaterally symmetrical motor output, despite their broad and essential functions.

Drosophila larval crawling is one of the few genetically tractable model systems for investigating the molecular and neuronal underpinnings of symmetric motor output. Larval crawling is a simple, robust motor behavior that involves waves of rhythmic, bilaterally symmetric body wall muscle contractions (Heckscher et al., 2012). The segmented larva has ~30 bilateral body wall muscles per segment and a similar number of motor neurons, and their role during larval locomotion has been characterized (Berni et al., 2012; Crisp et al., 2008; Crisp et al., 2011; Dixit et al., 2008; Heckscher et al., 2012; Hughes and Thomas, 2007; Lahiri et al., 2011; Pulver and Griffith, 2010; Schaefer et al., 2010). In contrast, there are ~270 bilateral interneurons per segment, and their role in locomotion is virtually unknown (Kohsaka et al., 2014). Recently, we identified several hundred Gal4 lines that express in a sparse pattern of neurons (1-10 per hemisegment) in the late embryonic CNS (Manning et al., 2012), and we determined the expression pattern at single neuron resolution for 75 of these lines (Heckscher et al., 2014). We use this collection of sparsely-expressed Gal4 lines to express the warmth-activated TRPA1 cation channel, which allows us to transiently and reversibly induce neural activity in well-defined, sparse patterns of identified interneurons. We screened for interneurons that, when activated, disrupted larval locomotion (Clark, et al., in preparation). Here we focus on a small pool of interneurons ("ELs") that express the evolutionarily conserved homeodomain transcription factor Even-skipped (Eve; Evx1/2 in mammals).

Eve/Evx^{+} interneurons are found in the nerve cord of almost all bilateral animals examined to date, including annelids, chordates, insects, fish, birds and mammals, as well

as the presumed last common ancestor between invertebrates and vertebrates, the bristleworm (Avaron et al., 2003; Copf et al., 2003; Denes et al., 2007; Ferrier et al., 2001; Holland, 2013; Ikuta et al., 2004; Moran-Rivard et al., 2001; Sordino et al., 1996; Takatori et al., 2008; Thaeron et al., 2000). In the cases where the morphology of Eve/Evx^{+} interneurons has been examined, morphological features are conserved (**Figure 1A**). In flies, in addition to expression in a small pool of EL interneurons, Eve is expressed in seven pairs of motor neurons per segment in the nerve cord, but no cells in the central brain express Eve (Frasch et al., 1987). The Eve/Evx transcription factor is well known to specify neuronal identity and regulate axon pathfinding in fly and worm motor neurons as well as in mammalian interneurons (Broihier and Skeath, 2002; Doe et al., 1988; Esmaeili et al., 2002; Fujioka et al., 2003; Landgraf et al., 1999; Moran-Rivard et al., 2001; Zarin et al., 2014). However, despite years of intense study the behavioral role for Eve/Evx^{+} interneurons remains undefined. Our data support the hypothesis that ELs are part of a "perturbation-compensation" circuit that controls the left-right balance of muscle contraction amplitude during linear crawling in *Drosophila* larvae.

Results

The EL interneurons are required for left-right symmetric larval locomotion

We used a collection of Gal4 lines that sparsely label neurons in the late embryonic CNS (Heckscher et al., 2014; Manning et al., 2012) to express the warmth-activated cation channel TRPA1 (Pulver et al., 2009). We screened newly hatched larvae for defects in locomotion following activation of TRPA1 (28^{o}C) that were reversed following inactivation of TRPA1 (23^{o}C). We identified many pools of interneurons

whose activation induced a variety of phenotypes: slow crawling, turning, or phenotypes similar to activation of known motor neuron populations (Clark, et al., in preparation). Here we focus on interneurons whose activation disrupts left-right symmetrical locomotion, as judged by slow locomotion and 'wavy' body posture (**Figure 1**).

One group of interneurons that results in slow locomotion and 'wavy' body posture upon activation is the evolutionarily conserved Eve^{+} lateral interneurons ("ELs"). In flies ELs project contralaterally and rostrally like their homologs in fish (CoSAs) and mouse (V0vs) (Moran-Rivard et al., 2001; Suster et al., 2009)(**Figure 1A**). Because in mice V0vs are excitatory (Moran-Rivard et al., 2001), we asked whether in fly ELs are excitatory. ELs do not express markers for neuropeptides (Heckscher, 2015). Using both genomic reporters and antibodies for the three major insect neurotransmitters: glutamate, acetylcholine or GABA we find most ELs are cholinergic; a single EL is often, but not always labeled by GABAergic markers (Fig S1). We conclude that a majority of ELs are cholinergic, and therefore likely to be excitatory similar to mammalian Evx^{+} interneurons.

To understand the role of EL interneurons in regulating larval locomotion, we used the *EL-Gal4* line on the third chromosome (Fujioka et al., 1999) that has specific and reproducible expression in all but one EL as well as expression in few, variable, off-target cells (**Figure 1B**). Normally, first instar larvae crawl forward or backward with a linear posture at both 23°C and 28°C, although they crawl faster at the higher temperature (Heckscher et al., 2012). First instar larvae expressing TRPA1 in the ELs showed normal linear crawling at 23°C (**Figure 1C**; Movie S1**)**. Raising the temperature to 28°C to activate TRPA1 and induce EL activity resulted in slow a crawling phenotype (Table S1).

Importantly, activation of ELs leads to a profound defect in left-right symmetric body posture including pronounced C-bends (**Figure 1C-D,** Movie S2). Activation of ELs in the absence of heat using optogenetic simulation also resulted in pronounced C-bends at later larval stages (**Figure 1E,** Movies S3-4). C-bends are different from normal larval turning because they can occur in posterior segments, whereas larval turning is performed by anterior segments (Berni, 2015; Lahiri et al., 2011). We conclude that bilateral activation of EL interneurons is sufficient to disrupt left-right symmetric locomotion.

Next, to determine whether EL interneurons are necessary for normal locomotion, we asked whether removal of ELs from the larval CNS had a locomotion phenotype. We used *EL-Gal4* to drive expression of the pro-apoptotic Hid/Reaper proteins to ablate the interneurons. This manipulation removed all but one EL per hemisegment (**Figure 2A-B**). Interestingly, similar to EL activation, ablation of the ELs led to slow crawling speeds and "wavy" body posture, including C-bends (**Figure 2C-E,** Movie S5). Because ablation removes statistically similar numbers of ELs from the right and left sides of the nerve cord (**Figure 2B**), and because C-bends can occur in both directions within the same animal (**Figure 2C**), we conclude that bilateral ablation leads to a randomized asymmetric crawling phenotype. To our knowledge the EL interneurons are the first neurons that are required to ensure bilaterally symmetric locomotion in any system. Although EL interneurons are present only in the nerve cord, the *EL-Gal4* line can stochastically express in a few cells in the brain (Figure S2). To test whether ablation of these brain neurons caused locomotion defects, we used *tsh-Gal80* (Clyne and Miesenbock, 2008) to inhibit *EL-Gal4* in the nerve cord but not in the brain. We found that ablation of the *EL-Gal4* neurons in only the brain had no locomotion phenotype

(**Figure 2E**). We conclude that the Eve^{+} ELs within the nerve cord are required for bilaterally symmetrical crawling in *Drosophila* larvae, and thus the normal function of EL interneurons is to maintain symmetric left-right muscle contractions during linear locomotion.

EL interneurons are required to match left-right muscle contraction amplitude without affecting left-right muscle contraction timing

There are two ways in which EL interneurons could generate asymmetric larval locomotion: either by disrupting left-right symmetric muscle contraction amplitude, or by disrupting left-right synchronous muscle contraction timing. We quantified larvae for muscle contraction timing, muscle resting length, and maximum contraction amplitude using the pan-muscle marker MHC:GFP. We found that control, EL ablation, and EL activation larvae all showed synchronous timing of left-right muscle contractions (**Figure 3**, Table S2). These findings indicate that EL interneurons do not impact the proper timing of left-right motor output.

We next measured left-right muscle contraction amplitude. As expected control larvae showed bilateral symmetry in resting muscle length and maximum contraction amplitude (**Figure 3A**, Movie S6, Table S2). In contrast, both EL ablation and EL activation showed significant left-right differences in resting muscle length and maximum muscle contraction amplitude during forward locomotion (**Figure 3B-C**, Movie S7-8, Table S2). We conclude that the EL interneurons are required to maintain bilaterally symmetric muscle contraction amplitude, both at rest and during active muscle contraction. To our knowledge, these are the first neurons shown to have this function in

any organism, and this finding raises the possibility that the highly conserved Evx^+ interneurons may have similar functions in other animals (see Discussion).

Calcium imaging reveals interactions among EL interneurons

To characterize the neural circuit containing the EL interneurons, we asked how ELs respond to bilateral activation. We expressed the thermogenetic activator, TRPA1 and the calcium sensor GCaMP6m in ELs. We imaged isolated CNS preparations to reduce movement artifacts and eliminate sensory input (**Figure 4A**). The EL responses to bilateral stimulation fell into three groups (**Figure A-C**, i-iii). The most commonly observed group showed a left-right asymmetric response profile: on one side, either left or right at random, the ELs were strongly activated (bright side) whereas the ELs on other side were weakly activated (dim side). At stimulus offset the response reliably switched sides, with the initially dim side becoming brighter (**Figure 4B-C** i, n = 10, Movie S9). The second group showed bilaterally symmetrical activity that was low during stimulation and increased at stimulus offset (**Figure 4B-C** ii, n = 6). The third group also showed a bilaterally symmetrical response whose dynamics followed the TRPA1-induced stimulus (**Figure 4B-C** iii, n = 6). Notably in all three groups the response profile of ELs on the left and right sides were in synch with each other (**Figure 4A-C**). We conclude that there are functional interactions within the population of EL interneurons: invariably ipsilateral ELs are coupled, whereas left-right EL interneurons can show asymmetric or symmetrical activation (see Discussion).

Calcium imaging in intact, freely-moving larvae provide functional evidence that EL

interneurons are part of a sensorimotor circuit

To determine whether left-right asymmetrical activation of EL interneurons can occur *in vivo*, we extended our calcium imaging to intact, freely moving larvae. We expressed both TRPA1 and GCaMP6 in ELs, and imaged larvae held chronically at high temperature for ~2 minutes. We saw epochs of left-right asymmetric EL activity in 100% of the larvae recorded (n=5) (**Figure 5A**). We this supports the idea that *in vivo* EL interneurons can be asymmetrically activated.

Next, we asked whether left-right asymmetrical EL interneuron activity has a correlated motor response. We repeated the experiment above using a low-power objective to measure the left-right EL calcium signal while simultaneously monitoring body position using weak the autofluorescence of the larvae. The relationship between EL calcium signal and body position was complex (data not shown), so we focused our analysis on epochs where the left-right asymmetrical EL activation switched from high on one side of the midline to high on the other. We selected ten epochs that contained the largest switches in left-right EL activity (without attention to the behavioral data) and aligned the traces to the moment EL activity switched from highest on left to highest on right, or vice versa (e.g., **Figure 5B-D**, Movie S10). In each of these ten cases, we found that a switch in activation of EL activity was accompanied by contralateral muscle contraction, as inferred from larval body bending (**Figure 5E**). We conclude that large left-right switches in EL interneuron activation have a behavioral correlate: contralateral larval body bending.

In intact animals left-right switches in EL interneuron activation occurred multiple times even though the temperature was constant (**Figure 5A**). In contrast, left-right

switching of EL activation was never observed at constant high temperature within an isolated CNS (**Figure 4A-C**). This is consistent with the idea that sensory input present only in the intact larval preparation triggers left-right switching by modifying EL activity. Thus, we hypothesize that ELs receive sensory input. The alternative hypothesis is that ELs receive central input, and below we test this alternative hypothesis. We expressed GCaMP6 in ELs, or—as a control, in motor neurons, whose activity should be driven by the central pattern generator (CPG) for locomotion. We made isolated CNS preparations to remove sensory input and imaged spontaneous neuronal activity. As expected, we observed locomotion-like activity in motor neurons, finding at least one robust posterior to anterior wave of activity in over 40% of preparations (Figure S3**,** Movie S11). In contrast, we never observed organized waves of activity in ELs, although we saw spontaneous activity of individual ELs (Figure S3, Movie S12). We conclude that ELs are neither part of the CPG for locomotion, nor do they receive central input from the locomotor CPG; these observations support the hypothesis that EL interneurons require sensory input for their activation.

Identification of individual EL interneurons by light and electron microscopy

Our functional data support the hypothesis that EL interneurons are part of a sensorimotor circuit that regulates muscle contraction amplitude. To gain a more complete view of the network context in which the ELs operate, we identified their pre- and post-synaptic partners using the "gold standard" transmission electron microscopy (TEM) analysis for tracing anatomical connectivity. Because TEM reconstruction of neuronal morphology and connectivity is laborious, before attempting to reconstruct all

ELs we asked whether we could identify, and thus reconstruct a smaller subset of functionally important ELs. We used a previously identified transgene, R11F02 line that is expressed in a subset of ELs (Heckscher et al., 2014). We combined R11F02-gal4^{AD} and EL-gal4^{DBD} lines to label only the R11F02^{+} EL^{+} double positive neurons (here after referred to as 11F02 ∩ EL interneurons), which labeled just five ELs per hemisegment (**Figure 6A**). Activation of these five neurons produced a similar phenotype as that seen when activating all ELs with EL-Gal4 (**Figure 6B-C,** Movie S13-14). We conclude that the 11F02 ∩ ELs are functionally relevant elements of the EL interneuron circuit that maintains left-right balanced locomotion.

To identify individual 11F02 ∩ EL interneurons using TEM, we determined both the shared and distinct features of 11F02 ∩ ELs. Shared features include: adjacent cell bodies in a characteristic position within the CNS (ventro-lateral near the anterio-posterior border of each segment), a common proximal axon fascicle, and neural processes that project across the midline through the anterior commissure (**Figure 6A**). To determine the unique features of each 11F02 ∩ EL, we used multicolor flip-out (MCFO) (Nern et al., 2015) to visualize the morphology of single interneurons within the 11F02 ∩ EL population. We found three neurons with local contralateral projections (A08e1-3, hereafter local ELs) and two neurons with contralateral projections ascending to the brain (A08c, A08s; **Figure 6D**). The 11F02 ∩ ELs can be distinguished from each other based on a unique pattern of neural arbors (**Figure 6D,** Table S3). We conclude that each 11F02 ∩ EL interneuron has a distinctive morphology, giving us template "ground truth" images with which to search the TEM volume for morphologically identical interneurons.

By matching features of each 11F02 ∩ EL interneuron seen by light microscopy we identified their cognate interneurons in TEM reconstructions. We reconstructed 11F02 ∩ ELs in two different TEM volumes: a slightly younger "Larva 1", in which the TEM dataset includes the entire CNS, and a slightly older "Larva 2", in which the TEM dataset contained only segment A3. In Larva 1 we reconstructed all five 11F02 ∩ ELs in the left and right sides of segment A1 (**Figure 6E)**, and many of the neurons in segments A2-A3 (**Figure 6G-H**); in Larva 2 we reconstructed the three local ELs in the left and right sides of segment A3 (**Figure 6F**). For a given 11F02 ∩ EL (e.g. A08e3) we observed a stereotyped morphology from larva to larva, segment to segment and on left and right sides (**Figure 6E-I**). We conclude that we identified all 11F02 ∩ EL interneurons using TEM reconstruction.

Mono- and di-synaptic proprioceptive inputs into EL interneurons

Because we hypothesize that EL interneurons function as part of a sensorimotor circuit, we used TEM to test for direct sensory-EL connectivity. This is possible because all of the sensory neurons in Larva 1 and Larva 2 have been previously identified (Ohyama et al., 2015). In *Drosophila* there are several sensory modalities: e.g., mechanosensation, nociception and proprioception (Singhania and Grueber, 2014). Strikingly, we found that both local and projection ELs received strong direct input from proprioceptive neurons; in contrast ELs received little other direct sensory input **(Figure 7A,C)**. Interestingly, dorsal (e.g., dbd) and ventral (e.g. vbd) proprioceptive inputs into the ELs are segregated (**Figures 7A,D**, S4). Proprioceptive input into the 11F02 ∩ ELs was highly reproducible from segment to segment and larva to larva; for example vbd

invariably formed synapses within the same arbor domains of A08e3 in all hemisegments examined (e.g., **Figure 7D**). We conclude that proprioceptive sensory neurons form monosynaptic connections with 11F02 ∩ ELs, providing the opportunity to transduce body wall contraction information to the EL interneurons.

Although EL interneurons have a large number (~60) of synapses with proprioceptive sensory neurons, this accounts for less than 10% of the total synapses onto the ELs (**Figure 8B**). Thus we asked what other inputs do ELs receive? Unlike sensory neurons, interneurons in the TEM volume have not been fully reconstructed or annotated for synaptic partners. Rather than reconstruct and annotate the connectivity for all 11F02 ∩ EL presynaptic partners, which is far beyond the scope of this study, we reconstructed interneurons that formed multiple synapses within a restricted domain of an EL interneuron arbor, thereby preferentially identifying interneurons that make multiple synaptic contacts with ELs. We identified two interneurons with a large number of synapses onto the 11F02 ∩ ELs, and named them HMD1 and HMD3 (**Figure 8A)**; HMD2 is similar in morphology and proprioceptive inputs, but connects to the EL interneurons indirectly via HMD1 (**Figure 8A, inset**). Together HMD1 and HMD3 provide 50-75 additional input synapses onto local ELs (~8% of the total synaptic input, **Figure 8B**). We conclude that the HMD interneurons are major presynaptic partners of local 11F02 ∩ EL interneurons.

To gain insight into the type of information that HMD interneurons could provide to EL interneurons we examined the inputs to the HMDs. Strikingly, over 35% of HMD input synapses come directly from proprioceptors with no other direct sensory input (**Figure 8B**). The network topology from proprioceptors to HMDs is complex (**Figure**

8A). Interestingly, in contrast to the distributed nature of proprioceptor to HMD connectivity, HMD to EL connections display synapse specificity. HMD1 forms synapses with A08e1; HMD3 forms synapses with A08e2; there are no HMD to A08e3 synapses (**Figure 8A,C**). We conclude that there is a multi-synaptic proprioceptor to EL pathway providing further opportunity for the transduction of body wall contraction information to the EL interneurons.

Mono- and di-synaptic output from EL interneurons to motor neurons

Because activation of EL interneurons results in altered muscle contraction, ELs must influence the activity of motor neurons either directly or indirectly. Using TEM reconstruction, we tested for direct connectivity between 11F02 ∩ EL interneurons and motor neurons, which is possible because nearly all motor neurons in A1 of Larva 1 and A3 of Larva 2 have been fully identified (by us for this study or previously, (Ohyama et al., 2015). In both TEM reconstructions from Larva 1 and Larva 2 we find direct synaptic connections between all local ELs and contralateral dorsally-projecting motor neurons (**Figure 7A,D-E,** data not shown). We conclude that local ELs have monosynaptic connectivity to a specific subset of motor neurons, providing the opportunity for EL interneuron activity to influence motor output.

Because EL interneurons have only a modest number of output synapses with motor neurons (~3% total output), we asked what other interneurons could receive information from the ELs (**Figure 9B).** We reconstructed interneurons that receive input from local ELs, and neurons that showed multiple inputs within the same domain were fully reconstructed. In this way we identified two interneurons with a large number of synapses (~50, or 10% of total output) from local ELs, which we named AAZ1 and

AAZ2 (**Figure 9**). Notably, all three local ELs make contralateral contacts with both AAZs; moreover these contacts converge onto a relatively small region with the contralateral arbor of each AAZ (**Figure 9A,C**). We conclude that AAZ interneurons are major outputs of 11F02 ∩ EL interneurons.

To understand the significance of synaptic contacts from local EL interneurons to AAZ interneurons, we reconstructed neurons receiving the greatest amount of synaptic input from the AAZs. We found that both AAZs make a large number (~150, or ~20% total output) of output synapses to all three classes of motor neurons (those with projections to dorsal, ventral, and lateral/transverse muscles) (**Figure 9A**). Interestingly, whereas the 11F02 ∩ ELs form direct monosynaptic connections with motor neurons that project to the contralateral muscle field, the disynaptic EL-AAZ-motor neuron pathway connects 11F02 ∩ ELs with ipsilateral motor neurons (**Figure 9A**); We conclude that the ELs could regulate motor neuron output via at least two pathways: a monosynaptic, contralateral pathway and disynaptic, ipsilateral pathway (see Discussion). Overall, our anatomical data shows EL interneurons positioned at the heart of a sensorimotor circuit that is suited for detecting and modifying body wall muscle contraction.

Discussion

Drosophila larvae: a model system for investigating left-right symmetric motor output

Bilaterally symmetric motor patterns—those with muscle contractions on the left and right sides of the body occurring synchronously and with equal amplitude—have broad and essential functions. Despite the nearly ubiquitous use of bilaterally symmetric

motor patterns throughout the animal kingdom we understand surprisingly little about the neural circuitry underlying bilaterally symmetric motor output. Here we introduce a new model system in which to study this important motor pattern: *Drosophila* larval crawling. We conducted a behavior screen and identified a set of evolutionarily conserved interneurons (see below), the Even-skipped^{+} interneurons ("ELs") that are required to produce symmetrical motor output. Ablation or activation of ELs prevents the larva from maintaining left-right matching muscle contraction amplitudes without affecting the left-right synchronous timing of muscle contraction (**Figures 1-3**). To our knowledge, the ELs are the first identified interneurons to be specifically involved in regulation of muscle contraction amplitude. Further our data show that the amplitude and synchrony of left-right muscle contraction can be independently regulated.

In mouse the V3 interneurons have been implicated in establishing a robust and balanced locomotion rhythm during walking (Zhang et al., 2008). Similar to the ELs, V3 interneurons are excitatory and project across the midline and thus provide the opportunity for communication between left and right sides of the nerve cord. In the future, it will be interesting to examine muscle contraction amplitude in "V3 mutant" mice to determine whether this class of neuron is responsible for balancing amplitude of left-right muscle contraction during alternating motor patterns such as vertebrate walking.

EL interneurons are part of a sensorimotor circuit

Multiple lines of evidence show that EL interneurons do not act as part of the CPG for locomotion, but rather in a parallel sensorimotor circuit. First, in the absence of sensory input ELs do not fire in locomotion-like patterns of activity (Figure S3). Second,

perturbation of ELs is not sufficient to alter left-right timing of muscle contraction (**Figure 3**). Third, perturbations of ELs alter muscle contraction amplitude both during contraction and at rest (**Figure 3**). Thus, we favor the hypothesis that EL interneurons act in a pathway parallel to the CPG for locomotion.

Our data support the idea that EL interneurons receive sensory input. Using calcium imaging we find evidence for dynamic left-right EL asymmetrical activation *in vivo* (**Figure 5**). Yet, these dynamics are missing from similar experiments done in the isolated CNS, which lack sensory afferents (**Figure 4**). Using TEM reconstruction of the EL circuit we find direct and indirect sensory input pathways into 11F02 ∩ ELs (**Figures 7-8,** S4). Thus, we conclude that EL interneurons should respond to sensory stimuli (see below).

Additionally, our data demonstrate that EL interneurons modify motor output. Perturbation of ELs (either activation or ablation) results in slow crawling, "wavy" body posture (**Figures 1-2**), and imbalance of left-right muscle contraction amplitude (**Figure 3**). Changes in left-right asymmetrical EL activity have behavioral correlates (contralateral body bend, **Figure 5**). Moreover TEM reconstruction identifies EL to motor neuron pathways (**Figures 7,9**). Taken together these data demonstrate that EL activity regulates motor output, and place EL interneurons in a sensorimotor circuit.

TEM reconstruction reveals a complex proprioceptive input pathway to EL interneurons

One striking result of our TEM analysis is that we find strong mono- and di-synaptic pathways from proprioceptors to EL interneurons. Because proprioceptive neurons can detect muscle length and movement (Simon and Trimmer, 2009; Tamarkin

and Levine, 1996), they are perfectly suited to convey muscle amplitude information to the ELs. Closer inspection of the proprioceptor to EL connectivity generates interesting hypotheses. First, some local ELs also receive direct input from lesA, which is an extra-sensory neuron about which little is known (**Figure 7A**). Depending on the type of stimuli that activate lesA, the ELs could be a point for multi-modal sensory integration. Second, proprioceptors make direct synapses with both projection and local 11F02 ∩ ELs (**Figures 7,** S4). Thus, it is possible that the ELs generate an efference copy of body posture that is sent to the brain, as well as participate in a local feedback circuit. Finally, the complexity of the multi-synaptic SN-HMD-EL pathway—with multiple nodes available for integration of proprioceptive information between left and right as well as dorsal and ventral (**Figure 8A**)—suggests that sensory information can be processes before being transmitted to the ELs. Notably, we do not know the neurotransmitter expression profile of any of the HMD interneurons. Given the anatomical complexity of the SN-HMD-EL pathway it is hard to infer function, but raises the question as to whether EL interneurons have state dependent responses to proprioceptive inputs.

EL interneuron activity and contralateral muscle contraction

Anatomical connectivity shows two pathways from EL interneurons to motor neurons. The first pathway is a monosynaptic, contralateral pathway (**Figure 7A**). Because the a majority of ELs are cholinergic (Figure S1) and therefore likely to be excitatory, and in *Drosophila* larva motor neurons are excitatory (Kohsaka et al., 2012) increased EL activity on one side of the body should result in increased contralateral motor neuron activity and contralateral muscle contraction. There is a second pathway from ELs to motor neurons: a disynaptic (EL-AAZ-MN), ipsilateral pathway (**Figure 9A**). The

transmitter type of the AAZ interneurons is currently unknown, but one possibility is that AAZs are inhibitory. If this were the case then increased EL activity would decrease ipsilateral motor neuron activity and allow for ipsilateral muscle lengthening. Ipsilateral muscle lengthening—via the EL-AAZ-MN pathway, together with contralateral muscle contraction—via the direct EL-MN pathway could facilitate larval body bending. It is interesting to note that calcium imaging in intact larvae, shows that a behavioral correlate to increasing EL activity on one side of the body is contralateral body bending (**Figure 5).** In this case our functional data and TEM data seem to be in agreement. Important questions for the future include how exactly the motor neuron activity is altered by EL interneuron activity, and how this results in differential muscle contraction amplitude.

Interactions among EL interneurons

Contralateral projecting interneurons such as EL interneurons mediate communication across the midline. Because the ELs are likely excitatory, one expects the ELs would coordinate left-right neuronal activity. It is therefore surprising that we see left-right asymmetrical activation of ELs in intact freely moving larva (**Figure 5**). We also see a similar phenomenon in isolated CNS preparations: bilateral stimulation of ELs with TRPA1 often results in asymmetrical left-right responses in EL activity (Group 1, Fi**gure 4**). One simple explanation for this asymmetrical activation phenomenon is that ELs could inhibit each others' activity: ELs on one side of the midline might start in a more activated state, or respond more robustly to an initial TRPA1 stimulus. Then during prolonged TRPA1 stimulation this slight difference could be amplified, because the more active ELs would inhibit the activity of ELs on the other side of the midline. In isolated CNS preparations when the TRPA1 stimulation is removed, the asymmetry of EL activation

flips (Group 1, Fi**gure 4**). This could be due to synaptic fatigue in the initially bright side neurons occurring during the stimulus, or post-inhibitory rebound in the initially dim side neurons after the stimulus—either of which would allow the initially dim side neurons to become more active after stimulus offset. The idea of inhibition is also consistent with a second group of EL responses, but not the third group of responses (**Figure 4**). The origin of this variation in response is not clear. It could come from experimental differences (e.g., dissection, mounting, slight stimulus variance), or it could come from network differences (e.g., differences in network architecture or state).

The network architecture mediating interactions among EL interneurons is not clear. For the hypothesized left-right EL-EL inhibition, the only mechanism we can rule out is direct 11F02 ∩ EL to 11F02 ∩ EL connectivity. We find only a few synapses connecting contralateral pairs of ELs (**Figure 7B**). Moreover, 11F02 ∩ ELs do not label with GABA (data not shown), and thus are not likely to be inhibitory. This leaves open the possibility that there is a multi-synaptic inhibitory pathway. Additionally, our data are consistent with the idea that the activity of ipsilateral ELs can be coupled (**Figure 4)**. Because the ELs are likely excitatory, one might predict ipsilateral synaptic connectivity among ELs would mediate this coupling. Using TEM reconstruction, we find only weak and variable ipsilateral connections among ELs both intra- and inter-segmentally (data not shown). It is unclear whether these connections would be sufficient to account for the observed ipsilateral EL coupling, or whether there is an additional multi-synaptic ipsilateral EL-EL interneuron pathway.

How does ablation and activation of EL interneurons result in same phenotype?

One interesting finding is that both activation and ablation of EL interneurons lead

to strikingly similar phenotypes: a mismatch of the left-right amplitude of muscle contraction (**Figures 1-3**). We favor a model in which ELs are part of a "perturbation-compensation" circuit. The idea is that during locomotion asymmetrical perturbations exist; these perturbations could be environmental (e.g., a bump on the substrate) or CNS derived (e.g., differences in the drive to left-right muscle pairs) (Frigon and Rossignol, 2006). Without proper compensation, these perturbations would result in mismatched muscle contraction amplitude on left-right sides of the body. We hypothesize that normally the EL sensorimotor circuit provides the needed compensation. Sensory input into the ELs might allow the state of ELs to represent the curvature of the body wall. Left-right interactions among ELs would allow for comparison between left versus the right sides of the body. Modulating EL activity could result in adjusting muscle contraction amplitude in responses to in appropriate muscle elongation. In the case of EL ablation, perturbations would persist due the lack of EL-mediated compensation, and thus a "wavy" crawling phenotype results. In the case of EL activation, compensation provided by ELs would be chronically active, thereby over compensating for non-existent perturbations, again resulting in a "wavy" crawling phenotype. In this way two "opposite" manipulations would the yield the "same" phenotype. An alternative less, mechanistic explanation for the similarity in phenotypes is that both ablation and activation of EL interneurons cause them to be non-functional in their normal context.

A conserved function of Eve/Evx$^+$ interneurons in neuronal circuitry and behavior?

There is deep conservation of genetic programs that specify neuronal fate. This is particularly true for the Even-skipped$^+$ (Eve or Evx$^+$ in vertebrates) interneurons, which have been found in virtually all bilateral animals examined to date (except *C. elegans*).

Annelids, chordates, insects, fish, birds, and mammals—as well as the presumed last common ancestor between invertebrates and vertebrates, the bristleworm—all contain Eve/Evx^{+} interneurons (Avaron et al., 2003; Copf et al., 2003; Denes et al., 2007; Ferrier et al., 2001; Fujioka et al., 2003; Holland, 2013; Ikuta et al., 2004; Landgraf et al., 1999; Moran-Rivard et al., 2001; Sordino et al., 1996; Suster et al., 2009; Takatori et al., 2008; Thaeron et al., 2000). Where examined (fish, flies, mice) they all have commissural ascending projections. In addition, we now know that like their homologs in mice EL interneurons are likely to be excitatory (Figure S1) and make direct synaptic connections with motor neurons (**Figure 7**). One hypothesis to explain the remarkable parallels between Eve/Evx^{+} interneurons is that the last common ancestor between vertebrates and invertebrates was segmented and motile; and thus the genetic programs used to create locomotion circuitry may be evolutionarily ancient.

Because of the ubiquity of Eve/Evx^{+} interneurons throughout the animal kingdom an important question is: what is the role of Eve/Evx^{+} interneurons in any species? The first attempt to answer this question came from a molecular genetic removal of Evx1 in mice. However, this approach did not reveal any specific function for Evx1^{+} interneurons in either gross motor patterns or in the timing of left-right alternating motor neuronal activity as assayed by nerve root recordings (Lanuza et al., 2004; Moran-Rivard et al., 2001). Subsequently, ablation of a subset of Dbx1^{+} neurons, using Vglut2::Cre; Dbx1^{DTA}—which reduced the number of Evx1^{+} interneurons to 25% of wild type levels, as well as ablating a large, but unspecified number of Vglut2^{+} Dbx1^{+} Evx1^{-} neurons that could potentially include a population of Pitx2^{+} cells—resulted in a hind limb hopping phenotype during fast locomotion in mice (Talpalar et al., 2013). This study raises the

possibility that Evx1^{+} interneurons do indeed play an important role in regulation of locomotion in mice. In our study we show that specific ablation or activation of Eve^{+} interneurons, the ELs leads to defects in *Drosophila* larval crawling. Thus, our study is the first to demonstrate a role for Eve^{+} interneurons in any motor pattern in any organism. It will be interesting in the future to determine whether Evx1^{+} interneurons in other systems such as the mouse play a role in regulation of muscle amplitude, and to determine whether the *Drosophila* larval EL interneurons play a role during asymmetric behavior such as turning.

Materials and methods

Fly genetics

For complete list of fly stocks see Supplemental Experimental Procedures. For *EL-AD* molecular constructs and transgenic flies were generated using standard methods as previously described (Pfeiffer et al., 2008; Pfeiffer et al., 2010). See Supplemental Experimental Procedures. All stocks were raised at room temperature; EL ablated larvae and controls were raised at 30^{o}C.

Embryo immunostaining

We used standard methods to stain *Drosophila* embryos and larvae (Manning et al., 2012). For list of primary antibodies see Supplemental Experimental Procedures. Secondary antibodies were from Invitrogen/Molecular Probes (Eugene, OR) and were used according to manufacturer's instructions Images were acquired on a Zeiss 700 or 710 confocal microscope with a 40X objective. Images were cropped in ImageJ (NIH).

Larval behavior

We recorded behavior in 0-4 h first instar larvae, except late first instar to second larvae

were recorded for experiments using Chrimson. *Brightfield whole larval recordings*. Behavior arenas were made of 6% agar in grape or apple juice, 2 mm thick. Behavior was recorded at 23^{o}C, unless otherwise noted. Temperature was measured using Omega HH508 thermometer, and controlled with a custom-built thermoelectric controller and peltier device. Arenas were placed under a Leica S8APO dissecting microscope and a red light (700 nm, Metaphase Technologies) illuminated a single larva. The microscope was equipped with a Scion 1394 Camera, using Scion VisiCapture software. Images were acquired at either 4 HZ or 7.5 HZ. All larvae were fed yeast paste lacking all-trans-retinal (ATR) except where noted. Also see Supplemental Experimental Methods. *Fluorescent whole larval recordings* (*muscle kinematics)* Behavior arenas were placed on sapphire slides. Larva were allowed to cross the field of view then the stage was manually moved to keep the larvae in view of the camera. This resulted in several short fragments of behavioral recordings for each larva. Images were acquired at 10 HZ with a 10x objective on a McBain spinning disc confocal microscope equipped with a Hamamatsu EM-CCD camera, and Volocity software (PerkinElmer). For image analysis see Supplemental

Experimental Methods.

Calcium imaging

For intact larval recordings see muscle kinematics section above. For Figure 4, a freshly dissected CNS from newly-hatched larvae was placed directly on sapphire slides in HL3.1 saline. For Figure S3 we used the protocol as described above except we used Baine's saline (Marley and Baines, 2011), and maintained a constant temperature between 26-28^{o}C. Temperature was controlled as described above. Imaging was done with a 40x

objective on the McBain spinning disc, as described above. For details of image analysis see Supplemental Experimental Methods.

Multicolor flip out (MCFO) to label and name single EL interneurons

We used published methods to label single EL interneurons in first instar larvae (Nern et al., 2015). The stock MCFO-3 was crossed to EL-gal4 (Supplemental Experimental Procedures). The progeny first instar larvae were dissected, stained for the MCFO epitopes and Eve protein, and imaged on a Zeiss 700 or 710 confocal microscope. Segments containing single MCFO+ Eve+ neurons were analyzed in dorsal view and posterior view, which allowed each neuron to be classified as one of the five 11F02 ∩ EL neurons. The name of the neuron was chosen to match the neuron naming scheme developed to classify third instar abdominal neurons (JT, unpublished).

Reconstructing single EL interneurons and determining their synaptic partners within the serial section TEM volumes

We reconstructed neurons in CATMAID using a Google Chrome browser as previously described (Ohyama et al., 2015). To identify single EL interneurons within the TEM volume we used the following features observed in the MCFO "ground truth" data set: (1) All 11F02 ∩ EL neurons share a common ventro-anterior cell body position; (2) all 11F02 ∩ EL neurons share a common proximal axon fascicle; (3) all 11F02 ∩ EL neurons have contralateral projections; (4) each 11F02 ∩ EL neuron has a characteristic morphology when viewed dorsally and posteriorly (Table S3). Using these criteria, we reconstructed neurons with ventro-anterior soma until we found one that matched the morphology of an individual 11F02 ∩ EL neuron; we then reconstructed adjacent neurons projecting in a common proximal axon fascicle to "enrich" for the remaining 11F02 ∩ EL neurons.

Principle component analysis of the 11F02 ∩ EL neurons was performed using the principle component tool in CATMAID.

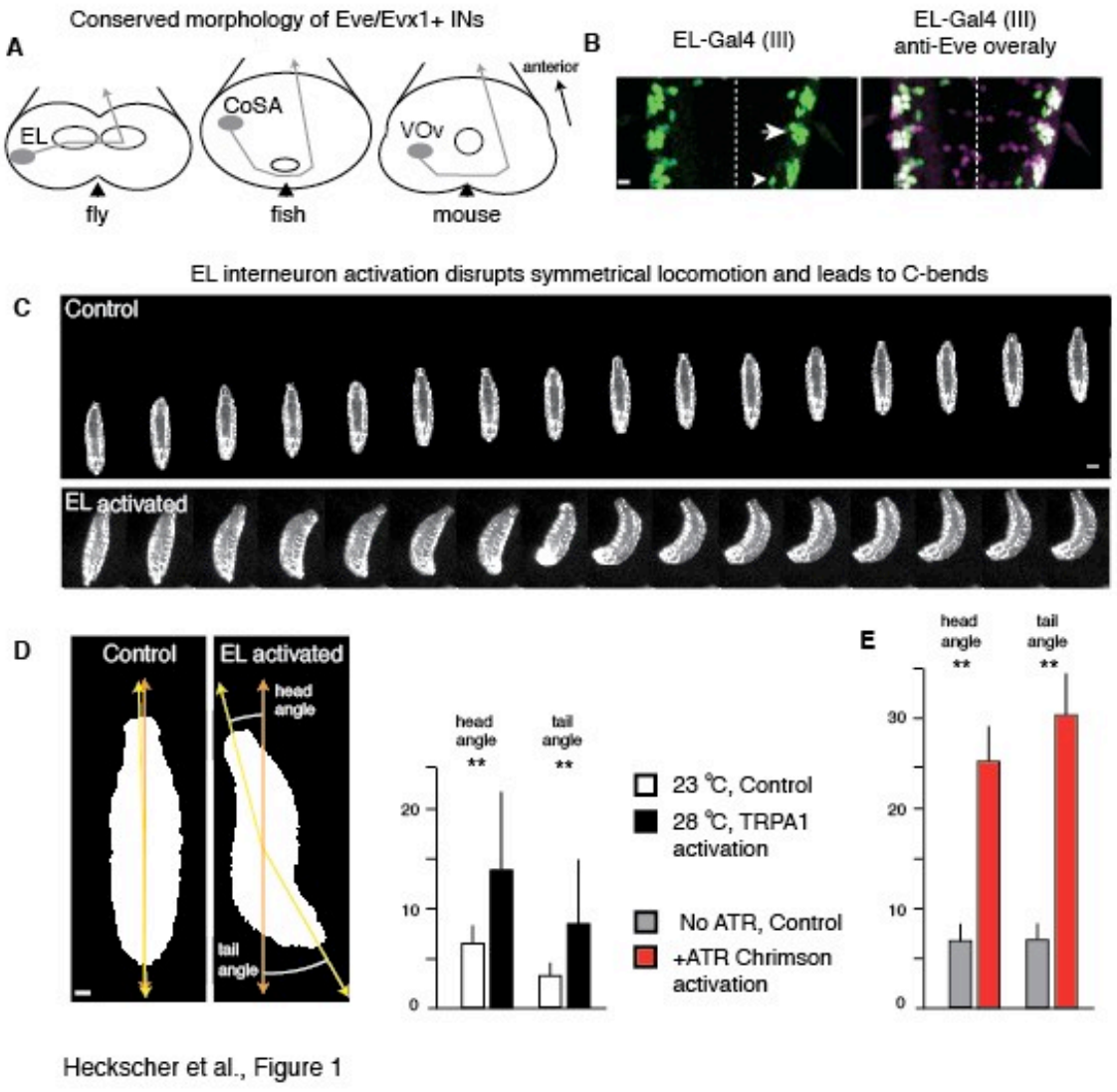

Figure 1. Activation of EL interneurons causes larval crawling defects.

(A) Eve/Evx1+ interneurons have commissural ascending axons in flies, fish and mouse. Midline, black arrowheads; anterior, up in all figures unless noted.

(B) *EL-Gal4* (green) is consistently in nine EL interneurons (arrow) and stochastically in few non-EL cells (arrowhead). Eve protein, magenta; midline, dashed. Scale bar, 10 µm. Genotype: *EL-Gal4 / UAS-nls-GFP*.

(C) Activation of EL interneurons reduces larval crawl speed and induces C-bends. Frames shown at 0.5 second intervals. Scale bar, 150 µm. Genotype: *UAS-dTRPA1/+; EL-Gal4(III)/EL-Gal4(III)*. Control: 23 oC, EL activated: 28 oC.

(D) Thermogenetic, TRPA1-mediated activation of EL interneurons results in larval C-bends with laterally displaced head and tail. Scale bar, 40 µm. See Movies S1-S2Average and SEM shown, ** $p<0.05$, t-test. Genotype as in C. See Movies S1-S2.

(E) Optogenetic, Chrimson-mediated activation of EL interneurons results in larval C-bends. Average and SEM shown, ** $p<0.05$, t-test. Genotype: *UAS-Chrimson.mVenus/+;*

EL-Gal4(III)/+. Control: larvae raised on food without all-trans-rentinal (ATR), EL activated: raised on food with ATR. See Movies S3-S4.

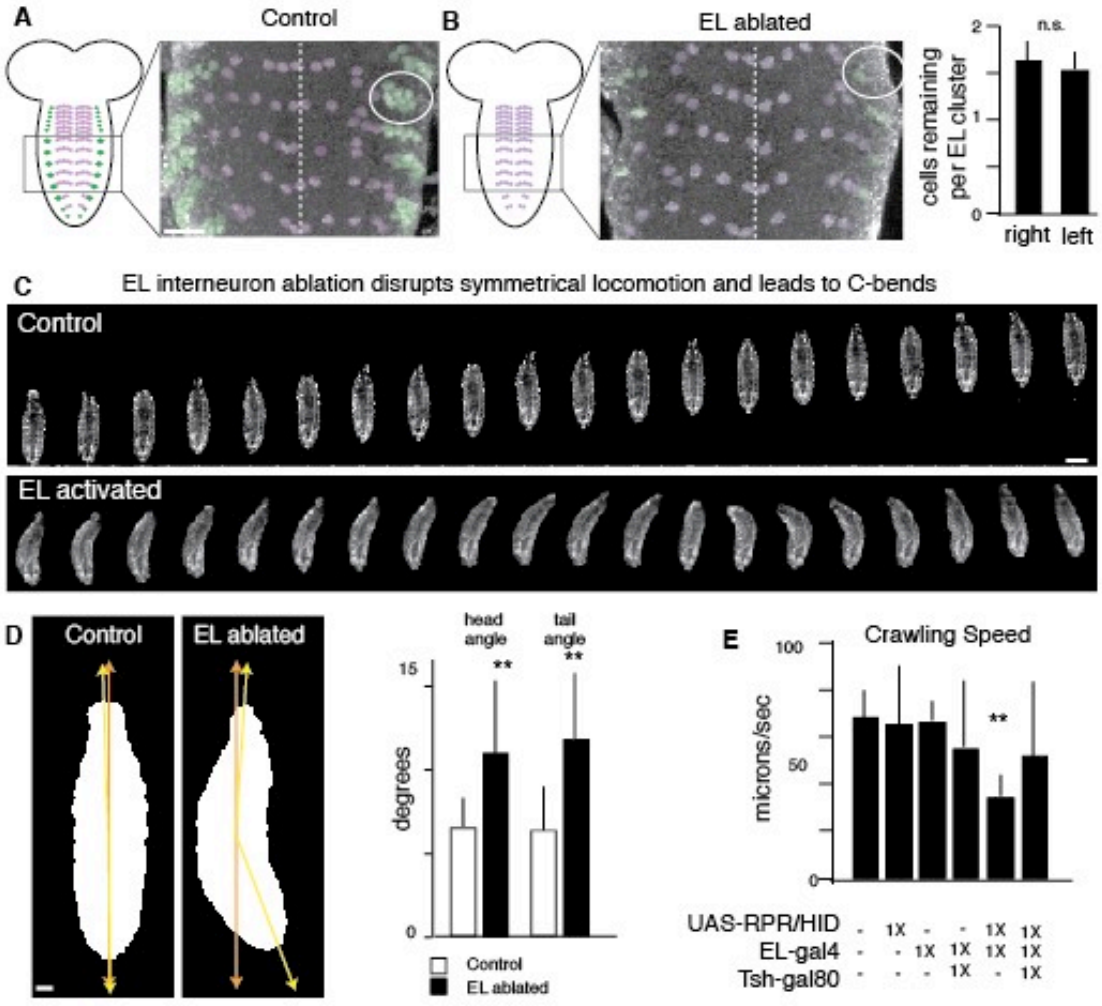

Heckscher et al., Figure 2

Figure 2. Ablation of EL interneurons causes significant crawling defects in L1 larvae.
(A-B) Eve+ motor neurons and Eve+ EL interneurons are pseudocolored green and magenta, respectively. EL ablation reduces EL interneuron number from ~10 to 1.63 ± 0.21 (left) and 1.54 ± 0.19 (right). The left-right difference is not significant (t-test, n = 4 animals). Scale bar, 10 µm. Control genotype: *UAS-reaper, UAS-hid / Y.* EL ablated genotype: *UAS-reaper, UAS-hid / Y;;EL-Gal4/+*.
(C-D) Ablation of EL interneurons decreases larval crawling speed and induces C-bends. Genotypes as in A. (C) Frames are shown at 0.5 second intervals. See Movie S5. Scale bar, 150 µm. (D) Scale bar, 40 µm.
(E) EL-Gal4 expressing brain neurons are not required for normal locomotion. Genotypes from left: (1) *y w*; (2) *UAS-reaper, UAS-hid / Y;* (3) *EL-Gal4 (III)/+;* (4) *UAS-reaper, UAS-hid /Y;;EL-Gal4 /+; (5) tsh-Gal80/+; EL-Gal4 /+; (6) UAS-reaper, UAS-hid /Y; tsh-Gal80/+; EL-Gal4 /+* (in this genotype only EL-Gal4+ neurons in the brain are ablated). (B,D,E) Average and SEM shown, ** $p<0.05$, t-test.

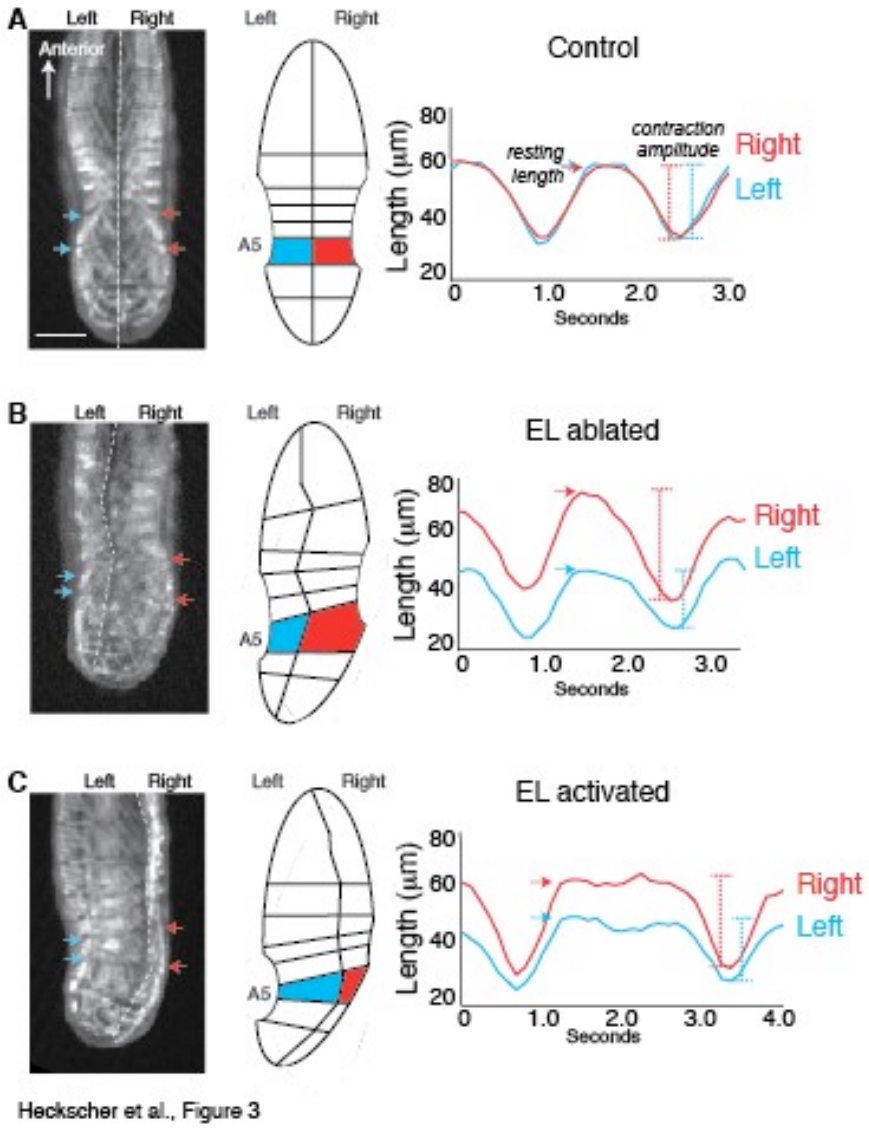

Figure 3. Ablation or activation of EL interneurons results in failure to maintain symmetrical left-right muscle length without affecting left-right timing in L1 larvae. **(A-C)** Control larvae (A), EL ablated larvae (B) and EL activated larvae (C) quantified for resting muscle length, muscle contraction amplitude, and muscle contraction timing. Left: Muscle marker MHC:GFP. Center: schematic of raw data. Right: plot of A5 muscle length on the left (blue) or right (red) over two cycles of relaxation and contraction. Scale bar, 100 µm. See Movies S6-S8. Top and bottom genotypes are *UAS-dTRPA1, MHC:GFP/ UAS-dTRPA1* at 23oC (control) or 30oC (activated). Middle genotype: *UAS-reaper, UAS-hid/+; MHC:GFP/+; EL-Gal4 /+.*

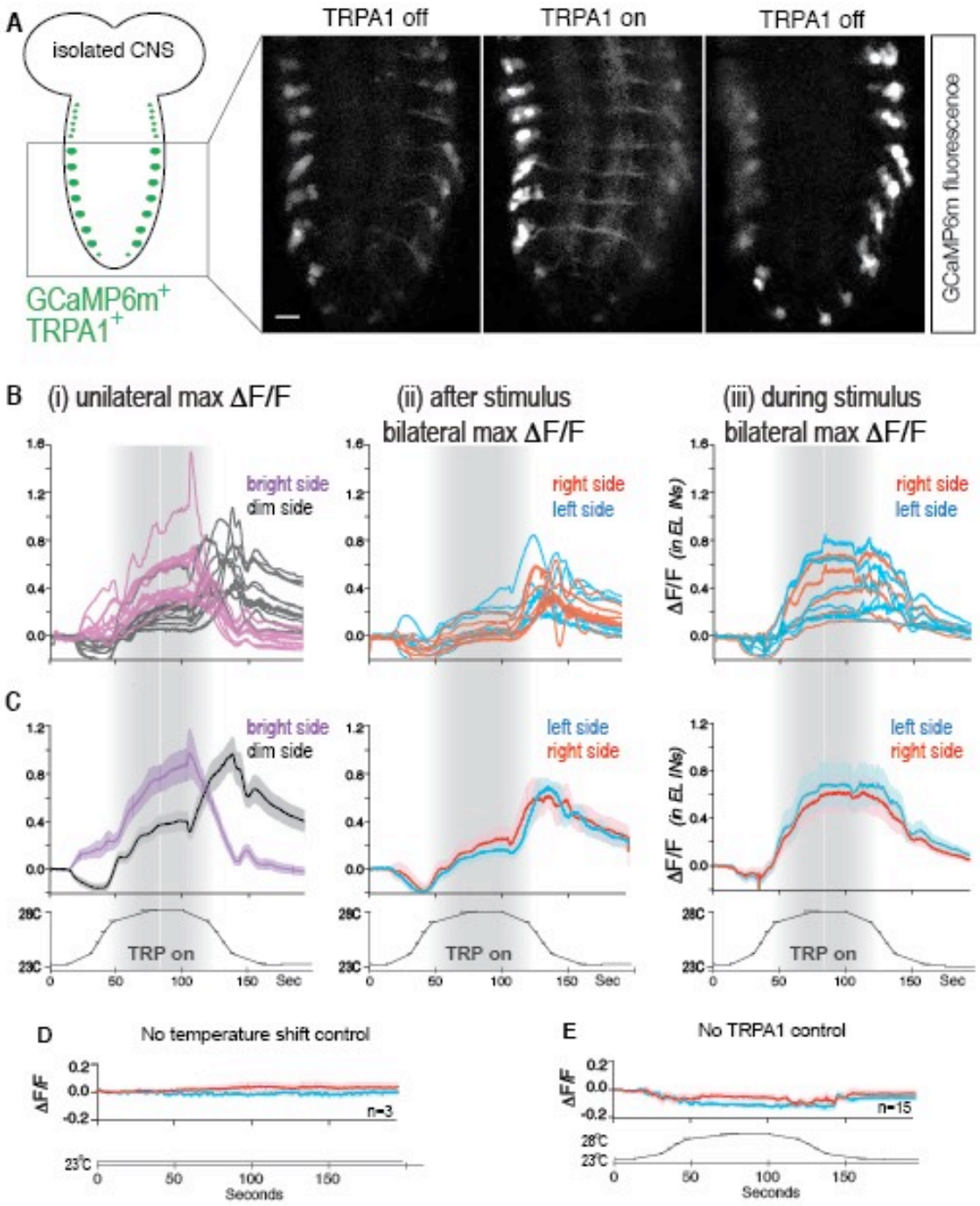

Heckscher, Figure 4

Figure 4. Intersegmental and bilateral EL interactions in response to bilateral EL stimulation

(A-C) Isolated L1 CNS expressing GCaMP6m and TRPA1 in EL interneurons. (A) Left, schematic of preparation and GCaMP6m/TRPA1 expression in EL interneurons; right, frames from Movie S9 when TRPA1 is off (23oC), TRPA1 is on (28oC), and is TRPA1 off (23oC) taken from group iii in (B). Scale bar, 25 μm. (B) Individual plots of GCaMP6m

fluorescence (ΔF/F) over time for each phenotypic category. (C) Group average plots of GCaMP6m fluorescence (ΔF/F) over time for each phenotypic category, with standard error. Genotype: *UAS-dTRPA1/UAS-GCaMP6m; EL-Gal4 /EL-Gal4*.
(D-E) Controls for isolated CNS preparation experiments. (D) Isolated brains expressing GCaMP6m and TRPA1 in EL interneurons held at baseline temperature (23oC). (E) Isolated brains expressing only GCaMP6m in EL interneurons with temperature shifts as in B-C. Genotypes: *UAS-dTRPA1/UAS-GCaMP6m; EL-Gal4 /EL-Gal4* and *UAS-GCaMP6m/UAS-GCaMP6m; EL-Gal4 /EL-Gal4*.

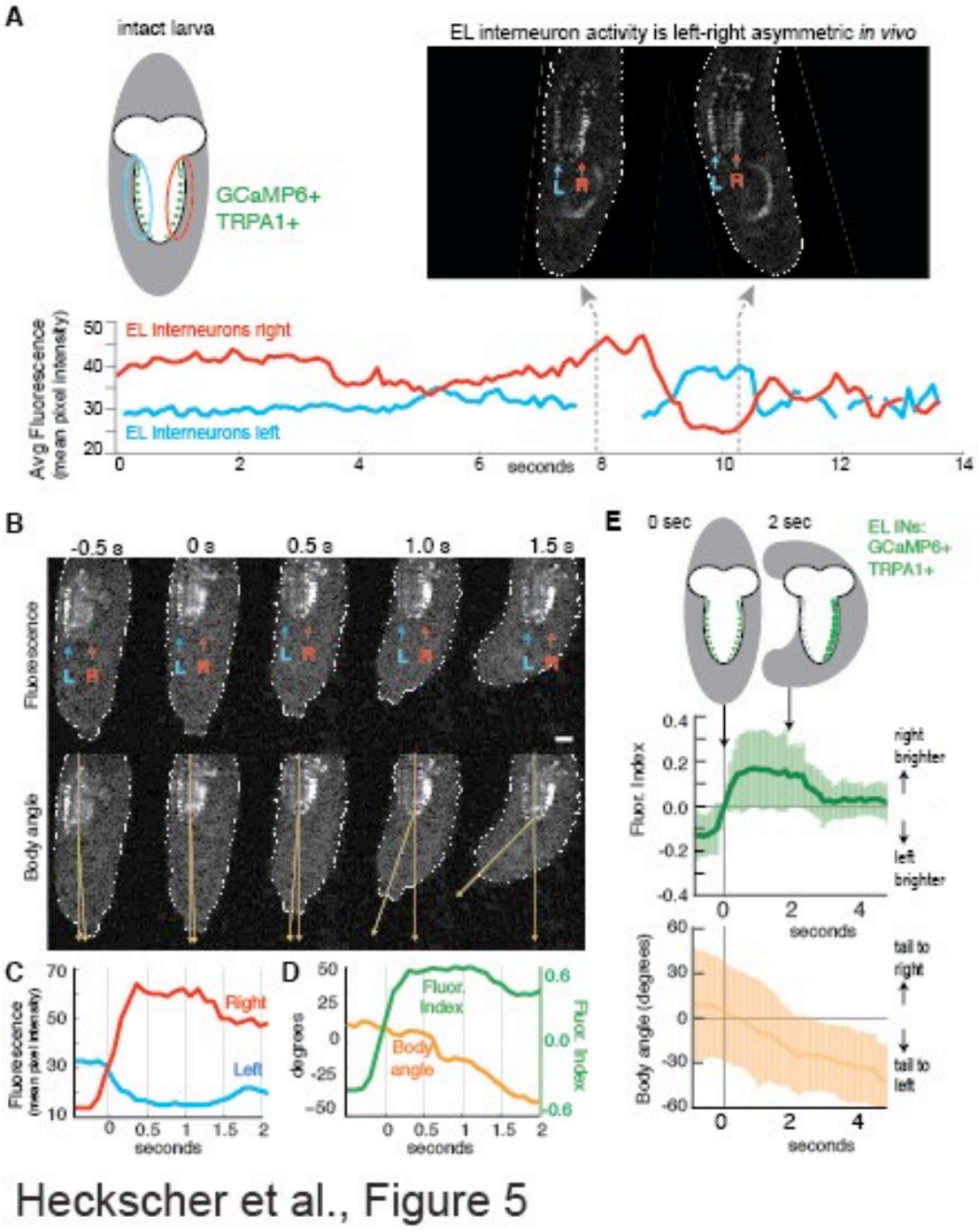

Figure 5. EL interneurons show left-right asymmetrical activity that correlates with contralateral muscle contractions.

(A) Top left: schematic of intact larval preparation and GCaMP6m/TRPA1 expression in EL interneurons. Top right: left-right (L-R) asymmetric GCaMP6m fluorescence in EL interneurons taken from indicated times during plot below (arrows). Bottom: Intact L1 larvae expressing GCaMP6m and TRPA1 in EL interneurons were held at 32oC and mean fluorescence intensity in left (blue) and right (red) EL interneuron clusters was measured. Genotype: *UAS-dTRPA1 / UAS-GCaMP6m; EL-Gal4 / EL-Gal4*.

(B-D) Representative single larva data from Movie S10. (B) Frames showing GCaMP6m fluorescence in the left-right (L-R) EL interneurons and body angle; the top row labeled for EL interneurons, bottom row labeled for body angle (arrows). Scale bar, 50 μm. (C) Plot of left and right EL fluorescence intensity over the time interval shown in B. (D) Plot of fluorescence index (bright side fluorescence - dim side fluorescence / total fluorescence) and body angle for the same time interval shown in B. Genotype as in A.
(E) Summary of group data. EL interneuron activity (green) is correlated with contralateral body bending (orange). Average and standard deviation shown (n=10 switches from 3 larvae). Genotype as in A.

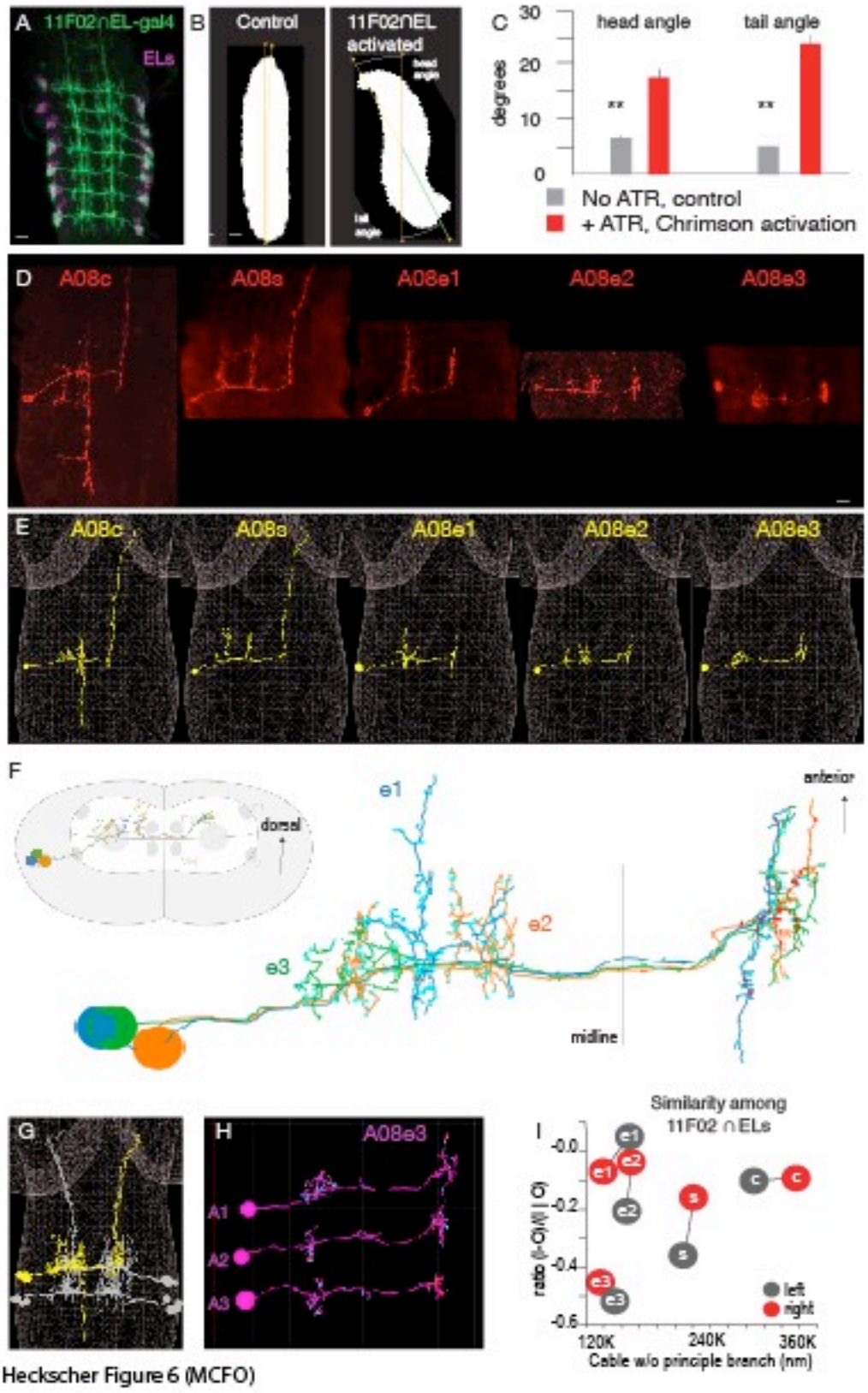

Figure 6. Identification of individual EL interneurons by light and electron microscopy.

(A-C) Activation of a subset of EL interneurons is sufficient to cause C-bending in *Drosophila* larvae. (A) A subset of ELs (anti-Eve, magenta) label with 11F02 ∩ EL Gal4 driving myr:GFP (green). (B-C) Optogenetic activation of 11F02 ∩ EL interneurons results in larval C-bends. Average and SEM shown, ** $p<0.05$, t-test.
Genotype: *UAS-Chrimson.mVenus/EL-AD; R11F02-DBD*/+. Control: larvae raised on food without all-trans-rentinal (ATR), 11F02 ∩ EL activated: raised on food with ATR.
(D) Individual 11F02 ∩ EL neurons detected using the MCFO method. There are two projection neurons (A08c, A08s) and three local neurons (A08e1-e3); all have contralateral projections. Anterior, up; midline, arrowhead. (**E-H**) Reconstructions of 11F02 ∩ EL neurons by electron microscopy. (E) Individual 11F02 ∩ EL neurons were identified and traced within a TEM serial section of an entire L1 CNS. Individual 11F02 ∩ EL neurons shown below their cognate neurons from the "ground truth" light microscopy analysis. Anterior, up. (F) Local ELs reconstructed from segment A3 of a second larval CNS. Anterior up, (or dorsal up in inset). (G) All 11F02 ∩ EL neurons reconstructed in segment A1 and A2; A1L colored yellow. (H) Segmentally homologous neurons are highly similar (A08e3 shown in A1, A2, A3 left hemisegments).
(I) Bilaterally homologous 11F02 ∩ EL neurons are more similar to each other than to other EL neurons by principle component analysis (lines shown have the shortest total path length for the indicated 10 neurons). Y axis: ratio of input-output/input+output synapse number; X axis: neurite branch length (total neurite length – principle branch in nm).

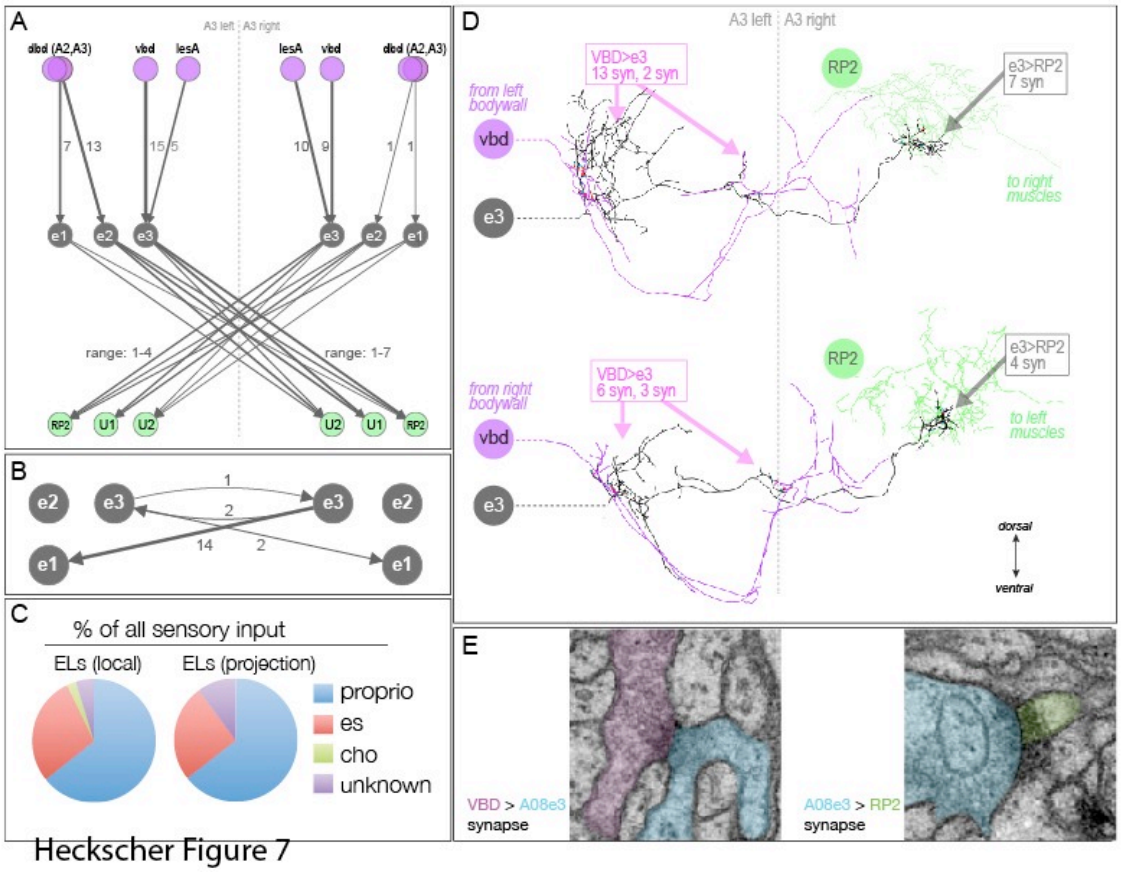

Figure 7. A08e1-e3 local interneurons have monosynaptic proprioceptive inputs and motor outputs.

Anatomical circuit reconstruction of sensory-EL-motor neuron connectome from Larva 1 segment A3 reveals the local 11F02 ∩ EL neurons have direct proprioceptive input and direct motor output.

(A, B) Summary of the connectome showing the indicated number of synapses between proprioceptive sensory neurons EL local interneurons (black), and motor neurons (green). For clarity, the connectivity between EL local interneurons is shown separately (B).

(C) Proprioceptive neurons (dbd, dmd1, vpd, vpda) are the major input into the EL interneurons.

(D) The vbd-A08e3-RP2 connectome is bilaterally symmetric. Top: the A3L vbd has two zones of pre-synaptic contacts with A08e3, which forms synapses with the ventral-most region of the RP2 motor neuron dendritic arbor. Bottom: the A3R vbd-e3-RP2 connectome has the identical location of synaptic contacts, with only minor variation in synapse numbers. Posterior view; dorsal up, midline, dashed line.

(E) Examples of synapse morphology in the TEM reconstruction for vbd-A08e3 (left) and A08e3-RP2 (right). Note the pre-synaptic vesicle accumulation and electron density at the synapse.

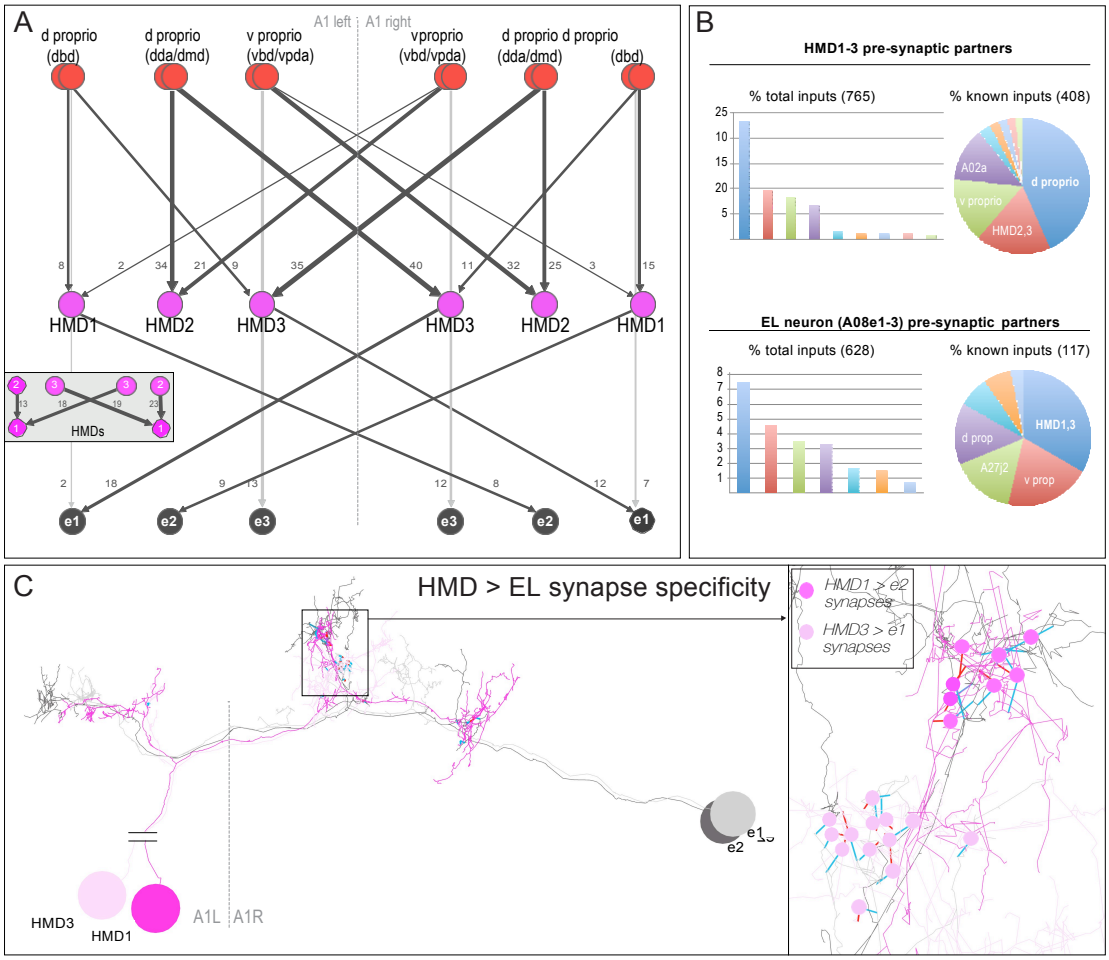

Figure 8. EL interneurons have disynaptic proprioceptive inputs.
Anatomical circuit reconstruction of sensory-HMD-EL connectome from Larva 2 segment A1 reveals the 11F02 ∩ EL neurons have disynaptic proprioceptive input via the HMD neurons.
(A) Summary of the connectome showing the indicated number of synapses between proprioceptive sensory neurons (red), HMD interneurons, and EL local interneurons (black). For clarity, the connectivity between HMD interneurons is shown separately (inset).
(B-C) Proprioceptive neurons (dbd, dmd1, vpd, vpda) are the major input into the HMD interneurons in both % of total inputs (left, includes unannotated neurons) and % of known inputs (right, only annotated neurons). HMD interneurons are the major input into the EL local interneurons in both % of total inputs (left, includes unannotated neurons) and % of known inputs (right, only annotated neurons). **(D)** Each HMD interneuron forms synapses within a characteristic region of the EL dendritic arbors: HMD neurons project contralaterally (from left to right) and target either a ventral domain of the EL arbor (HMD3, light magenta) or a dorsal domain of the EL arbor (HMD1, dark magenta) as seen in the inset. Posterior view; dorsal up, midline, dashed line.

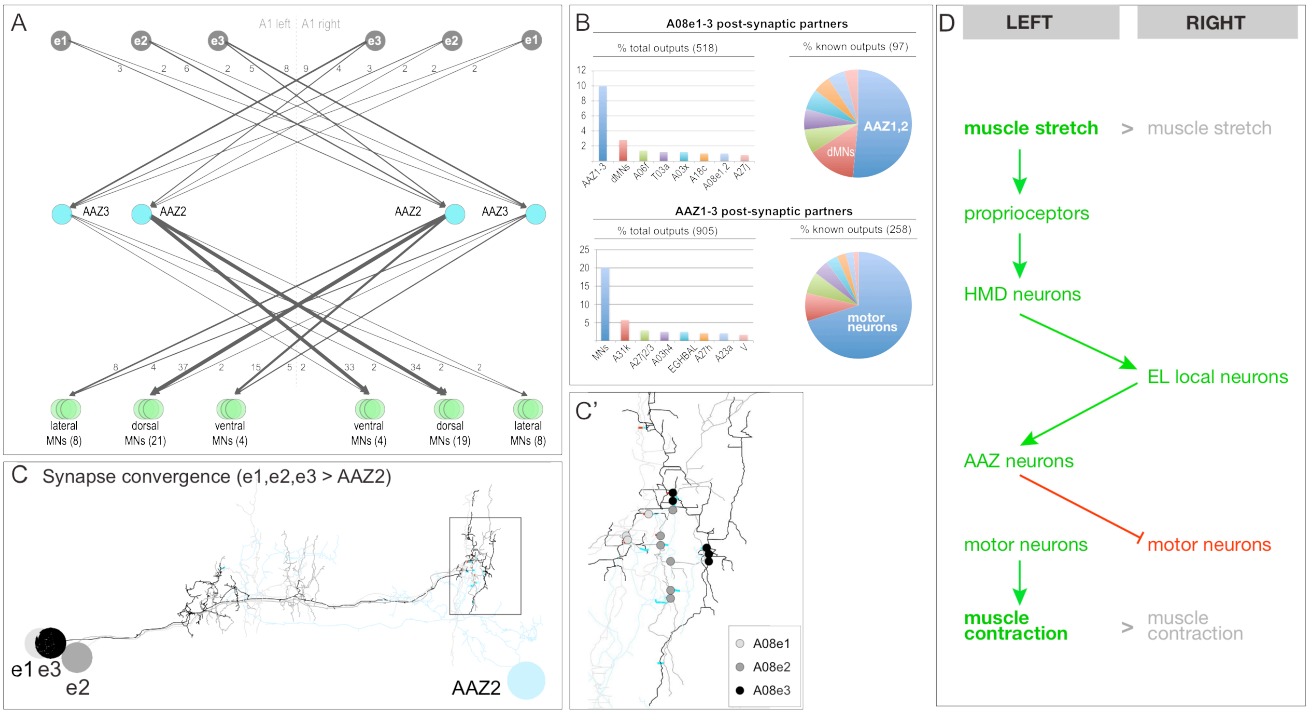

Heckscher Figure 9

Figure 9. EL interneurons have disynaptic motor neuron outputs.
Anatomical circuit reconstruction of EL-AAZ-motor neuron connectome from Larva 2 segment A1 reveals the 11F02 ∩ EL neurons have disynaptic motor output via the AAZ neurons.
(A) Summary of the connectome showing the indicated number of synapses between EL local interneurons (black), AAZ pre-motor interneurons (cyan), and motor neurons (green).
(B-C) The major output of the 11F02 ∩ EL neurons are the AAZ neurons, in both % of total inputs (left, includes unannotated neurons) and % of known inputs (right, only annotated neurons). The major output of the AAZ interneurons are motor neurons, in both % of total inputs (left, includes unannotated neurons) and % of known inputs (right, only annotated neurons).
(D) The 11F02 ∩ EL neurons project to a common region of the AAZ neurons dendritic arbor; see inset for details (D'). Posterior view; dorsal up, midline, dashed line.

BRIDGE TO CHAPTER IV

Following from the results of the thermogenetic screen we sought to elucidate neurons in given patterns that were triggering certain behaviors. Here we explore the reverse phenotype.

CHAPTER IV

MOONWALKING MAGGOTS: IDENTIFICATION OF DESCENDING COMMAND INTERNEURONS THAT GOVERN BACKWARDS LOCOMOTION

Matthew Clark, Laurina Manning, Chris Q. Doe*

Institute of Neuroscience, Institute of Molecular Biology, Howard Hughes Medical Institute, University of Oregon, Eugene, OR 97403.

*Correspondence

Chris Q. Doe

E-mail: cdoe@uoregon.edu

key words: sensorimotor, wave propagation, descending interneuron, navigation, neurodevelopment, multisensory integration, aversion, neural circuit

Abstract

Animals rely on sensory systems to navigate various stimuli (thermal, chemosensory, etc.) by relaying environmental information to the central brain for processing. When encountering noxious or aversive stimuli, it becomes necessary to alter trajectory by reversing the standard mode of locomotion forward and move backwards. Little is known about the identity and function of central neurons that govern these processes. In a previous behavior activation screen of over 200 Gal4 lines we identified a unique driver line that when activated via UAS-dTrpA1, generated chronic backwards

locomotion. Here we identify a unique pair of descending neurons dubbed the 'Mooncrawler' descending neurons (McDNs) to be sufficient to generate reverse locomotion. We show that the McDNs are present at larval hatching, function during larval life, and are remodeled during metamorphosis while maintaining basic morphological features and neural functions necessary to generate backwards locomotion. Finally, using Electron Microscopy (TEM) to map neural connections to upstream and downstream elements provides a mechanistic view of how sensory information is received by the McDNs and transmitted to the VNC motor system to perform reverse locomotion. Finally, we show that these McDNs are the same as those identified in recent work in *Drosophila* adults (Bidaye et al. 2014) to be sufficient to generate reverse locomotion.

Introduction

The nervous systems of animals have the innate ability to respond to various sensory cues in their environment allowing them to avoid noxious stimuli and approach attractive ones (Fraenkel and Gunn 1961; Bullock et al. 1977). Indeed, in a life or death struggle for survival, when attacked by the parasitic wasp *Leptopilina boulardi*, *Drosophila* larvae may show characteristic evasive maneuvers of rolling, fast crawling forwards or rapidly crawling backwards (Hwang *et al.* 2007). Recent work using the advanced neurogenetic toolkit of *Drosophila* has dissected the precise neural mechanisms of the evasive 'goro-goro' or rolling escape behavior (Ohyama *et al.* 2015b). In this landmark study, Ohyama and colleagues found command-like local as well as descending interneurons that could trigger the larval motor system to perform complex rolling and fast crawl behavior, mimicking the natural escape sequence elicited by *Leptopilina*. Escape

neurons allowing the larvae to crawl backwards were not identified and could provide valuable insight into strategies of how to rapidly transmit information from sensory to motor systems.

For all animals, a fundamental function of the nervous system is locomotion. How nervous systems rapidly process sensory cues and transmit them into executable motor programs has been an area of great interest in both vertebrate and invertebrate systems (Drew et al. 2004; Bouvier et al. 2015; Hsu and Bhandawat 2016). One of the earliest systems to explore how these functions are executed has been the command neurons that trigger crayfish escape behavior (Wiersma and Ikeda 1964). Work by Wiersma and colleagues demonstrated that specific, naturally occurring behavior patterns could be initiated by the activity of single (or small groups of) neurons (Kupfermann et al. 1978). However, historically it has been difficult to demonstrate that the activity of command neurons that have been experimentally manipulated has a behavioral correlate in intact and freely moving animals.

The advent of advanced neurogenetic techniques in *Drosophila* has allowed researchers unprecedented ability to dissect neural circuits (Luan, Peabody, *et al.* 2006; Hamada *et al.* 2008; Manning *et al.* 2012; Jenett *et al.* 2012; Klapoetke *et al.* 2014; Pulver *et al.* 2015c). This progress has allowed targeted and reversible activation of increasingly specific populations of neurons in freely moving animals. For example, activation of specific neuronal types in the larval brain can elicit stereotyped feeding, locomotion, or escape behaviors (Ohyama *et al.* 2013b; Huckesfeld *et al.* 2015; Tastekin *et al.* 2015; Clark *et al.* 2016; Wreden *et al.* 2017). A powerful component of circuit breaking in the larval system is the ability to anatomically identify individual circuit components and map them

into a broader collaborative effort to map the connectome of the entire brain via TEM (Schneider-Mizell *et al.* 2015; Berck *et al.* 2016a; Eichler *et al.* 2017; Larderet *et al.* 2017). This allows investigators to formulate, test and validate hypothesis related to anatomical structure and neural circuit function (Kohsaka, Takasu, Morimoto, Nose, *et al.* 2014; Heckscher *et al.* 2015; Fushiki *et al.* 2016a; Jovanic *et al.* 2016; Zwart *et al.* 2016; Schlegel *et al.* 2016).

Drosophila larval crawling is an attractive system to study patterned motor output at the level of animal behavior. *Drosophila* larval crawling consists of forward crawls (runs), turns, head casts and backwards movements. Radially symmetric peristaltic waves of muscle contractions generate forward or reverse locomotion, with asymmetric contractions yielding turns (Lahiri et al. 2011). Reverse locomotion can be initiated by mechanosensative escape circuits (as in the case of wasp attacks) or can be driven by the activation of sensory systems upon encountering aversive stimuli such as high concentrations of salt, light, and heat (Hamada *et al.* 2008; Apostolopoulou *et al.* 2015; Humberg and Sprecher 2017). How signals are mediated by the central brain and transformed by the ventral nerve cord (VNC) to perform locomotor output functions is not well known. In adult flies and other insects, descending neurons integrate information to rapidly relay signals to the VNC (Mu *et al.* 2014; von Reyn *et al.* 2014; Suver *et al.* 2016; Schnell *et al.* 2017). Furthermore, recent work in adult *Drosophila* has shown how aversive light signals mediated by the visual system can be relayed from a descending neuron to generate a response to walk backwards (Sen *et al.* 2017).

Using the warmth gated neural activator dTrpA1, our previous work demonstrated that unique subsets of neurons could trigger distinct behaviors when activated. In this study

we identified a Gal4 line that could trigger chronic backwards locomotion in larvae (Clark *et al.* 2016). In our present study, we have gone on to identify two unique bilateral pairs of descending neurons within this pattern that are capable of initiating reverse locomotion, which we've dubbed the Mooncrawler descending neurons (McDNs). Further, these larval McDNs function to trigger reverse locomotion throughout larval life, are remodeled during metamorphosis, and is the equivalent to the previously described Moonwalker descending neuron (MwDN) (Bidaye *et al.* 2014). With its characteristically unique morphology and using serial section transmission electron microscopy tracing methods we were able to chart these neurons and map their connectivity network.

Results

Interneurons in the central brain are sufficient but not necessary to induce backward larval locomotion

Using the neural activator UAS-dTrpA1, we previously screened ~200 Gal4 Lines with expression in subsets of sparse interneuronal lines (Clark *et al.* 2016). One such line, R53F07-Gal4, showed only reverse locomotion when activated via UAS-dTrpA1. Intermittently, we observed a tonic muscle contraction phenotype that was synonymous with tonic motor neuron activation. Using VGlut-Gal80 to inhibit expression of Gal4 in glutamatergic and motor neurons yielded larvae that chronically crawled backwards, yet had no contractile phenotype (Figure 1A). In conjunction with VGlut-Gal80, we used Tsh-LexA, LexAop-Gal80 to block expression of Gal4 in the ventral nerve cord (VNC) and observed similar results (Figure 1F). Strikingly, there appeared to be many descending neurons projecting from the central brain into the ventral nerve cord (Figure 1B).

Neuroanatomical expression was still broad (~100 neurons in the central brain and ~200 in VNC), thus to refine expression we utilized a split-gal4 intersectional strategy (Luan, Peabody, *et al.* 2006). We generated homozygous viable UAS-Chrimson::mVenus; *R53F07-Gal4^{DBD}*, to screen through roughly 75 *Gal4^{AD}* strains for lines that showed reverse locomotion when triggered via 605nm light stimulation (Klapoetke *et al.* 2014). We found four split Gal4 lines, which for simplicity we named Mooncrawler 1-4-Gal4 (McDN1-4-Gal4). *R49F02^{AD}∩ R53F07-Gal4^{DBD}* (McDN1-Gal4) expressed most consistently starting at early first instar (L1) until third instar (L3), with approximately 10 neurons per brain lobe, and 10 neurons per hemisegment throughout the VNC (Figure 1C). *VT050660^{AD}∩ R53F07-Gal4^{DBD}* (McDN2-Gal4) expressed in the fewest neurons (2 per brain lobe, 2 in the VNC) however expression was somewhat sporadic and expressed only in late wandering L3. *VT037740^{AD}∩ R53F07-Gal4^{DBD}* (McDN3-Gal4) and *VT044504^{AD}∩ R53F07-Gal4^{DBD}* (McDN4-Gal4) also expressed in few cells in the central brain and VNC and began expressing early L3 (expression data not shown).

To narrow expression and distinguish whether the backward-inducing neurons were located in the central brain we used a further intersectional technique. To limit expression of the McDN1-4-Gal4 lines to the central brain, we combined them with LexA/LexAop driven expression of a "Killer Zipper" construct in the VNC, which inhibits split Gal4 activity (Dolan *et al.* 2017). We found that all four central brain (CB) expressing McDN split lines to be sufficient to trigger reverse locomotion via Chrimson activation. We conclude one or more neurons in these patterns to be sufficient to induce backward locomotion.

We noticed that with smaller CB Split Gal4 patterns, after a 5 second Chrimson pulse

stimulation we observed fairly continual backwards locomotion (Figure 1F), however, the number of sequential reverse waves generated was diminished during 10 sec pulse when compared to the broader pattern (Figure 1G). It was possible to stimulate subsequent reverse waves, but only after a brief latency period. We consistently observed descending neurons in each of the CB Split Gal4 lines, with a the most consistent across all genotypes containing an axon terminating in abdominal segment 5 (A5), though in McDN1 we also observed an axon terminating in A4.

Unique pairs of 'Mooncrawler' descending neurons are sufficient to induce backward larval locomotion

We next sought to determine if unique identifiable neurons within these patterns were capable of triggering reverse locomotion. We stochastically expressed CsChrimson in subsets of interneurons via heat-shock mediated flippase expression and excision of a stop cassette to create mosaic larvae (Supplemental Figure 1A). We further restricted expression to the CB by using Teashirt Killer Zipper to prevent expression in the VNC (genotype: hsFlpG5.PEST, R49F02-Gal4^{AD}∩ R53F07-Gal4^{DBD}, Tsh-LexA, LexAop-Killer Zipper, UAS.dsFRT.Chrimson::mVenus). We found that when larvae were raised at 25ºC there were low enough levels of activity of the heat-shock promoter so single clones of phenotypically relevant reverse behavior neurons were generated. Upon CsChrimson stimulation we could pick 1-5 larvae (out of ~200) and upon dissection observe as few as 1-2 neurons per brain lobe that were sufficient to trigger reverse locomotion (Figure 1E, Supplemental Figure 1B-B’’).

Anatomical features of the individual neurons we observed were dorsally located cell

bodies directly adjacent to each other, their neurites fasciculating from the cell bodies, as well as fasciculating as they crossed the commissure. Contralateral projections into the subesophageal zone (SEZ) continued to fasciculate out into the VNC while following a common trajectory. The major distinguishing characteristics between the two neurons included descending axons that terminated in abdominal segment 4 (A4) or abdominal segment 5 (A5). We also noted that the A4 terminating neuron had an ipsilateral branch in the central brain that projected ventrally, whereas the A5 terminating axon did not have this feature.

While individual neurons with their axons terminating in A4 or A5 were capable of generating reverse locomotion, we most often observed a mix of A4/A4, A4/A5, or a combination of all bilateral pairs of descending neurons. We did not note any handedness in the crawl patterns of the sparse clones, rather larvae crawled symmetrically backwards. We conclude that there are 2 pairs of bilaterally symmetric sister McDNs that are all capable of independently triggering reverse locomotion.

Mooncrawler descending neurons are not required for multimodal aversive sensory induced backward larval locomotion

To asses the possible role of the MDNs we used the optogenetically reversible neural silencing tool, anion-conducting channelrhodopsin GtACR (Mohammad *et al.* 2017b) in a broad (genotype: Tsh-LexA, LexAop-Gal80; R53F07-Gal4, UAS-GtACR1) and refined (genotype: R49F02-Gal4^{AD}∩ R53F07-Gal4^{DBD}, Tsh-LexA, LexAop-Killer Zipper, UAS-GtACR-EYFP) pattern. Using these two patterns and an empty vector control (pBDP-Gal4), we assayed three sensory modalities (heat, salt, mechanosensation) with aversive levels of stimulation (37ºC, 1M NaCl, three consecutive gentle touch stimuli to

anterior mouth hook region). To ensure the larvae would a set choice of forward or reverse locomotion when presented with the stimulus, we affixed them to a narrow channel carved into the agar substrate. When presented with aversive stimuli, controls showed the stereotypic response of aversion by generating a series of backwards waves (Figure 1H). In all three scenarios, silencing CB neurons in the R53F07 showed a reversible loss-of-function phenotype, where they failed to show a response to the aversive stimuli. The refined pattern however did not show a phenotype when silenced, and exhibited behaviors more in line with the controls. We conclude that there must be redundant neurons in the broader pattern that when silenced yield a phenotype, whereas the refined pattern neurons alone are not solely necessary for reverse locomotion upon aversive stimulus.

Identification of the Mooncrawler descending neurons by transmission electron microscopy

To provide insight into fine morphological features of the McDNs we obtained single cell resolution at L1 using the technique known as MultiColor FlpOut (MCFO) (Nern *et al.* 2015) (genotype: hsFlpG5.PEST; R49F02-Gal4^{AD}∩ R53F07-Gal4^{DBD}, Tsh-LexA, LexAop-Killer Zipper, UAS-MCFO2). We found reproducibly similar anatomical features to that of our behavior FlpOut experiments, yet with improved dendritic branching morphologies due to the optimized features of the MCFO constructs (Figure 2).

With refined anatomical features of the McDNs, we next began searching for the neurons amongst the thousands of neurons annotated in CATMAID as part of a broader collaborative effort to map the entire connectome (Schneider-Mizell *et al.* 2016). To identify candidate neurons in CATMAID we used a number known anatomical features of

the MDNs including contralaterally projecting neurites traveling through the posterior commissure, along the dorsal region of the neuropil, with axons that terminated in the A4 or A5 region. We fully reconstructed and annotated these neurons which belonged to the DPMm1 lineage (as annotated in CATMAID), and thus named them DPMm1a and DPMm1b, with the 1a designation belonging to the A4 terminating axon and 1b belonging to the A5 terminating axon (Figures 2A,A'-2D,D'). Indeed these neurons terminate and are situated in the same regions of the neuropil as those we observed with confocal (Figures 2E,E'-F,F'). As the neurite travels into the ventral never cord, the axon tract takes a path that is parallel and just adjacent to the DM fascicle tract labeled via FASII antibody staining (Landgraf, Sánchez-Soriano, *et al.* 2003). The region where the axon resides is between the motor and stretch receptor neuropils within the VNC (Zlatic *et al.* 2009). In the larval instar stages we tested (L1-L3), we consistently observed these neurons terminating in the A4 and A5 segments. We similarly observe either the presence (A4 terminating axon) or absence (A5 terminating axon) of a ventrally projecting ipsilateral neurite feature (Figure 2C,C'-D,D')

Identification of Mooncrawler descending neuron features and pre- and post-synaptic partners by electron microscopy

A powerful feature of CATMAID neural tracing is the annotation of pre- and postsynaptic sites on neuronal skeletons (Figure 3A and 3B). This allows features of neurons to be described as well as their connectivity. For instance, across the McDNs we observed that the primary input regions (presynaptic sites) on the McDNs reside in the central brain (Figure 3C). Furthermore, the ipsilateral branches contained many more pre-synaptic sites when compared to the contralateral dendritic branches (700 vs. 320

respective). We also observed relatively sparse postsynaptic sites in the CB, which emanated from connections between the McDNs. There was very dense clustering of postsynaptic sites in the SEZ, as well as an equal number of postsynaptic sites evenly distributed throughout the VNC.

The McDN axons project through the region in the VNC to make them prime candidates to be presynaptic to pre-motor interneurons. Indeed, we found a monosynaptic direct connection to A18b pre-motors, and disynaptic indirect connection to the A27l and A27k pre-motors via a pair of thoracic descending neurons (ThDNs) (Figure 4D and 4F). There is also a route to A27h pre-motors via the Pair1 interneurons. The pre-motor groups span all motor neuron groups, which project along the dorsoventral axis to innervate all muscle groups and provide excitatory drive for muscle contraction.

We noted the convergence of many sensory pathways onto the McDNs via various polysynaptic pathways (data not shown), and have chosen to demonstrate previously published pathways from sensory systems to higher order regions. The olfactory receptor neurons (ORNs) as well as their downstream systems are well annotated (Berck *et al.* 2016). There appeared to be common multiglomerular projection neurons (mPNs) that were directly downstream various aversive ORNs. For example, aversive ORNs 45a and 82a (Kreher *et al.* 2005) both project to the iACT VUM and D mPNs. Both these mPNs have a common downstream target CZ2, which is one of the more highly represented pair of neurons presynaptic to the MDNs.

Mooncrawler neurons persist through metamorphosis and into the adult and are sufficient to induce adult backward walking

Due to the similarities in behavioral phenotype, cell body position, and descending nature of the McDNs, we next sought to determine if they were the same as the previously

described moonwalker descending neurons (MwDN) (Bidaye *et al.* 2014). To do this we first allowed animals from our behavior FlpOut experiments (Supplemental Figure 1) to achieve maturity. When the backwards-crawling larvae were allowed to undergo metamorphosis and raised to adults, we observed the same backwards locomotion phenotype upon CsChrimson stimulation (Figure 5F).

To confirm that the MwDNs are indeed the McDNs, we tracked the MDNs through pupal metamorphosis using MCFO. Starting at late L3 (wandering) stage we observed little morphological variation from the MCFO experiments performed at L1 (Figure 2). At early pupal stage (P4) we observed stereotypical shrinking of the abdominal segment (Veverytsa and Allan 2012). There were no changes in the position of the axon its terminal position. We did however note reduced dendritic branching. This trend continued into mid-pupal stage (P6), where it appears the branching pattern has undergone considerable pruning yet the axon position remains relatively stable. By late mid-pupal stage (P12), branching architecture appears to be undergoing regrowth and remodeling. Finally, by late pupal stage (P14), and MDN we observed as undergone considerable regrowth and has an elaborate branching pattern (relative to earlier L1 larvae). Based on morphological similarities throughout pupal developmental stages, and the adult evoked backwards walking behavior, we conclude that the larval McDNs survive metamorphosis and remodeling to become the MwDNs that provide the same basic function.

Discussion

We have demonstrated that unique pairs of interneurons, the McDNs, are sufficient to generate backwards locomotion. Furthermore, we show that these are the same descending interneurons, the MwDNs, that were previously identified in *Drosophila* adults

to be sufficient to generate backwards locomotion (Bidaye et al. 2014). For interneuronal function, it is remarkable and perhaps the first example if a single neuron controlling a similar feature of locomotion in limbless and limbed locomotion. In future studies it will be interesting to understand what elements of the locomotion circuitry are conserved from larva to adult. For example, there have been examples of aversive ORN sensory neurons, and aversive gustatory receptor neurons (GRN) that maintain their function through larval and adult life (Moon *et al.* 2009; Apostolopoulou *et al.* 2015). Since aversive ORNs are upstream of the McDNs, it will be interesting to determine if the downstream neural circuitry is also conserved in larval and adult life.

What mechanisms are in place to ensure proper pruning, maintenance and regrowth of appropriate connections during metamorphosis? It will be interesting to determine if elements downstream of the McDNs in locomotor system are preserved. If so, how is connectivity with a target such as the Pair1 neuron is maintained and how are new circuits integrated and built on these core components? Recently it was demonstrated that the adult MwDNs receive aversive visual input. By optogenetically recording from the lateral accessory lobe region of the central brain (downstream of the motor processing region) it was found that the MwDNs receive input from the visual system. In this study the authors posit that the MwDNs are being used as an output from the central complex to direct locomotion in the VNC. Though there is no defined central complex described in the larvae, it certainly may be performing the same function.

The Pair1 neurons had the highest number of synaptic inputs from the McDNs. They are upstream of a premotor network with A27h as the central component of a feed-forward circuit that promotes forward locomotion (Fushiki *et al.* 2016). The Pair1 neurons are inhibitory (personal communication M. Louis). In this scenario, McDNs would receive

aversive signals from the various upstream sensory pathways and activate the Pair1 SEZ neurons to halt forward locomotion via the inhibition of A27h. In this manner reverse locomotion could then be initiated.

What is the mechanism for backwards wave initiation? Perhaps the easiest mechanism to posit would be similar to the feedforward mechanism generated by the A27h neurons, but rather would be accomplished by a different set of analogous interneurons. A27h neurons are active only during forward peristalsis and act via the inhibitory GDL interneurons to ensure proper timing of motor neuron activation within a given segment (CITE FUSHIKI AGAIN). A18b, A27k and A27l appear to be prime candidates to fulfill this role for backwards locomotion, as these are the alternative divergent pathways from the MDNs (via the ThDNs) which are separate from the Pair1 stop function pathway. Furthermore, A18b interneurons appear to be active only during reverse locomotion, while A27l is inhibitory thus providing an analogous pair to neurons to the A27h (excitatory) and GDL (inhibitory) neurons (personal communication A. Zarin).

Is there a one site of multisensory integration that acts via the MDNs to trigger backwards locomotion or are there independent pathways through which this information can flow? Does all information regarding backwards locomotion initiation go through the McDNs identified here? Our loss-of-function necessity experiment initially suggested so, however, as we were able to focus expression of GtACR to a handful of neurons in the central brain, larvae were able to perform backwards locomotion. This outcome suggests that there may be redundant circuits to ensure reverse locomotion is achieved when needed. Alternatively, as observed in *Drosophila* and other systems, descending inputs from the brain are designed to rapid transmit information via chemical and electrical synapses

(Zucker *et al.* 1971; Phelan *et al.* 2008; Schnell *et al.* 2017; Miller *et al.* 2017). It may be that within the McDNs themselves there may be a redundancy via electrical synapses that our silencing tool would not affect.

Materials and Methods

The following fly stocks were used in this study: pBDP-Gal4 in attP2 (gift from B.D. Pfeiffer), *R49F02^{AD}* (a gift from G. Rubin), *VT050660^{AD}*, *VT037740^{AD}*, *VT044504^{AD}* (gifts from B Dickson), hsFlpG5.PEST; R49F02-Gal4^{AD}∩ R53F07-Gal4^{DBD}, UAS-MCFO2, UAS-GtACR (a gift from A. Claridge-Chang), R53F07-Gal4 , UAS-Chrimson::mVenus , UAS.dsFRT.Chrimson::mVenus (a gift from G. Rubin), Tsh LexA,LexAop-Gal80 (a gift from J. Simpson), and Tsh-LexA, LexAop-KZip+::3xHA (a gift from B. White). We made R53F07-Gal4^{DBD} according to standard procedures (Pfeiffer *et al.* 2008, 2010).

Optogenetic experiments, Bright-field whole larva behavioral recordings, and behavioral analysis

Adults and larvae were fed yeast supplemented with 1µM all-trans-retinal. McDN1 began showing phenotype as early as we could test at first larval instar (L1), whereas McDN3 and 4 began expressing at L2, and McDN2 began showing reverse phenotype late L3. For consistency of behavioral analysis all assays were performed at late third instar. All stochastic FlpOut behavior experiments were monitored using first instar larvae. Behavior arenas were made of 6% agar in grape juice, 2 mm thick and 5.5 cm in diameter. The arenas were placed under a Leica S8APO dissecting microscope and red light (700 nm, Metaphase Technologies) illuminated a single larva. The microscope was equipped with a

Scion1394 monochrome CCD Camera, using Scion VisiCapture software. Images were acquired via ImageJ at 7.5 Hz for high magnification.

Standard confocal microscopy, immunocytochemistry and MCFO methods were performed as previous (Heckscher *et al.* 2015; Clark *et al.* 2016).

Reconstructing Single EL Interneurons and Determining Their Synaptic Partners within the Serial Section TEM Volumes

We reconstructed McDNs in CATMAID using a Google Chrome browser as previously described (Ohyama *et al.* 2015b). With the exception of the ThDNs, we relied on previously reconstructed elements within CATMAID to find the upstream and downstream elements.

Statistical analysis

We analyzed the data using Student's t test and one-way analysis of variance (ANOVA) Statistical significance is denoted by asterisks: ***$p<0.001$; **$p<0.01$; *$p<0.05$; n's., not significant. All statistical tests were performed using Excel software. The results are stated as mean ± Sc.D., unless otherwise noted.

Acknowledgements

We thank Avinash Kandelwal and Aref Zarin for their assistance in annotating downstream neurons in the EM and the Fly EM Project Team at HHMI Janelia for the gift of the EM volume. Laurina Manning for help with MCFO experiments, Keiko molecular biology,

Cooper Doe for dissections. We would also like to thank the invaluable resource to the fly community BDSC and Todd Laverty and Flycore facilities at JRC. Stocks obtained from the Bloomington *Drosophila* Stock Center (NIH P40OD018537) were used in this study. We also thank other labs for stocks: Gerry Rubin, Ben White, Julie Simpson and Adam Claridge-Chang. The transgenic lines were generated by BestGene Inc..

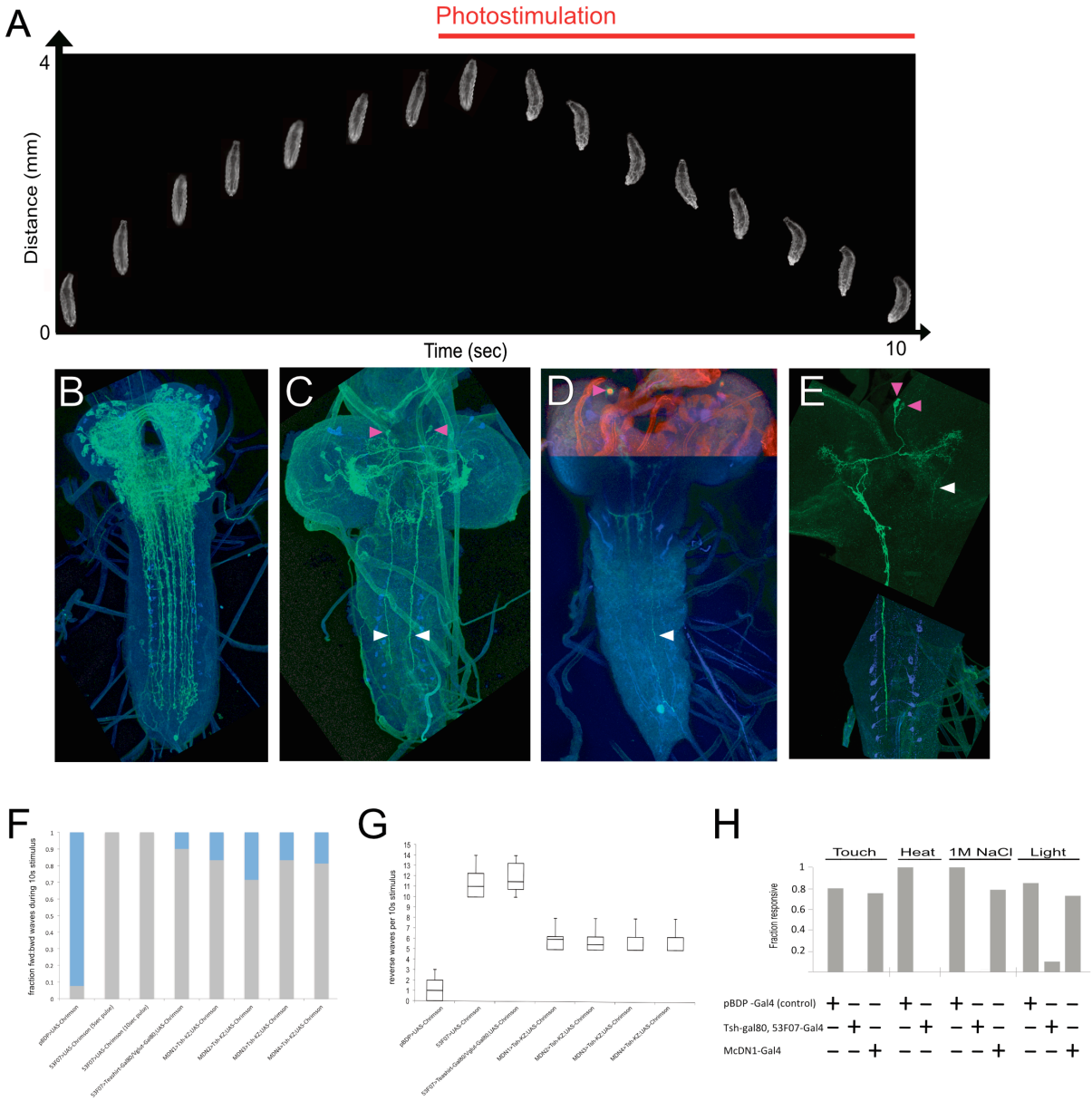

Figure 1. Interneurons in the Central Brain are Sufficient but not Necessary to Induce Backwards Larval Locomotion

(A) During period of Chrimson photostimulation, L1 larvae only crawl backwards (genotype: 53F07-Gal4, Tsh-LexA, LexAop-Gal80; UAS-Chrimson::mVenus) (B) Activation of a subset of interneurons in the central brain reveals a multitude of descending projections into the ventral nerve cord (Genotype: 53F07-Gal4, Tsh-LexA, LexAop-Gal80; UAS-Chrimson::mVenus)). Chrimson: Green, anti-GFP; segmental fiduciary marker: blue, anti-Corazonin. (C) Backwards locomotion triggered by the activation of bilateral pairs of descending interneurons with axons in the VNC (white arrows). Approximately 10 cell bodies per brain lobe with a pair in the dorsoposterior region of the central brain (magenta arrows) (Genotype: R49F02^{AD}∩ R53F07-Gal4^{DBD}, Tsh-LexA, LexAop-Killer Zipper; UAS-Chrimson::mVenus).

(D) Activation of a single descending interneuron (magenta arrow) in the central brain (magenta arrows) triggers backwards locomotion (Genotype: VT050660-Gal4^{AD}∩

R53F07-Gal4^{DBD}; UAS-Chrimson::mVenus, UAS-RedStinger). (E) Stochastic behavior FlpOut clones shows two descending neurons in the right lobe of the central brain (magenta arrows) that is sufficient to trigger backwards locomotion. White arrow denotes ipsilateral branching into the central brain (genotype: hsFlpG5.PEST, R49F02-Gal4^{AD}∩ R53F07-Gal4^{DBD}, Tsh-LexA, LexAop-Killer Zipper, UAS.dsFRT.Chrimson::mVenus). Chrimson: Green, anti-GFP; segmental fiduciary marker: blue, anti-Corazonin. (F) Chrimson activation of subsets of Gal4 patterns shows varying degrees of backwards locomotion during a 5s photostimulation period. (G) Quantification of the number of backwards waves during a 10s Chrimson activation period. Various subsets of Gal4 patterns shows that larger patterns are have more persistent backwards locomotion phenotype. (H) Neural silencing with anion-conducting channelrhodopsin GtACR showed a loss-of-function phenotype when presented with various aversive stimuli in the broader pattern expression of GtACR (Genotype: 53F07-Gal4, Tsh-LexA, LexAop-Gal80; UAS-GtACR-EYFP) while the narrower pattern does not (Genotype: R49F02-Gal4^{AD}∩ R53F07-Gal4^{DBD}, Tsh-LexA, LexAop-Killer Zipper, UAS-GtACR-EYFP).

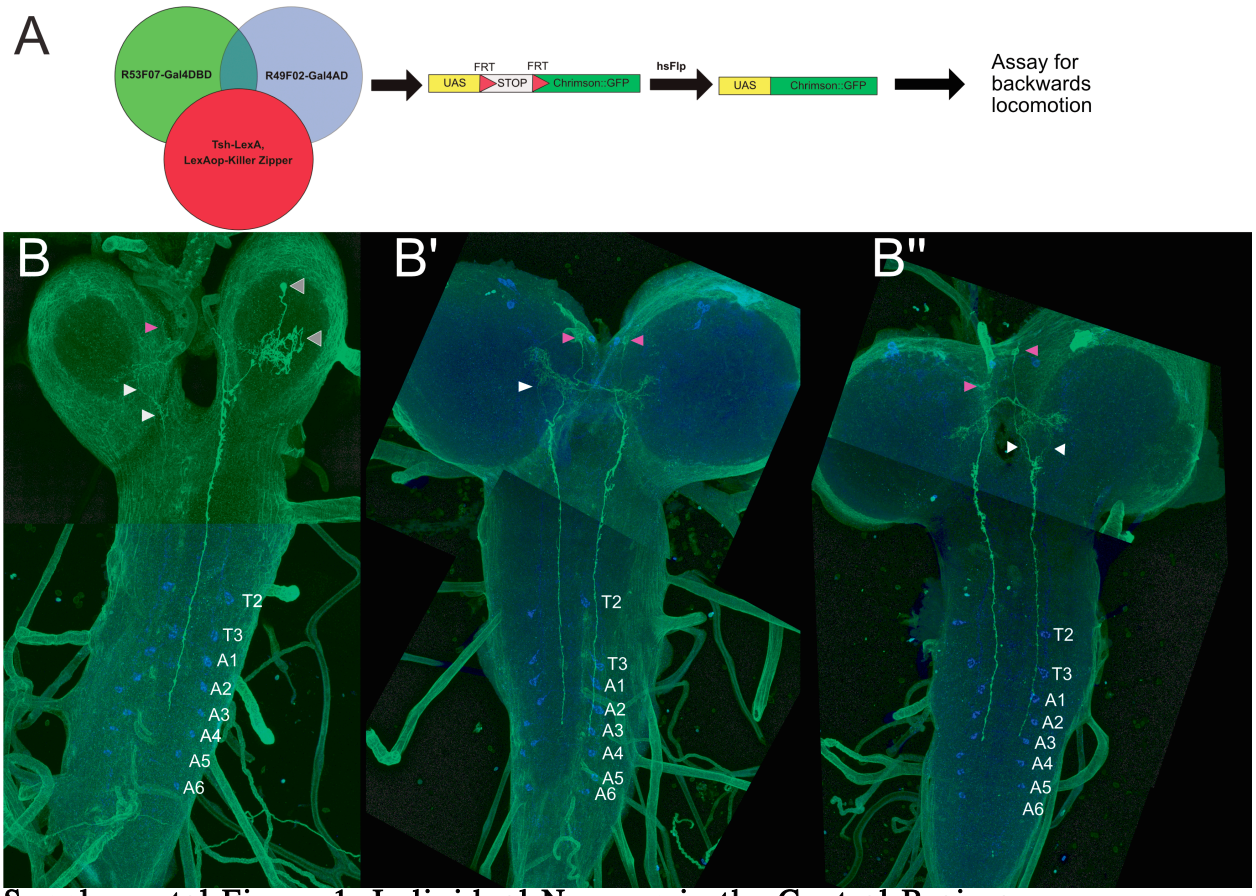

Supplemental Figure 1. Individual Neurons in the Central Brain are Sufficient to Induce Backwards Locomotion

(A) Genetic scheme of behavior FlpOut experiments where Tsh-LexA, LexAop-Killer Zipper (red circle) is used to restrict stochastic Chrimson expression to the central brain of split Gal4 pattern McDN1 (genotype: hsFlpG5.PEST, R49F02-Gal4^{AD}∩ R53F07-Gal4^{DBD}, Tsh-LexA, LexAop-Killer Zipper, UAS.dsFRT.Chrimson::mVenus). (B-B'') Representative expression of behavior FlpOut Chrimson expressing animals varying from one to two descending neurons. Axons projected to segments A4 or A5 (arrows: magenta=cell bodies, white=neurites, grey=off-target expression). Chrimson clones: Green, anti-GFP; segmental fiduciary marker: blue, anti-Corazonin.

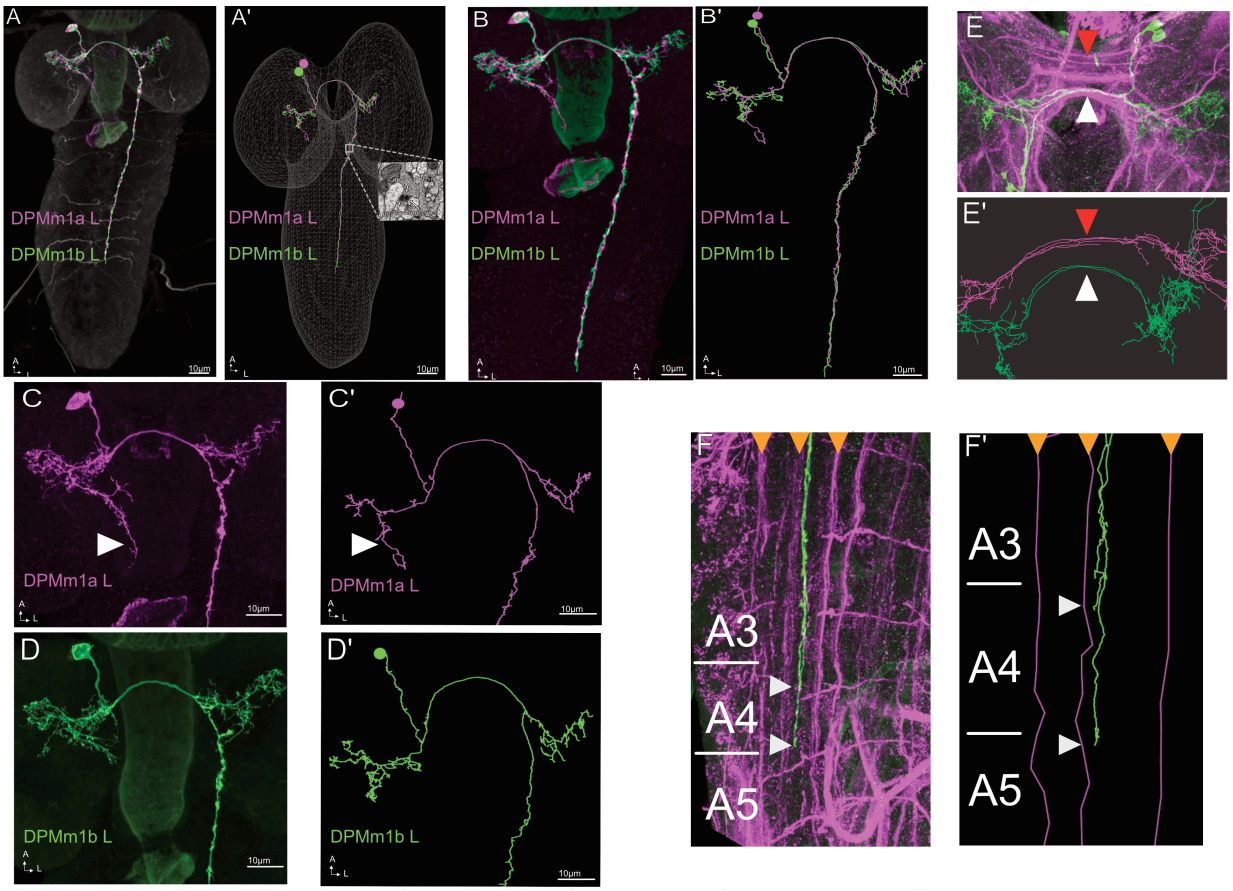

Figure 2. Identification of Individual Moonwalker Descending Interneurons by Light and Electron Microscopy

Moonwalker Descending Neurons (MDNs) feature comparisons via light microscopy and serial section TEM of a first instar larval brain.

(A-A') (A) MCFO identification of descending neurons matching behavior FlpOut clones from the McDN1-Gal4 pattern (see Supplemental Figure 1). (A') Serial section TEM reconstruction of corresponding MDNs, here designated DPMm1a and DPMm1b, where DPMm1a terminates in A4 and DPMm1b, A5. (B-B') ipsilateral branch descends into the brain of corresponding shorter terminating axon. (magenta). Green has no ipsilateral ventrally projecting neurite branch and the axon projects further into the nerve cord (green). (C-C') Interhemispheric commissarial trajectory comparisons of confocal light microcopy and ssTEM. Red arrow denotes anterior bundles and white are the MDNs emanating from the right hemisphere. FasII bundles: magenta, anti-FasII. MCFO clones: green, anti-GFP. (D-D') Similar branching features of DPMm1a in the left-brain lobe with similar descending ipsilateral branch in the central brain (white arrow). (E-E') Similar branching features of DPMm1b in the left brain lobe without the descending ipsilateral neurite branch observed in the DPMm1a neuron. (F-F') Terminal axon feature comparisons of MCFO clones and EM reconstruction, with the shorter axon terminating between segments A3 and A4 (white arrows), while the longer axon terminates at anterior border of A5 (Magenta, anti-FasII, MCFO clones: Green, anti-GFP) Orange triangles denote FasII landmarks DL, CI, DM (L to R respective).

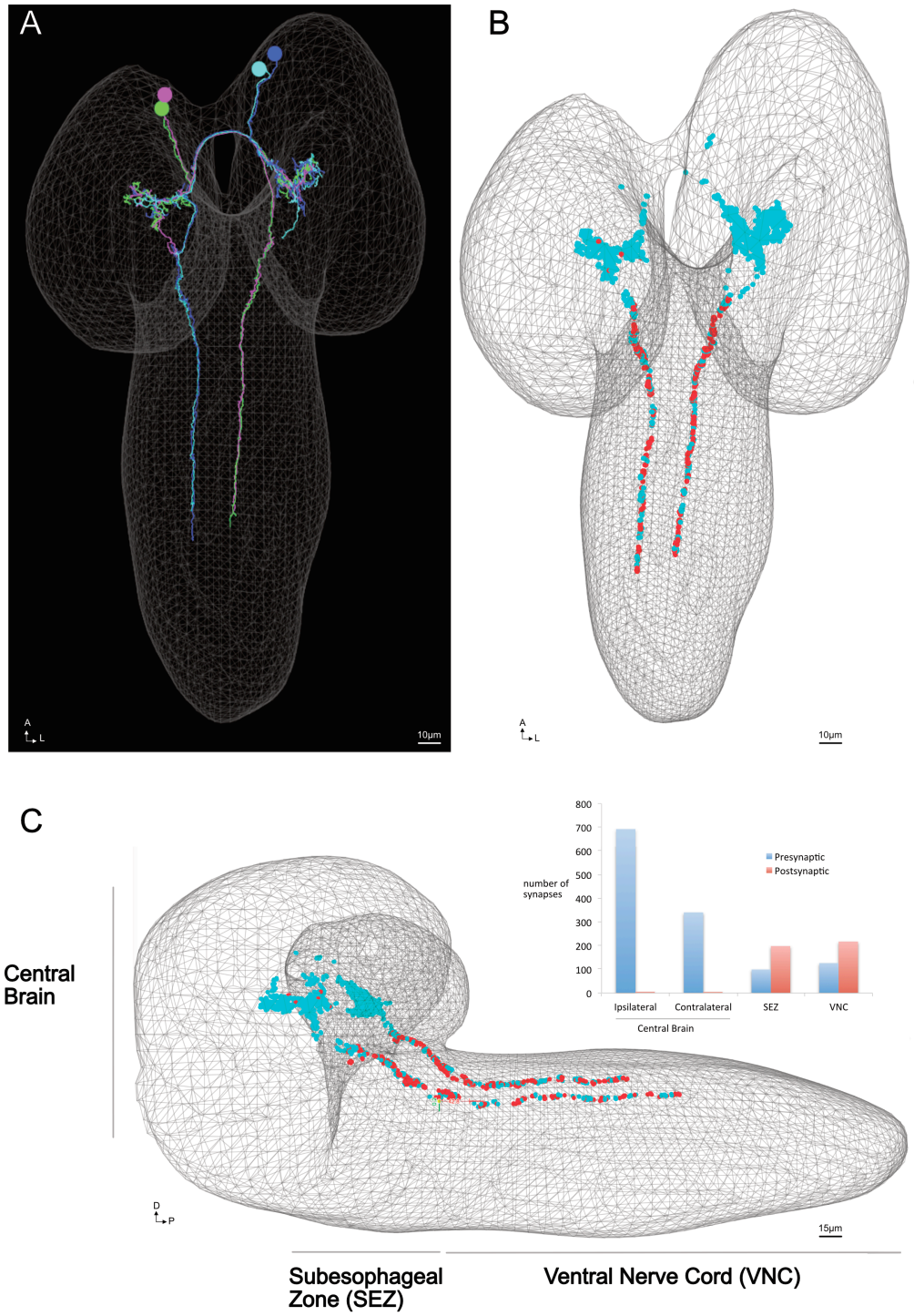

Figure 3. Moonwalker Descending Interneurons Have Inputs in the Central Brain and Outputs in the Subesophageal Zone and Ventral Nerve Cord
(A) ssTEM reconstruction of both bilateral pairs of MDNs DPMm1a and DPMm1b, left and right (anterior is up). (B) MDN presynaptic sites (blue dots) reside primarily in the central brain, whereas postsynaptic sites are in the SEZ and VNC. (C) Lateral view of the brain shows distribution of postsynaptic sites in the SEZ and VNC, with the number of pre and post-synaptic sites quantified (red and blue, respectively).

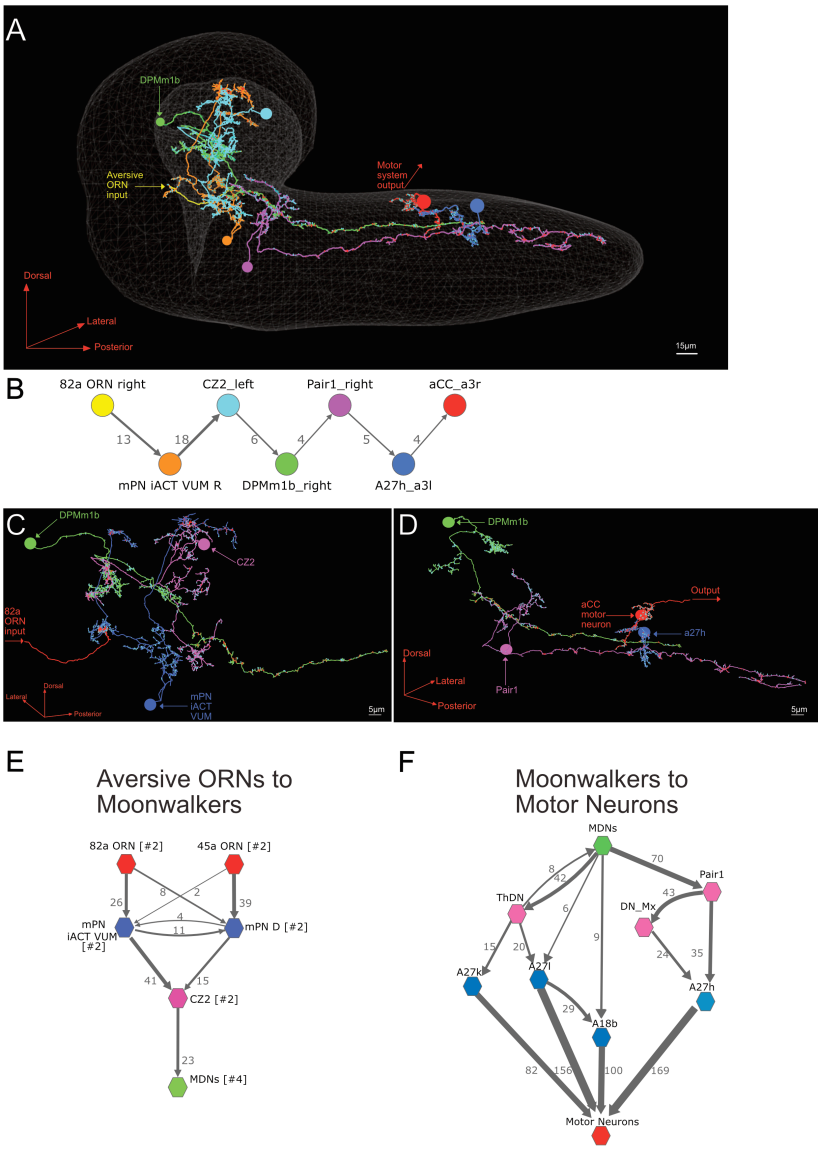

Figure 4. Moonwalker Descending Interneurons Receive Polysynaptic Aversive Olfactory Receptor Neuron Input and Have Polysynaptic Motor Output

(A) ssTEM reconstruction of a sensory to motor systems circuit with the MDNs as a core central component (green skeleton). (B) Colored circles representing nodes in the circuitry represented in (A). Arrows denote connections from presynaptic to postsynaptic neuron with the numbers corresponding to the number of synapses present. One member of the cohort, DPMm1b_right, represents the MDNs. (C) Aversive ORN 82a synapses with mPN iACT VUM which projects into the higher order region of the brain to synapse with MDN presynaptic partner, CZ2. Pre- and postsynaptic sites can be observed on the skeleton as blue and red dots (respective). (D) A primary downstream target of the MDNs is Pair1 that synapses with pre-motor neurons belonging to the neuroblasts lineage A27h. (E) A pair of aversive ORNs upstream to mPNs are coupled to MDN presynaptic partner CZ2. Groups of similar, or bilateral pairs of neurons are represented as colored hexagons. (F) Polysynaptic input from the MDNs to the motor system via a direct route via the A18b neurons, and indirectly through two separate pathways to pre-motors, via the Pair1s and the ThDNs.

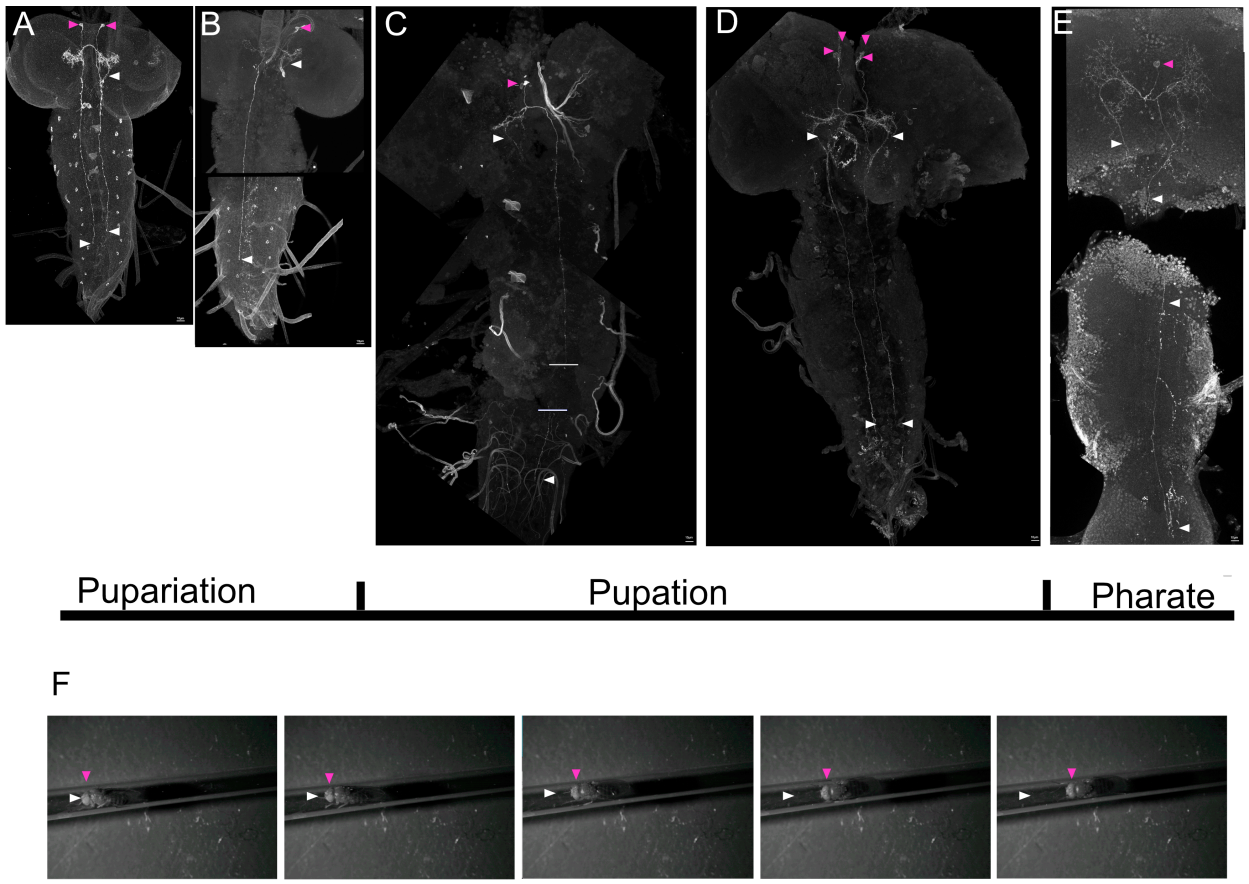

Figure 5. Moonwalker Descending Interneurons are Present Throughout Metamorphosis and Trigger Reverse Locomotion in Adults
(A) Late third instar larva (wandering) MCFO showing MDNs with magenta arrows denoting cell body location, and white arrows highlighting neurite features including ipsilateral descending dendritic projection and terminal descending axon. (B) Early pupal stage (P4) MCFO of DPMm1a Right. (C) Early mid-pupal stage (P6) MCFO featuring DPMm1a left (horizontal white bars indicate artifactual dissection damage break in the VNC). Pruning of dendritic branching in the central brain can be observed (white arrow). (D) Late mid-pupal stage (P12) MCFO with both pairs of MDNs present (magenta arrows). Regrowth of dendritic branches in the central brain has begun. (E) Late pupal stage (P14) MCFO of an MDN featuring extensive regrowth of dendritic branches in the central brain. Considerable shrinking of the abdominal segments has occurred with the major regrowth projections in the VNC occurring in the thoracic region (white arrows). (F) Montage of behavior FlpOut clone flies raised from a larva (see Supplemental Figure 1), stimulated with 605nm light. White triangle represents the initial position of fly upon stimulus, while magenta represents body position as the fly progressively walks backwards.

REFERENCES CITED

Akerboom, J., T.-W. Chen, T. J. Wardill, L. Tian, J. S. Marvin *et al.*, 2012 Optimization of a GCaMP calcium indicator for neural activity imaging. J. Neurosci. 32: 13819–13840.

Aleman-Meza, B., S.-K. Jung, and W. Zhong, 2015 An automated system for quantitative analysis of Drosophila larval locomotion. BMC Dev. Biol. 15: 11.

Almeida-Carvalho, M. J., D. Berh, A. Braun, Y. Chen, K. Eichler *et al.*, 2017 The Ol1mpiad: concordance of behavioural faculties of stage 1 and stage 3 Drosophila larvae. J. Exp. Biol. 220:.

Apostolopoulou, A. A., A. Rist, and A. S. Thum, 2015 Taste processing in Drosophila larvae. Front. Integr. Neurosci. 9: 1–9.

Aso, Y., D. Sitaraman, T. Ichinose, K. R. Kaun, K. Vogt *et al.*, 2014 Mushroom body output neurons encode valence and guide memory-based action selection in Drosophila. Elife 3: e04580.

Atwood, H., 2008 PARALLEL `PHASIC' AND `TONIC' MOTOR SYSTEMS OF THE CRAYFISH ABDOMEN. J. Exp. Biol. 211:.

Baines, R. A., J. P. Uhler, A. Thompson, S. T. Sweeney, and M. Bate, 2001 Altered electrical properties in Drosophila neurons developing without synaptic transmission. J. Neurosci. 21: 1523–31.

Barbagallo, B., and P. A. Garrity, 2015 Temperature sensation in Drosophila. Curr. Opin. Neurobiol. 34: 8–13.

Bargmann, C. I., and W. T. Newsome, 2014 The Brain Research Through Advancing Innovative Neurotechnologies (BRAIN) initiative and neurology. JAMA Neurol. 71: 675–676.

Berck, M. E., A. Khandelwal, L. Claus, L. Hernandez-Nunez, G. Si *et al.*, 2016a The wiring diagram of a glomerular olfactory system: Cold Spring Harbor Labs Journals.

Berck, M. E., A. Khandelwal, L. Claus, L. Hernandez-Nunez, G. Si *et al.*, 2016b The

wiring diagram of a glomerular olfactory system. Elife 5:.

Berni, J., 2015 Genetic Dissection of a Regionally Differentiated Network for Exploratory Behavior in Drosophila Larvae. Curr. Biol. 25: 1319–26.

Berni, J., S. R. Pulver, L. C. Griffith, and M. Bate, 2012 Autonomous circuitry for substrate exploration in freely moving Drosophila larvae. Curr. Biol. 22: 1861–1870.

Bidaye, S. S., C. Machacek, Y. Wu, and B. J. Dickson, 2014 Neuronal control of Drosophila walking direction. Science 344: 97–101.

Birkholz, O., C. Rickert, J. Nowak, I. C. Coban, and G. M. Technau, 2015 Bridging the gap between postembryonic cell lineages and identified embryonic neuroblasts in the ventral nerve cord of Drosophila melanogaster. Biol. Open 4: 420–434.

Bouvier, J., V. Caggiano, R. Leiras, V. Caldeira, C. Bellardita *et al.*, 2015 Descending Command Neurons in the Brainstem that Halt Locomotion. Cell 163: 1191–203.

Branson, K., A. A. Robie, J. Bender, P. Perona, and M. H. Dickinson, 2009 High-throughput ethomics in large groups of Drosophila. Nat. Methods 6: 451–7.

Brooks, D. S., K. Vishal, J. Kawakami, S. Bouyain, and E. R. Geisbrecht, 2016 Optimization of wrMTrck to monitor Drosophila larval locomotor activity. J. Insect Physiol. 93–94: 11–17.

Bullock, T. H., R. Orkand, and A. Grinnell, 1977 *Introduction to nervous systems*. W.H. Freeman.

Burrows, M., 1996 *The Neurobiology of an Insect Brain*. Oxford University Press.

Büschges, A., H. Scholz, and A. El Manira, 2011 New moves in motor control. Curr. Biol. 21: R513-24.

Cardona, A., 2013 Towards semi-automatic reconstruction of neural circuits. Neuroinformatics 11: 31–3.

Cardona, A., S. Saalfeld, S. Preibisch, B. Schmid, A. Cheng *et al.*, 2010 An integrated micro- and macroarchitectural analysis of the Drosophila brain by computer-assisted serial section electron microscopy. PLoS Biol. 8: 2564.

Chen, T.-W., T. J. Wardill, Y. Sun, S. R. Pulver, S. L. Renninger *et al.*, 2013 Ultrasensitive fluorescent proteins for imaging neuronal activity. Nature 499: 295–300.

Choi, J. C., D. Park, and L. C. Griffith, 2004 Electrophysiological and morphological characterization of identified motor neurons in the Drosophila third instar larva central nervous system. J. Neurophysiol. 91: 2353–2365.

Clark, M. Q., S. J. McCumsey, S. Lopez-Darwin, E. S. Heckscher, and C. Q. Doe, 2016 Functional Genetic Screen to Identify Interneurons Governing Behaviorally Distinct Aspects of Drosophila Larval Motor Programs. G3 Genes, Genomes, Genet. 6:.

Denes, A. S., G. J??kely, P. R. H. Steinmetz, F. Raible, H. Snyman *et al.*, 2007 Molecular Architecture of Annelid Nerve Cord Supports Common Origin of Nervous System Centralization in Bilateria. Cell 129: 277–288.

Dixit, R., K. VijayRaghavan, and M. Bate, 2008 Hox genes and the regulation of movement in *Drosophila*. Dev. Neurobiol. 68: 309–316.

Doe, C. Q., 1992 Molecular markers for identified neuroblasts and ganglion mother cells in the Drosophila central nervous system. Development 116: 855–863.

Dolan, M.-J., H. Luan, W. C. Shropshire, B. Sutcliffe, B. Cocanougher *et al.*, 2017 Facilitating Neuron-Specific Genetic Manipulations in Drosophila melanogaster Using a Split GAL4 Repressor. Genetics 206:.

Drew, T., S. Prentice, and B. Schepens, 2004 Cortical and brainstem control of locomotion, pp. 251–261 in.

Edwards, D. H., W. J. Heitler, and F. B. Krasne, 1999 Fifty years of a command neuron: the neurobiology of escape behavior in the crayfish. Trends Neurosci. 22: 153–161.

Eichler, K., A. Litwin-Kumar, F. Li, Y. Park, I. Andrade *et al.*, 2017 The Complete Connectome Of A Learning And Memory Center In An Insect Brain. bioRxiv.

Flood, T. F., S. Iguchi, M. Gorczyca, B. White, K. Ito *et al.*, 2013 A single pair of interneurons commands the Drosophila feeding motor program. Nature 499: 83–7.

Fox, L. E., D. R. Soll, and C.-F. Wu, 2006 Coordination and modulation of locomotion

pattern generators in Drosophila larvae: effects of altered biogenic amine levels by the tyramine beta hydroxlyase mutation. J. Neurosci. 26: 1486–1498.

Fraenkel, G., and D. Gunn, 1961 The orientation of animals: kineses, taxes and compass reactions.

Fushiki, A., M. F. Zwart, H. Kohsaka, R. D. Fetter, A. Cardona *et al.*, 2016a A circuit mechanism for the propagation of waves of muscle contraction in Drosophila. Elife 5:.

Fushiki, A., M. F. Zwart, H. Kohsaka, R. D. Fetter, A. Cardona *et al.*, 2016b A circuit mechanism for the propagation of waves of muscle contraction in Drosophila. Elife 5:.

Gage, F. H., and S. Temple, 2013 Neural stem cells: generating and regenerating the brain. Neuron 80: 588–601.

Gerhard, S., I. Andrade, R. D. Fetter, A. Cardona, and C. M. Schneider-Mizell, 2017 Conserved Neural Circuit Structure Across Drosophila Larva Development Revealed By Comparative Connectomics. bioRxiv.

Gjorgjieva, J., J. Berni, J. F. Evers, and S. J. Eglen, 2013 Neural circuits for peristaltic wave propagation in crawling Drosophila larvae: analysis and modeling. Front. Comput. Neurosci. 7: 24.

Gomez-Marin, A., G. J. Stephens, and M. Louis, 2011 Active sampling and decision making in Drosophila chemotaxis. Nat. Commun. 2: 441.

Green, C., B. Burnet, and K. Connolly, 1983 Organization and patterns of inter-and intraspecific variation in the behaviour of Drosophila larvae. Anim. Behav. 1: 282–291.

GRILLNER, S., J. HELLGREN, A. MENARD, K. SAITOH, and M. WIKSTROM, 2005 Mechanisms for selection of basic motor programs – roles for the striatum and pallidum. Trends Neurosci. 28: 364–370.

Hamada, F. N., M. Rosenzweig, K. Kang, S. R. Pulver, A. Ghezzi *et al.*, 2008 An internal thermal sensor controlling temperature preference in Drosophila. Nature 454: 217–220.

Harris-Warrick, R. M., 2011 Neuromodulation and flexibility in Central Pattern Generator networks. Curr. Opin. Neurobiol. 21: 685–92.

Harris, R. M., B. D. Pfeiffer, G. M. Rubin, and J. W. Truman, 2015 Neuron hemilineages provide the functional ground plan for the Drosophila ventral nervous system. Elife 4: e04493.

HARTLINE, H. K., and F. RATLIFF, 1957 Inhibitory interaction of receptor units in the eye of Limulus. J. Gen. Physiol. 40: 357–76.

HARTLINE, H. K., and F. RATLIFF, 1958 Spatial summation of inhibitory influences in the eye of Limulus, and the mutual interaction of receptor units. J. Gen. Physiol. 41: 1049–66.

Heckscher, E. S., S. R. Lockery, and C. Q. Doe, 2012 Characterization of Drosophila larval crawling at the level of organism, segment, and somatic body wall musculature. J. Neurosci. 32: 12460–71.

Heckscher, E. S., F. Long, M. J. Layden, C.-H. Chuang, L. Manning *et al.*, 2014 Atlas-builder software and the eNeuro atlas: resources for developmental biology and neuroscience. Development 141: 2524–2532.

Heckscher, E. S., A. A. Zarin, S. Faumont, M. Q. Clark, L. Manning *et al.*, 2015 Even-Skipped+ Interneurons Are Core Components of a Sensorimotor Circuit that Maintains Left-Right Symmetric Muscle Contraction Amplitude. Neuron.

Hooper, S. L., and R. A. DiCaprio, 2004 Crustacean Motor Pattern Generator Networks. NeuroSignals 13: 50–69.

Hsu, C. T., and V. Bhandawat, 2016 Organization of descending neurons in Drosophila melanogaster. Sci. Rep. 6: 20259.

Hu, C., M. Petersen, N. Hoyer, B. Spitzweck, F. Tenedini *et al.*, 2017 Sensory integration and neuromodulatory feedback facilitate Drosophila mechanonociceptive behavior. Nat. Neurosci.

Huckesfeld, S., A. Schoofs, P. Schlegel, A. Miroschnikow, and M. J. Pankratz, 2015

Localization of Motor Neurons and Central Pattern Generators for Motor Patterns Underlying Feeding Behavior in Drosophila Larvae. PLoS One 10: e0135011.

Hückesfeld, S., A. Schoofs, P. Schlegel, A. Miroschnikow, and M. J. Pankratz, 2015 Localization of Motor Neurons and Central Pattern Generators for Motor Patterns Underlying Feeding Behavior in Drosophila Larvae. PLoS One 10: e0135011.

Hughes, C. L., and J. B. Thomas, 2007 A sensory feedback circuit coordinates muscle activity in Drosophila. Mol. Cell. Neurosci. 35: 383–96.

Humberg, T.-H., and S. G. Sprecher, 2017 Age- and Wavelength-Dependency of Drosophila Larval Phototaxis and Behavioral Responses to Natural Lighting Conditions. Front. Behav. Neurosci. 11: 66.

Hwang, R. Y., L. Zhong, Y. Xu, T. Johnson, F. Zhang *et al.*, 2007 Nociceptive neurons protect Drosophila larvae from parasitoid wasps. Curr. Biol. 17: 2105–16.

Ito, K., K. Shinomiya, M. Ito, J. D. Armstrong, G. Boyan *et al.*, 2014 A systematic nomenclature for the insect brain. Neuron 81: 755–765.

Iyengar, B. G., C. J. Chou, K. M. Vandamme, M. K. Klose, X. Zhao *et al.*, 2011 Silencing synaptic communication between random interneurons during Drosophila larval locomotion. Genes. Brain. Behav. 10: 883–900.

Jenett, A., G. M. Rubin, T.-T. B. Ngo, D. Shepherd, C. Murphy *et al.*, 2012 A GAL4-driver line resource for Drosophila neurobiology. Cell Rep. 2: 991–1001.

Jorgenson, L. A., W. T. Newsome, D. J. Anderson, C. I. Bargmann, E. N. Brown *et al.*, 2015 The BRAIN Initiative: developing technology to catalyse neuroscience discovery. Philos. Trans. R. Soc. Lond. B. Biol. Sci. 370: 20140164.

Jovanic, T., C. M. Schneider-Mizell, M. Shao, J. B. Masson, G. Denisov *et al.*, 2016 Competitive Disinhibition Mediates Behavioral Choice and Sequences in Drosophila. Cell 167:.

Kabra, M., A. A. Robie, M. Rivera-Alba, S. Branson, and K. Branson, 2013 JAABA: interactive machine learning for automatic annotation of animal behavior. Nat.

Methods 10: 64–7.

Kandel, E. R., 2001 The molecular biology of memory storage: a dialogue between genes and synapses. Science 294: 1030–8.

Kaneko, T., and B. Ye, 2015 Fine-scale topography in sensory systems: insights from Drosophila and vertebrates. J. Comp. Physiol. A. Neuroethol. Sens. Neural. Behav. Physiol. 201: 911–20.

Klapoetke, N. C., Y. Murata, S. S. Kim, S. R. Pulver, A. Birdsey-Benson *et al.*, 2014 Independent optical excitation of distinct neural populations. Nat. Methods 11: 338–346.

Kohsaka, H., E. Takasu, T. Morimoto, and A. Nose, 2014 A group of segmental premotor interneurons regulates the speed of axial locomotion in Drosophila larvae. Curr. Biol. 24: 2632–42.

Kohsaka, H., E. Takasu, T. Morimoto, A. Nose, E. Marder *et al.*, 2014 A Group of Segmental Premotor Interneurons Regulates the Speed of Axial Locomotion in Drosophila Larvae. Curr. Biol. 24: 2632–2642.

Kohwi, M., and C. Q. Doe, 2013 Temporal fate specification and neural progenitor competence during development. Nat. Rev. Neurosci. 14: 823–838.

Kreher, S. A., J. Y. Kwon, and J. R. Carlson, 2005 The molecular basis of odor coding in the Drosophila larva. Neuron 46: 445–56.

Kupfermann, I., K. R. Weiss, J. Diamond, P. D. Evans, B. R. Talamo *et al.*, 1978 The command neuron concept. Behav. Brain Sci. 1: 3.

Kvon, E. Z., T. Kazmar, G. Stampfel, J. O. Yáñez-Cuna, M. Pagani *et al.*, 2014 Genome-scale functional characterization of Drosophila developmental enhancers in vivo. Nature 512: 91–5.

Lacin, H., J. W. Truman, M. Abbott, T. Kaufman, M. Abbott *et al.*, 2016 Lineage mapping identifies molecular and architectural similarities between the larval and adult Drosophila central nervous system. Elife 5: e13399.

Lahiri, S., K. Shen, M. Klein, A. Tang, E. Kane *et al.*, 2011 Two alternating motor programs drive navigation in Drosophila larva. PLoS One 6: e23180.

Lai, S.-L., and T. Lee, 2006 Genetic mosaic with dual binary transcriptional systems in Drosophila. Nat. Neurosci. 9: 703–709.

Landgraf, M., N. Sanchez-Soriano, G. M. Technau, J. Urban, and A. Prokop, 2003 Charting the Drosophila neuropile: a strategy for the standardised characterisation of genetically amenable neurites. Dev. Biol. 260: 207–225.

Landgraf, M., N. Sánchez-Soriano, G. M. Technau, J. Urban, and A. Prokop, 2003 Charting the Drosophila neuropile: a strategy for the standardised characterisation of genetically amenable neurites. Dev. Biol. 260: 207–25.

Landgraf, M., and S. Thor, 2006 Development of Drosophila motoneurons: Specification and morphology. Semin. Cell Dev. Biol. 17: 3–11.

Larderet, I., P. Fritsch, N. Gendre, L. Maier, R. D. Fetter *et al.*, 2017 Organization Of The Drosophila Larval Visual Circuit. bioRxiv.

Lemon, W. C., S. R. Pulver, B. Höckendorf, K. McDole, K. Branson *et al.*, 2015 Whole-central nervous system functional imaging in larval Drosophila. Nat. Commun. 6: 7924.

Li, H.-H., J. R. Kroll, S. M. Lennox, O. Ogundeyi, J. Jeter *et al.*, 2014 A GAL4 driver resource for developmental and behavioral studies on the larval CNS of Drosophila. Cell Rep. 8: 897–908.

Luan, H., W. C. Lemon, N. C. Peabody, J. B. Pohl, P. K. Zelensky *et al.*, 2006 Functional dissection of a neuronal network required for cuticle tanning and wing expansion in Drosophila. J. Neurosci. 26: 573–84.

Luan, H., N. C. Peabody, C. R. Vinson, and B. H. White, 2006 Refined spatial manipulation of neuronal function by combinatorial restriction of transgene expression. Neuron 52: 425–36.

Maia Chagas, A., L. L. Prieto-Godino, A. B. Arrenberg, and T. Baden, 2017 The €100 lab:

A 3D-printable open-source platform for fluorescence microscopy, optogenetics, and accurate temperature control during behaviour of zebrafish, Drosophila, and Caenorhabditis elegans. PLOS Biol. 15: e2002702.

Manning, L., E. S. Heckscher, M. D. Purice, J. Roberts, A. L. Bennett *et al.*, 2012 A resource for manipulating gene expression and analyzing cis-regulatory modules in the Drosophila CNS. Cell Rep. 2: 1002–1013.

Marder, E., 2007 Searching for Insight: Using Invertebrate Nervous Systems to Illuminate Fundamental Principles in Neuroscience, pp. 1–18 in *Invertebrate Nervous Systems*, edited by R. North, G, Greenspan.

Marder, E., and D. Bucher, 2001 Central pattern generators and the control of rhythmic movements. Curr. Biol. 11: R986-96.

Marder, E., and D. Bucher, 2007 Understanding circuit dynamics using the stomatogastric nervous system of lobsters and crabs. Annu. Rev. Physiol. 69: 291–316.

Marder, E., and R. L. Calabrese, 1996 Principles of rhythmic motor pattern generation. Physiol. Rev. 76: 687–717.

Matsunaga, T., H. Kohsaka, and A. Nose, 2017 Gap Junction–Mediated Signaling from Motor Neurons Regulates Motor Generation in the Central Circuits of Larval Drosophila. J. Neurosci. 37:.

Mauss, A., M. Tripodi, J. F. Evers, M. Landgraf, and M. Tessier-Lavigne, 2009 Midline Signalling Systems Direct the Formation of a Neural Map by Dendritic Targeting in the Drosophila Motor System (R. O. L. Wong, Ed.). PLoS Biol. 7: e1000200.

Melcher, C., and M. J. Pankratz, 2005 Candidate gustatory interneurons modulating feeding behavior in the Drosophila brain. PLoS Biol. 3: e305.

Mendell, L. M., 2005 The size principle: a rule describing the recruitment of motoneurons. J. Neurophysiol. 93:.

Merritt, D., and P. Whitington, 1995 Central projections of sensory neurons in the Drosophila embryo correlate with sensory modality, soma position, and proneural

gene function. J. Neurosci. 15:.

Miller, A. C., A. C. Whitebirch, A. N. Shah, K. C. Marsden, M. Granato *et al.*, 2017 A genetic basis for molecular asymmetry at vertebrate electrical synapses. Elife 6:.

Mirth, C., J. W. Truman, and L. M. Riddiford, 2005 The Role of the Prothoracic Gland in Determining Critical Weight for Metamorphosis in Drosophila melanogaster. Curr. Biol. 15: 1796–1807.

Mohammad, F., J. C. Stewart, S. Ott, K. Chlebikova, J. Y. Chua *et al.*, 2017a Optogenetic inhibition of behavior with anion channelrhodopsins. Nat. Methods 14:.

Mohammad, F., J. C. Stewart, S. Ott, K. Chlebikova, J. Y. Chua *et al.*, 2017b Optogenetic inhibition of behavior with anion channelrhodopsins. Nat. Methods 14: 271–274.

Moon, S. J., Y. Lee, Y. Jiao, and C. Montell, 2009 A Drosophila Gustatory Receptor Essential for Aversive Taste and Inhibiting Male-to-Male Courtship. Curr. Biol. 19: 1623–1627.

Mu, L., J. P. Bacon, K. Ito, and N. J. Strausfeld, 2014 Responses of Drosophila giant descending neurons to visual and mechanical stimuli. J. Exp. Biol. 217: 2121–9.

Mullins, O. J., J. T. Hackett, J. T. Buchanan, and W. O. Friesen, 2011 Neuronal control of swimming behavior: Comparison of vertebrate and invertebrate model systems. Prog. Neurobiol. 93: 244–269.

Nern, A., B. D. Pfeiffer, and G. M. Rubin, 2015 Optimized tools for multicolor stochastic labeling reveal diverse stereotyped cell arrangements in the fly visual system. Proc. Natl. Acad. Sci. U. S. A. 112: E2967-76.

Newman, Z. L., A. Hoagland, K. Aghi, K. Worden, S. L. Levy *et al.*, 2017 Input-Specific Plasticity and Homeostasis at the Drosophila Larval Neuromuscular Junction. Neuron 93: 1388–1404.e10.

Nicolai, L. J. J., A. Ramaekers, T. Raemaekers, A. Drozdzecki, A. S. Mauss *et al.*, 2010 Genetically encoded dendritic marker sheds light on neuronal connectivity in Drosophila. Proc. Natl. Acad. Sci. U. S. A. 107: 20553–20558.

Nusbaum, M. P., and M. P. Beenhakker, 2002 A small-systems approach to motor pattern generation. Nature 417: 343–350.

Ohyama, T., T. Jovanic, G. Denisov, T. C. Dang, D. Hoffmann *et al.*, 2013a High-Throughput Analysis of Stimulus-Evoked Behaviors in Drosophila Larva Reveals Multiple Modality-Specific Escape Strategies. PLoS One 8:.

Ohyama, T., T. Jovanic, G. Denisov, T. C. Dang, D. Hoffmann *et al.*, 2013b High-throughput analysis of stimulus-evoked behaviors in Drosophila larva reveals multiple modality-specific escape strategies. PLoS One 8: e71706.

Ohyama, T., C. M. Schneider-Mizell, R. D. Fetter, J. V. Aleman, R. Franconville *et al.*, 2015a A multilevel multimodal circuit enhances action selection in Drosophila. Nature 520: 633–9.

Ohyama, T., C. M. Schneider-Mizell, R. D. Fetter, J. V. Aleman, R. Franconville *et al.*, 2015b A multilevel multimodal circuit enhances action selection in Drosophila. Nature 520: 633–639.

Pauls, D., A. von Essen, R. Lyutova, L. van Giesen, R. Rosner *et al.*, 2015 Potency of transgenic effectors for neurogenetic manipulation in Drosophila larvae. Genetics 199: 25–37.

Pehlevan, C., P. Paoletti, and L. Mahadevan, 2016 Integrative neuromechanics of crawling in *D. melanogaster* larvae. Elife 5:.

Pérez-Escudero, A., J. Vicente-Page, R. C. Hinz, S. Arganda, and G. G. de Polavieja, 2014 idTracker: tracking individuals in a group by automatic identification of unmarked animals. Nat. Methods 11: 743–8.

Peron, S., M. A. Zordan, A. Magnabosco, C. Reggiani, and A. Megighian, 2009 From action potential to contraction: Neural control and excitation–contraction coupling in larval muscles of Drosophila. Comp. Biochem. Physiol. Part A Mol. Integr. Physiol. 154: 173–183.

Pfeiffer, B. D., A. Jenett, A. S. Hammonds, T.-T. B. Ngo, S. Misra *et al.*, 2008 Tools for

neuroanatomy and neurogenetics in Drosophila. Proc. Natl. Acad. Sci. U. S. A. 105: 9715–20.

Pfeiffer, B. D., T.-T. B. Ngo, K. L. Hibbard, C. Murphy, A. Jenett *et al.*, 2010 Refinement of tools for targeted gene expression in Drosophila. Genetics 186: 735–55.

Pfeiffer, B. D., J. W. Truman, and G. M. Rubin, 2012 Using translational enhancers to increase transgene expression in Drosophila. Proc. Natl. Acad. Sci. U. S. A. 109: 6626–31.

Phelan, P., L. A. Goulding, J. L. Y. Tam, M. J. Allen, R. J. Dawber *et al.*, 2008 Molecular Mechanism of Rectification at Identified Electrical Synapses in the Drosophila Giant Fiber System. Curr. Biol. 18: 1955–1960.

von Philipsborn, A. C., T. Liu, J. Y. Yu, C. Masser, S. S. Bidaye *et al.*, 2011 Neuronal control of Drosophila courtship song. Neuron 69: 509–22.

Pulver, S. R., T. G. Bayley, A. L. Taylor, J. Berni, M. Bate *et al.*, 2015a Imaging fictive locomotor patterns in larval Drosophila. J. Neurophysiol. 114: 2564–77.

Pulver, S. R., T. G. Bayley, A. L. Taylor, J. Berni, M. Bate *et al.*, 2015b IMAGING FICTIVE LOCOMOTOR PATTERNS IN LARVAL DROSOPHILA. J. Neurophysiol. jn.00731.2015.

Pulver, S. R., T. G. Bayley, A. L. Taylor, J. Berni, M. Bate *et al.*, 2015c IMAGING FICTIVE LOCOMOTOR PATTERNS IN LARVAL DROSOPHILA. J. Neurophysiol. jn.00731.2015.

Pulver, S. R., N. J. Hornstein, B. L. Land, and B. R. Johnson, 2011 Optogenetics in the teaching laboratory: using channelrhodopsin-2 to study the neural basis of behavior and synaptic physiology in Drosophila. AJP Adv. Physiol. Educ. 35: 82–91.

Pulver, S. R., S. L. Pashkovski, N. J. Hornstein, P. A. Garrity, and L. C. Griffith, 2009 Temporal dynamics of neuronal activation by Channelrhodopsin-2 and TRPA1 determine behavioral output in Drosophila larvae. J. Neurophysiol. 101: 3075–3088.

von Reyn, C. R., P. Breads, M. Y. Peek, G. Z. Zheng, W. R. Williamson *et al.*, 2014 A

spike-timing mechanism for action selection. Nat. Neurosci. 17: 962–970.

Rickert, C., T. Kunz, K.-L. Harris, P. M. Whitington, and G. M. Technau, 2011 Morphological characterization of the entire interneuron population reveals principles of neuromere organization in the ventral nerve cord of Drosophila. J. Neurosci. 31: 15870–83.

Riedl, J., and M. Louis, 2012 Behavioral neuroscience: Crawling is a no-brainer for fruit fly larvae. Curr. Biol. 22: R867-9.

Risse, B., N. Otto, D. Berh, X. Jiang, and C. Klämbt, 2014 FIM imaging and FIMtrack: two new tools allowing high-throughput and cost effective locomotion analysis. J. Vis. Exp.

Risse, B., S. Thomas, N. Otto, T. Lopmeier, D. Valkov *et al.*, 2013 FIM, a novel FTIR-based imaging method for high throughput locomotion analysis. PLoS One 8: e53963.

Risse, B., S. Thomas, N. Otto, T. Löpmeier, D. Valkov *et al.*, 2013 FIM, a novel FTIR-based imaging method for high throughput locomotion analysis. PLoS One 8: e53963.

Rohrbough, J., and K. Broadie, 2002 Electrophysiological analysis of synaptic transmission in central neurons of Drosophila larvae. J. Neurophysiol. 88: 847–60.

Ruta, V., S. R. Datta, M. L. Vasconcelos, J. Freeland, L. L. Looger *et al.*, 2010 A dimorphic pheromone circuit in Drosophila from sensory input to descending output. Nature 468: 686–690.

Saalfeld, S., A. Cardona, V. Hartenstein, and P. Tomancak, 2009 CATMAID: collaborative annotation toolkit for massive amounts of image data. Bioinformatics 25: 1984–6.

Schaefer, J. E., J. W. Worrell, and R. B. Levine, 2010 Role of Intrinsic Properties in Drosophila Motoneuron Recruitment During Fictive Crawling. J. Neurophysiol. 104: 1257–1266.

Schlegel, P., M. J. Texada, A. Miroschnikow, A. Schoofs, S. Hückesfeld *et al.*, 2016 Synaptic transmission parallels neuromodulation in a central food-intake circuit. Elife 5:.

Schmid, A., A. Chiba, and C. Doe, 1999a Clonal analysis of.

Schmid, A., A. Chiba, and C. Q. Doe, 1999b Clonal analysis of Drosophila embryonic neuroblasts: neural cell types, axon projections and muscle targets. Development 126: 4653–4689.

Schneider-Mizell, C. M., S. Gerhard, M. Longair, T. Kazimiers, F. Li *et al.*, 2015 Quantitative neuroanatomy for connectomics in Drosophila: Cold Spring Harbor Labs Journals.

Schneider-Mizell, C. M., S. Gerhard, M. Longair, T. Kazimiers, F. Li *et al.*, 2016 Quantitative neuroanatomy for connectomics in Drosophila. Elife 5: e12059.

Schnell, B., I. G. Ros, and M. H. Dickinson, 2017 A Descending Neuron Correlated with the Rapid Steering Maneuvers of Flying Drosophila. Curr. Biol. 27: 1200–1205.

Scott, K., R. Brady, A. Cravchik, P. Morozov, A. Rzhetsky *et al.*, 2001 A chemosensory gene family encoding candidate gustatory and olfactory receptors in Drosophila. Cell 104: 661–73.

Sen, R., M. Wu, K. Branson, A. Robie, G. M. Rubin *et al.*, 2017 Moonwalker Descending Neurons Mediate Visually Evoked Retreat in Drosophila. Curr. Biol. 27: 766–771.

Siller, K., and C. Doe, 2009 Spindle orientation during asymmetric cell division. Nat. Cell Biol.

Singhania, A., and W. B. Grueber, 2014 Development of the embryonic and larval peripheral nervous system of *Drosophila*. Wiley Interdiscip. Rev. Dev. Biol. 3: 193–210.

Sivanantharajah, L., and B. Zhang, 2015 Current techniques for high-resolution mapping of behavioral circuits in Drosophila. J. Comp. Physiol. A. Neuroethol. Sens. Neural. Behav. Physiol.

Srinivasan, S., K. Lance, and R. B. Levine, 2012 Segmental differences in firing properties and potassium currents in Drosophila larval motoneurons. J. Neurophysiol. 107: 1356–1365.

Stepien, A. E., M. Tripodi, and S. Arber, 2010 Monosynaptic Rabies Virus Reveals Premotor Network Organization and Synaptic Specificity of Cholinergic Partition Cells. Neuron 68: 456–472.

Stockinger, P., D. Kvitsiani, S. Rotkopf, L. Tirian, and B. J. Dickson, 2005 Neural circuitry that governs Drosophila male courtship behavior. Cell 121: 795–807.

Suster, M. L., J.-R. Martin, C. Sung, and S. Robinow, 2003 Targeted expression of tetanus toxin reveals sets of neurons involved in larval locomotion in Drosophila. J. Neurobiol. 55: 233–46.

Suver, M. P., A. Huda, N. Iwasaki, S. Safarik, and M. H. Dickinson, 2016 An Array of Descending Visual Interneurons Encoding Self-Motion in Drosophila. J. Neurosci. 36: 11768–11780.

Takemura, S., A. Bharioke, Z. Lu, A. Nern, S. Vitaladevuni *et al.*, 2013 A visual motion detection circuit suggested by Drosophila connectomics. Nature 500: 175–181.

Tastekin, I., J. Riedl, V. Schilling-Kurz, A. Gomez-Marin, J. W. Truman *et al.*, 2015 Role of the subesophageal zone in sensorimotor control of orientation in Drosophila larva. Curr. Biol. 25: 1448–1460.

Thor, S., and J. B. Thomas, 2002 Motor neuron specification in worms, flies and mice: conserved and "lost" mechanisms. Curr. Opin. Genet. Dev. 12: 558–64.

Titlow, J. S., B. R. Johnson, and S. R. Pulver, 2015 Light Activated Escape Circuits: A Behavior and Neurophysiology Lab Module using Drosophila Optogenetics. J. Undergrad. Neurosci. Educ. 13: A166-73.

Tripodi, M., J. F. Evers, A. Mauss, M. Bate, and M. Landgraf, 2008 Structural Homeostasis: Compensatory Adjustments of Dendritic Arbor Geometry in Response to Variations of Synaptic Input (A. L. Kolodkin, Ed.). PLoS Biol. 6: e260.

Turner-Evans, D., S. Wegener, H. Rouault, R. Franconville, T. Wolff *et al.*, 2017 Angular velocity integration in a fly heading circuit. Elife 6:.

Veverytsa, L., and D. W. Allan, 2012 Temporally tuned neuronal differentiation supports

the functional remodeling of a neuronal network in Drosophila. Proc. Natl. Acad. Sci. U. S. A. 109: E748-56.

Vogelstein, J. T., Y. Park, T. Ohyama, R. A. Kerr, J. W. Truman *et al.*, 2014 Discovery of Brainwide Neural-Behavioral Maps via Multiscale Unsupervised Structure Learning. Science (80-.). 344: 386–392.

Wiersma, C. A. G., and K. Ikeda, 1964 Interneurons commanding swimmeret movements in the crayfish, Procambarus clarki (girard). Comp. Biochem. Physiol. 12: 509–525.

WILSON, D. M., 1961 The Central Nervous Control of Flight in a Locust. J. Exp. Biol. 38:.

Wilson, R. I., G. C. Turner, and G. Laurent, 2004 Transformation of olfactory representations in the Drosophila antennal lobe. Science 303: 366–70.

WILSON, D. M., and R. J. WYMAN, 1965 MOTOR OUTPUT PATTERNS DURING RANDOM AND RHYTHMIC STIMULATION OF LOCUST THORACIC GANGLIA. Biophys. J. 5: 121–43.

Wolfram, V., T. D. Southall, A. H. Brand, and R. A. Baines, 2012 The LIM-homeodomain protein islet dictates motor neuron electrical properties by regulating K(+) channel expression. Neuron 75: 663–74.

Wreden, C. C., J. L. Meng, W. Feng, W. Chi, Z. D. Marshall *et al.*, 2017 Temporal Cohorts of Lineage-Related Neurons Perform Analogous Functions in Distinct Sensorimotor Circuits. Curr. Biol. 27: 1521–1528.e4.

Wu, Z., L. B. Sweeney, J. C. Ayoob, K. Chak, B. J. Andreone *et al.*, 2011 A combinatorial semaphorin code instructs the initial steps of sensory circuit assembly in the Drosophila CNS. Neuron 70: 281–298.

Xiang, Y., Q. Yuan, N. Vogt, L. L. Looger, L. Y. Jan *et al.*, 2010 Light-avoidance-mediating photoreceptors tile the Drosophila larval body wall. Nature 468: 921–926.

Yang, L., R. Li, T. Kaneko, K. Takle, R. K. Morikawa *et al.*, 2014 Trim9 regulates activity-dependent fine-scale topography in Drosophila. Curr. Biol. 24: 1024–30.

Yoshikawa, S., H. Long, and J. B. Thomas, 2016 A subset of interneurons required for Drosophila larval locomotion. Mol. Cell. Neurosci. 70: 22–9.

Yu, J. Y., M. I. Kanai, E. Demir, G. S. X. E. Jefferis, and B. J. Dickson, 2010a Cellular organization of the neural circuit that drives Drosophila courtship behavior. Curr. Biol. 20: 1602–14.

Yu, J. Y., M. I. Kanai, E. Demir, G. S. X. E. Jefferis, and B. J. Dickson, 2010b Cellular organization of the neural circuit that drives Drosophila courtship behavior. Curr. Biol. 20: 1602–1614.

Zarin, A. A., J. Asadzadeh, and J.-P. Labrador, 2014 Transcriptional regulation of guidance at the midline and in motor circuits. Cell. Mol. Life Sci. 71: 419–432.

Zlatic, M., F. Li, M. Strigini, W. Grueber, and M. Bate, 2009 Positional Cues in the Drosophila Nerve Cord: Semaphorins Pattern the Dorso-Ventral Axis (L. Luo, Ed.). PLoS Biol. 7: e1000135.

Zucker, R. S., D. Kennedy, and A. I. Selverston, 1971 Neuronal circuit mediating escape responses in crayfish. Science 173: 645–50.

Zwart, M. F., S. R. Pulver, J. W. Truman, A. Fushiki, R. D. Fetter *et al.*, 2016 Selective Inhibition Mediates the Sequential Recruitment of Motor Pools. Neuron 91: 615–628.

Zwart, M. F., O. Randlett, J. F. Evers, and M. Landgraf, 2013 Dendritic growth gated by a steroid hormone receptor underlies increases in activity in the developing Drosophila locomotor system. Proc. Natl. Acad. Sci. U. S. A. 110: E3878-87.